RESEARCH

UDOT udot.utah.gov

Utah Department of Transportation - Research Division
4501 South 2700 West - P.O. Box 148410 - SLC,UT 84114-8410

SIMPLIFIED SPT PERFORMANCE-BASED ASSESSMENT OF LIQUEFACTION AND EFFECTS: *TASKS 5 AND 6 (YEAR 2)*

Prepared For:

Utah Department of Transportation
Research Division

Submitted By:

Brigham Young University
Department of Civil and Environmental Engineering

Authored By:

Kevin W. Franke
Lucy Astorga
Braden Error

**Year 2, Quarter 2 Update Report for the TPF-5(296) Technical Advisory Committee
December 2015**

DISCLAIMER

The authors alone are responsible for the preparation and accuracy of the information, data, analysis, discussions, recommendations, and conclusions presented herein. The contents do not necessarily reflect the views, opinions, endorsements, or policies of the Utah Department of Transportation or the U.S. Department of Transportation. The Utah Department of Transportation makes no representation or warranty of any kind, and assumes no liability therefore.

ACKNOWLEDGMENTS

The authors acknowledge the Utah, Idaho, Montana, Alaska, South Carolina, and Connecticut Departments of Transportation for funding this research for pooled fund study TPF-5(296). The views and opinions presented in this report represent those of its authors, and may not represent those of the state agencies funding this research.

TECHNICAL REPORT ABSTRACT

1. Report No.	2. Government Accession No.	3. Recipient's Catalog No.
NA	NA	NA

4. Title and Subtitle SIMPLIFIED SPT PERFORMANCE-BASED ASSESSMENT OF LIQUEFACTION AND EFFECTS: *TASKS 5 AND 6 (YEAR 2)*	5. Report Date December 2015 6. Performing Organization Code NA
7. Author(s) Kevin W. Franke, Lucy Astorga, Braden Error	8. Performing Organization Report No. NA
9. Performing Organization Name and Address Brigham Young University Department of Civil and Environmental Engineering 368 Clyde Building Provo-UT 84602-4009	10. Work Unit No. 4206515D 11. Contract or Grant No. 148753
12. Sponsoring Agency Name and Address Utah Department of Transportation 4501 South 2700 West P.O. Box 148410 Salt Lake City, UT 84114-8410	13. Type of Report & Period Covered Year 2, Quarter 2 TAC Update June - December 2015 14. Sponsoring Agency Code PIC No. UT13.407

15. Supplementary Notes

Prepared in cooperation with the Utah Department of Transportation and the U.S. Department of Transportation, Federal Highway Administration

16. Abstract

The purpose of the research being performed is to provide the benefit of the full performance-based probabilistic earthquake hazard analysis, without requiring special software, training, and experience. To do this, simplified models of liquefaction triggering and lateral spread displacements that approximate the results of the full probabilistic analysis were developed in the Year 1 Quarter 1 report. These simplified methods require liquefaction parameter maps. This report describes the process of creating these parameter maps, addressing the Year 2 portion of Tasks 5 and 6 of the TPF-5(296) research contract.

To create proper parameter maps, it was necessary to define a set of rules for optimum grid spacing which would keep the error due to interpolation within a reasonable amount. As shown in this report, such a set of rules was derived. Assuming that these rules are followed, the grid spacings should result in a 5% or less difference between an interpolated value and the value that would have been produced if a full analysis were performed at that location. The set of grid spacing rules were used in creating the grid of points used for map making.

Using the set of rules developed in the grid spacing study, a set of points was determined for each state to be used in analysis. A full performance-based analysis was performed at each point for three return periods (475, 1033, and 2475 years) yielding three different values for each return period: vertical strain (ε^{ref}) in units of percent for post-liquefaction settlement and seismic slope displacement (D^{ref}) in units of centimeters. The values at each point were used to create a surface raster file in ArcMap using Kriging-style interpolation. This raster was then used to create contour maps for each parameter in each state. These contour maps can be re-formatted as desired from the raster file in ArcMap. Sample contour maps created by the research team can be found in the Appendix of this report.

17. Key Words	18. Distribution Statement	23. Registrant's Seal
Post-Liquefaction Settlement, Seismic Slope Displacement, Performance-based Engineering, Reference Maps, Simplified Models, Seismic Hazards	Not restricted. Available through: UDOT Research Division 4501 South 2700 West P.O. Box 148410 Salt Lake City, UT 84114-8410 www.udot.utah.gov/go/research	NA

19. Security Classification (of this report)	20. Security Classification (of this page)	21. No. of Pages	22. Price
Unclassified	Unclassified	92	NA

TABLE OF CONTENTS

LIST OF TABLES

LIST OF FIGURES

UNIT CONVERSION FACTORS

Units used in this report and not conforming to the UDOT standard unit of measurement (U.S. Customary system) are given below with their U.S. Customary equivalents:

SI* (MODERN METRIC) CONVERSION FACTORS				
APPROXIMATE CONVERSIONS TO SI UNITS				
Symbol	**When You Know**	**Multiply By**	**To Find**	**Symbol**
		LENGTH		
in	inches	25.4	millimeters	mm
ft	feet	0.305	meters	m
yd	yards	0.914	meters	m
mi	miles	1.61	kilometers	km
		AREA		
in^2	square inches	645.2	square millimeters	mm^2
ft^2	square feet	0.093	square meters	m^2
yd^2	square yard	0.836	square meters	m^2
ac	acres	0.405	hectares	ha
mi^2	square miles	2.59	square kilometers	km^2
		VOLUME		
fl oz	fluid ounces	29.57	milliliters	mL
gal	gallons	3.785	liters	L
ft^3	cubic feet	0.028	cubic meters	m^3
yd^3	cubic yards	0.765	cubic meters	m^3
		NOTE: volumes greater than 1000 L shall be shown in m^3		
		MASS		
oz	ounces	28.35	grams	g
lb	pounds	0.454	kilograms	kg
T	short tons (2000 lb)	0.907	megagrams (or "metric ton")	Mg (or "t")
		TEMPERATURE (exact degrees)		
°F	Fahrenheit	5 (F-32)/9 or (F-32)/1.8	Celsius	°C
		ILLUMINATION		
fc	foot-candles	10.76	lux	lx
fl	foot-Lamberts	3.426	candela/m^2	cd/m^2
		FORCE and PRESSURE or STRESS		
lbf	poundforce	4.45	newtons	N
lbf/in^2	poundforce per square inch	6.89	kilopascals	kPa
APPROXIMATE CONVERSIONS FROM SI UNITS				
Symbol	**When You Know**	**Multiply By**	**To Find**	**Symbol**
		LENGTH		
mm	millimeters	0.039	inches	in
m	meters	3.28	feet	ft
m	meters	1.09	yards	yd
km	kilometers	0.621	miles	mi
		AREA		
mm^2	square millimeters	0.0016	square inches	in^2
m^2	square meters	10.764	square feet	ft^2
m^2	square meters	1.195	square yards	yd^2
ha	hectares	2.47	acres	ac
km^2	square kilometers	0.386	square miles	mi^2
		VOLUME		
mL	milliliters	0.034	fluid ounces	fl oz
L	liters	0.264	gallons	gal
m^3	cubic meters	35.314	cubic feet	ft^3
m^3	cubic meters	1.307	cubic yards	yd^3
		MASS		
g	grams	0.035	ounces	oz
kg	kilograms	2.202	pounds	lb
Mg (or "t")	megagrams (or "metric ton")	1.103	short tons (2000 lb)	T
		TEMPERATURE (exact degrees)		
°C	Celsius	1.8C+32	Fahrenheit	°F
		ILLUMINATION		
lx	lux	0.0929	foot-candles	fc
cd/m^2	candela/m^2	0.2919	foot-Lamberts	fl
		FORCE and PRESSURE or STRESS		
N	newtons	0.225	poundforce	lbf
kPa	kilopascals	0.145	poundforce per square inch	lbf/in^2

*SI is the symbol for the International System of Units. (Adapted from FHWA report template, Revised March 2003)

LIST OF ACRONYMS

EDP	Engineering Demand Parameter
FHWA	Federal Highway Administration
GMPE	Ground Motion Predictive Equation
IM	Intensity Measure
PBEE	Performance-Based Earthquake Engineering
PSHA	Probabilistic Seismic Hazard Analysis
UDOT	Utah Department of Transportation

<u>**LIST OF TERMS**</u>

Post-Liquefaction Free-Field Settlement Terms

CRR	cyclic resistance ratio
CRR^{ref}	cyclic resistance ratio associated with the reference soil profile
CRR^{site}	cyclic resistance ratio for the site profile
CSR	cyclic stress ratio
CSR^{ref}	uniform hazard estimate of CSR associated with the reference soil profile
CSR^{site}	uniform hazard estimate of CSR associated with the site specific soil profile
$CSR_{SS,20,1D,atm}$	adjusted CSR to account for multi-directional shaking effects
CSR^{site}	site-specific uniform hazard estimate of CSR
DF_i	depth factor for soil sub-layer
D_R	relative density
FC	fines content (%)
F_{PGA}	soil amplification factor
FS_{Liq}	factor of safety against liquefaction triggering
FS_L^{site}	site-specific uniform hazard estimate of FS_L
F_α	limiting factor of safety (used in Ishihara and Yoshimine model)
F_α^{ref}	limiting factor of safety associated with reference soil profile
F_α^{site}	limiting factor of safety associate with site soil profile
K_{md}	multidirectional correction factor for unidirectional applied loading
K_{Mw}	magnitude correction factor
K_σ	non-linear increase in cyclic resistance correction factor
min(.)	use minimum value inside parentheses mathematical operator
M_w	mean moment magnitude
N	SPT blow count (uncorrected)
$(N_1)_{60}$	SPT resistance corrected to 60% efficiency and 1 atm pressure
$(N_1)_{60,cs}$	clean sand-equivalent SPT corrected to 60% efficiency and 1 atm pressure
N_{req}	SPT resistance required to resist or prevent liquefaction
N_{req}^{ref}	uniform hazard estimate of N_{req} associated with the reference soil profile
N_{req}^{site}	site-specific uniform hazard estimate of N_{req}

N_{site}	standard penetration test resistance of site profile layer
P_a	atmospheric pressure (1 atm, 101.3 kPa, 0.2116 psf)
PGA	peak ground acceleration
P_L	probability of liquefaction
$s_{profile}$	estimated total settlement for soil profile using equivalent strain approach
SPT	Standard Penetration Test
t_i	thickness of soil sub-layer
$V_{s,12}$	average shear wave velocity in upper 12 m (39.37 ft) of soil profile
z_{cr}	maximum depth at which vertical strain can occur (z_{cr} = *18 meters)*
$\Delta\varepsilon$	site-specific adjustment factor
ε_v	vertical strain
$\varepsilon_{v,calibrated}^{site}$	site-specific strain calibrated for model non-linearity
ε_v^{ref}	vertical strain for the reference soil profile
$\varepsilon_{Cetin}^{ref}$	vertical strain for the reference soil profile as calculated from Cetin (2009)
$\varepsilon_{IshaharaYoshimine}^{ref}$	vertical strain for the reference soil profile from Ishihara & Yoshimine (1992) model
ε_v^{site}	site-specific vertical strain
$\varepsilon_{v,eqv.}$	equivalent vertical strain for entire soil profile
$\varepsilon_{v,max}$	maximum limiting vertical strain for a soil layer
γ	unit weight of soil (e.g. pcf, kN/m^3, etc.)
γ_{max}	maximum limiting shear strain
γ_{min}	minimum limiting shear strain
$\lambda_{\varepsilon,v,i}$	mean annual rate of exceeding vertical strain
$\mu_{\ln\varepsilon}$	mean value of the natural logarithm of vertical strain
σ_ε	error term for either model + parametric uncertainty or parametric uncertainty
σ'_{vo}	effective vertical stress in the soil
Φ	standard normal cumulative distribution function
Φ^{-1}	inverse standard normal cumulative distribution function

Seismic Slope Displacement Terms

$\ln D$	natural logarithm of seismic slope displacement (cm)
k_y	yield acceleration (g)
PGA	peak ground acceleration (g)
M	earthquake moment magnitude (g)
σ_{ln}	standard deviation for the scalar model
λ_D	mean annual rate of not exceeding a seismic slope displacement value
D	seismic slope displacement (cm)
GM_i	single ground motion parameter
T_s	initial fundamental period of the sliding mass (s)
f_a	soil amplification factor (from AASHTO 2012 Values of site factor table)
$\ln D^{site}$	natural log of seismic slope displacement adjusted for the site-specific conditions
$\ln D^{ref}$	natural log of seismic slope displacement corresponding to the reference site
$\Delta \ln D$	adjustment factor for seismic slope displacement
k_y^{site}	yield acceleration adjusted for site-specific conditions (g)
PGA^{site}	peak ground acceleration adjusted for site-specific conditions (g)
k_y^{ref}	yield acceleration for the corresponding to the reference site (g)
PGA^{ref}	peak ground acceleration corresponding to the reference site (g)
f_a^{site}	soil amplification factor adjusted for site-specific conditions
f_a^{ref}	soil amplification factor corresponding to the reference site

EXECUTIVE SUMMARY

The purpose of the research being performed is to provide the benefit of the full performance-based probabilistic earthquake hazard analysis, without requiring special software, training, and experience. To do this, simplified models of post-liquefaction settlements and seismic slope displacements that approximate the results of the full probabilistic analysis were developed and validated in the Year 2 Quarter 1 update report. These simplified methods are designed to require only a few calculations programmed into a spreadsheet and a provided liquefaction parameter map. This report describes how to create these parameter maps, specifically addressing the Year 2 portion of Tasks 5 and 6 of the TPF-5(296) research contract.

Creating a contour map based on an infinite number of analyzed points is not possible for the scope of this research project. Therefore, it was necessary to define a finite number of points to analyze. Interpolation was then used to evaluate the values in between the points selected for analysis. Using a finite number of points introduces the possibility for error based on interpolation between these points. Thus it was necessary to define a set of rules for proper grid spacing which would keep the error due to interpolation within a reasonable amount. As shown in this report, such a set of rules was derived. Assuming that these rules are followed, the chosen grid spacing should result in an absolute error of 0.0015 or less for the post liquefaction volumetric strain or 5% error or less of seismic slope displacement between an interpolated value and the value that would have been produced if a full analysis were performed at that location. The set of grid spacing rules were used in creating the grid of points used for map making.

Using the set of rules developed in the grid spacing study, a set of points was determined for each state to be used in analysis. A full performance-based analysis was performed at each point for three return periods (475, 1033, and 2475 years) yielding four different values for each return period: post liquefaction volumetric strain for the Cetin (2009) model ($\varepsilon_{Cetin}^{ref}$), post liquefaction volumetric strain for Ishihara and Yoshimine 1992 ($\varepsilon_{IshiharaYoshi\min e}^{ref}$), seismic slope displacement for the Rathje and Saygili (2009) model ($D_{Rathje\&Saygili}^{ref}$), and Bray and Travasarou (2007) model ($D_{Bray\&Travasarou}^{ref}$). These values were calculated based on the reference soil profile introduced in the Year 2 Quarter 1 update report, not based on site-specific soil characteristics. The values at each point were used to create a surface raster file in ArcMap using Kriging-style interpolation. This raster was then used to create contour maps for each parameter in each state. These contour maps can be re-formatted as desired from the raster file in ArcMap. Sample contour maps created by the research team can be found in the Appendix of this report.

1.0 INTRODUCTION

1.1 Problem Statement

An important aspect of the simplified performance-based post-liquefaction settlement and seismic slope displacement models is the use of parameter and hazard maps. These maps are developed using a reference soil profile and require an analysis of a grid of points covering the desired area. The results of the analysis are then interpolated into a complete contour map providing the reference value. This quarterly report provides the methodology and process in developing these maps.

1.2 Objectives

The objective of this report is develop an optimum grid spacing for the development of the parameter and hazard maps as well as to explain the creation of these maps and the GIS files associated with them, addressing Tasks 5 and 6 of the TPF-5(296) research contract.

1.3 Scope

The tasks to be performed in this research will be: perform the grid spacing evaluation, generate the grid of points needed for the analysis for each state, perform the performance-based analysis for the grid points, and create the parameter and hazard maps.

1.4 Outline of Report

The research conducted for this report will contain the following:

- Introduction
- Evaluation of Grid Spacing
- Development of Maps
- Conclusions
- Appendices

2.0 EVALUATION OF GRID SPACING

2.1 Overview

Because biases due to spacing of grid points in gridded seismic hazard analyses are known to exist, the grid spacing study will evaluate the potential for bias to occur due to grid spacing effects in a gridded probabilistic liquefaction settlement and seismic slope displacement hazard assessment. Because the states involved in this study comprise areas of varying seismicity levels, evaluations will be performed in each of the states to assess the optimum grid spacing for development of liquefaction settlement and seismic slope displacement parameter maps in future tasks.

The grid spacing assessment was performed by comparing interpolated results from a simple 4-point grid placed in various parts of the country with site-specific results. The difference between the interpolated and site-specific results was quantified. By minimizing these computed differences, the optimum grid spacing for the liquefaction parameter maps in each state was obtained.

Note that this grid spacing study does not provide estimates of accuracy between the simplified performance-based method and the full performance-based method. The accuracy between the two methods is clearly explained in the quarter 1 year 2 report of the study. The measurements of error calculated in this grid spacing study reflect only the error involved in interpolation between grid points.

2.2 Performance-based Post-Liquefaction Settlement Evaluation

This section will describe the methods used to derive a correlation between optimum grid spacing and *PGA* for the simplified performance-based post-liquefaction settlement evaluation. The purpose of this correlation was to provide a simple, readily-available, well-defined set of rules for proper grid spacing across the states of interest. This set of rules is necessary because it is impractical to perform an infinite number of full performance-based analyses to create the liquefaction hazard contour maps. It was necessary to determine a finite number of points to analyze. The set of rules created in this grid spacing study was used to define the optimum number of points which would be feasible to analyze in the amount of time given and would yield an acceptable amount of error due to interpolation between analyzed points.

2.2.1 Methodology for Grid Spacing Study

Year 1 of this study performed a preliminary study in which it was hypothesized that expected *PGA* values have an effect on optimum grid spacing. Specifically, it was hypothesized that as *PGA* increases, the optimum grid spacing decreases. Please see the Year 1 report for more details on the preliminary study. This report builds on the premise introduced in Year 1 that *PGA* has an effect on the optimum grid spacing.

To estimate the effect of *PGA* on optimum grid spacing, a study was conducted focusing on 35 cities with a wide range of *PGA* values (Figure 2-1).

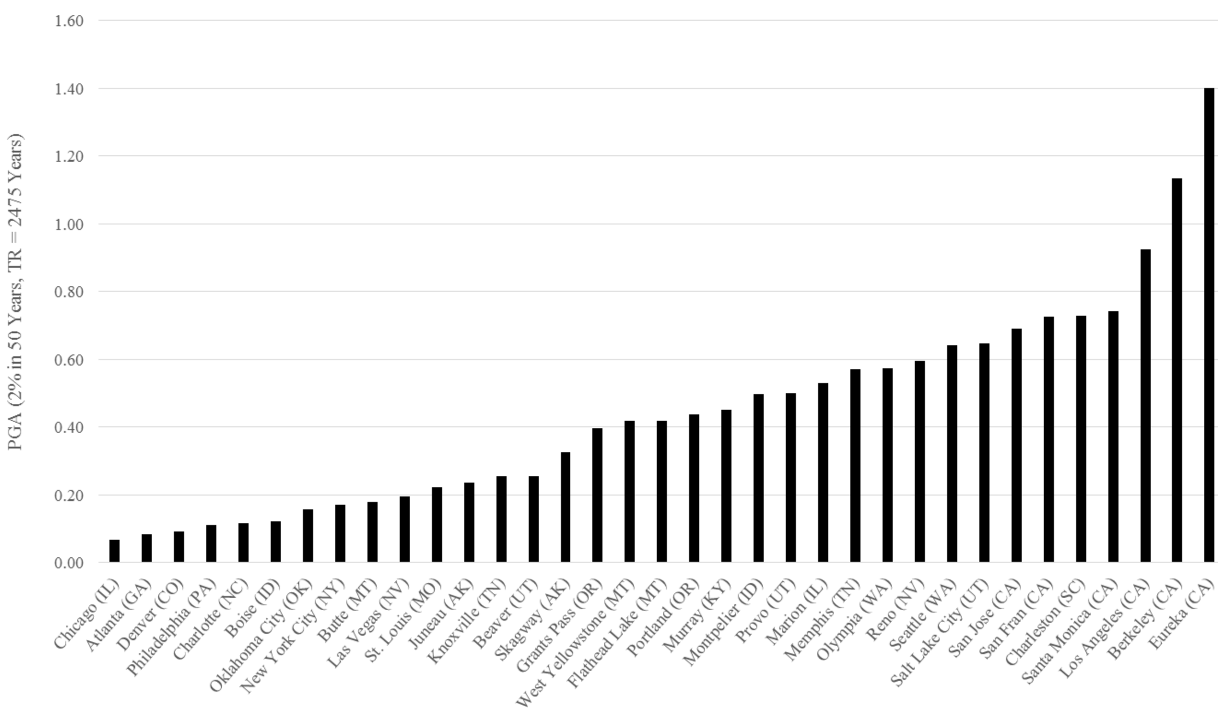

Figure 2-1 Cities used in grid spacing study and their respective expected *PGA* for the 2475 year return period.

For each city, the coordinates for an "anchor point" were selected. Using a square grid (like the one shown in Figure 2-2), a full performance-based liquefaction analysis was run for the anchor point using the reference soil profile to obtain values of $\varepsilon_{Cetin}^{ref}$ and $\varepsilon_{IshiharaYoshi\min e}^{ref}$ at three different return periods (475, 1033, and 2475 years). The full performance-based method was also run for four surrounding coordinates at varying grid spacings. The testing process included grid spacings of 1, 2, 4, 8, 16, 25, 35, and 50 kilometers (0.62, 1.24, 2.49, 4.97, 9.94, 15.5, 21.7, and 31.1 miles, respectively).

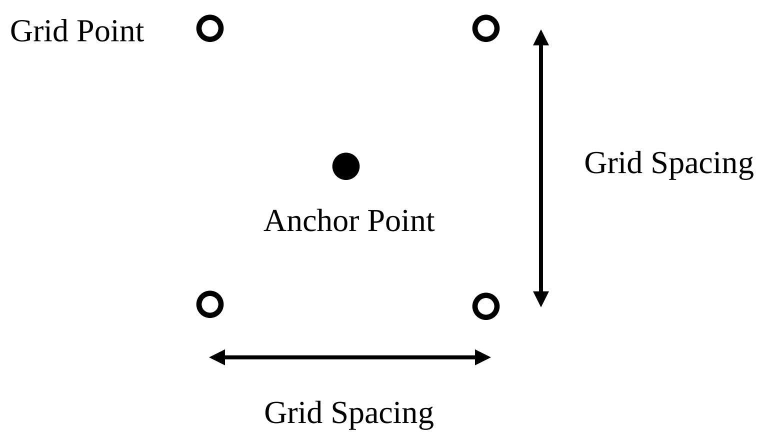

Figure 2-2 Layout of grid points centered on city's anchor point.

An estimate of the liquefaction hazard at the center point (i.e. the interpolated value of either $\varepsilon_{Cetin}^{ref}$ or $\varepsilon_{IshiharaYoshi\min e}^{ref}$) was calculated from the four corner points using a direct average of the four corner points. This interpolated value was then compared to the actual value of the center anchor point as calculated using a full performance-based liquefaction analysis. The absolute difference between the interpolated value and the true value at the center is called the error term. The error terms were calculated for each city at each grid spacing as follows:

$$AbsoluteError_{CITY,x} = \left| InterpolatedValue_{CITY,x} - AnchorValue_{CITY} \right| \quad (1)$$

where *CITY* indicates the city of interest and *x* is the grid spacing in question.

The error term calculated in equation (1) is different from the error term introduced in the Year 1 study which is a percent error. The absolute error was chosen as the error term for post-liquefaction strains due to the nature of the extremely small strain values. Even with very small magnitude strain values, slight fluctuations in strain values can lead to a high percent error even if the change is considered negligible.

The desired outcome of the grid spacing study was to create a correlation between *PGA* and optimum grid spacing in km. An equation for the best-fit trend line of *PGA* vs. optimum grid spacing alone would not be sufficient, because defining grid points to use in an analysis does not work well with non-integer values for grid spacing and constantly changing distances between points. Therefore, it was necessary to divide the different cities into *PGA* "bins" or defined ranges of values. These bins were determined using the USGS 2008 *PGA* hazard map (T_r = 2475 years) as shown in Figure 2-3. The *PGA* hazard map was chosen because it was clear and readily available as a well-documented definition of which areas in the country had significantly different seismicity levels compared to other areas' seismicity levels. Therefore, the objective of this study was to determine the optimum grid spacing for each color bin.

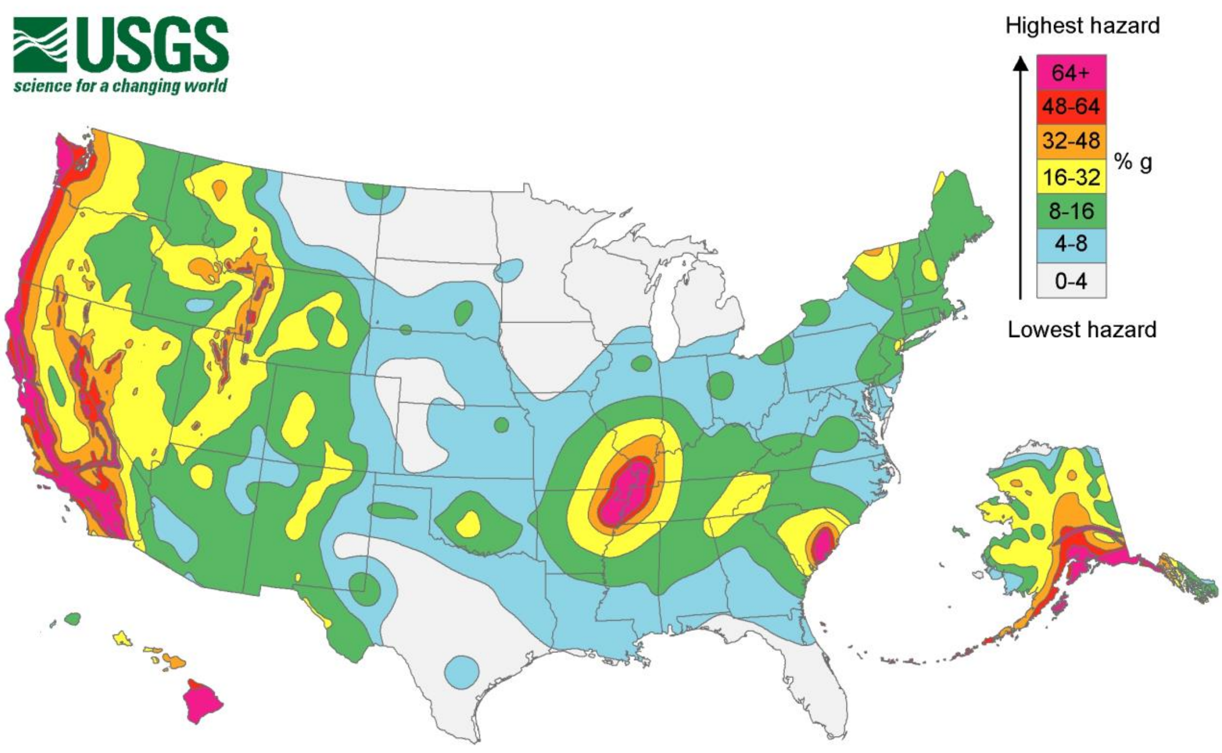

Figure 2-3 USGS 2008 *PGA* hazard map (T_r = 2475 years).

The maximum absolute error (i.e. the maximum absolute error between the Cetin (2009) and Ishihara and Yoshimine (1992) models across all return periods for a given anchor point) became the deciding parameter in selecting optimum grid spacing for a given location. The relationship between maximum absolute error and grid spacing was analyzed for each city and is discussed in the following section.

2.2.2 Results of Grid Spacing Study

The relationship between absolute error and grid spacing was analyzed for each city. It was determined that "optimum grid spacing" would be defined as the smallest grid spacing (i.e shortest distance between grid points) which yielded a maximum absolute error of 0.0015 (0.15%) across all return periods based on vertical strain. For example, if a full performance based analysis was run for an anchor point and returned a strain value of 0.02 (2%), an absolute error of 0.0015 means that the interpolated value from the four corner points would lie within 0.0185 and 0.0215 (1.85%-2.15%). In other words, for the reference soil profile as seen in Figure 2-4 which 12 is meters thick, an absolute error of 0.15% would result in settlement error of $\pm$1.8 cm. This seemed to be a reasonable amount of error, considering fluctuations in settlement of 1.8 cm would not necessarily change decision making and mitigation procedures.

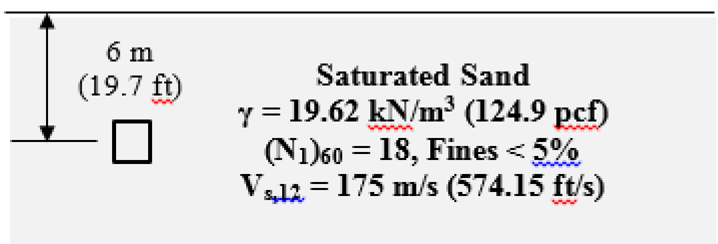

Figure 2-4: Reference soil profile used in the development of liquefaction loading maps

It is again worth noting that this study was performed in an attempt to limit spatial biases for *reference profile*. This study does not ensure that the simplified performance-based strains in the site profile will be within $\pm$0.15% of the full performance-based method. For a review on the accuracy of the simplified versus full performance-based method see the Year 2, Quarter 1 report of this study.

Optimum grid spacing was determined using a plot of absolute error vs grid spacing in km. Unique plots were created for each city to determine the optimum grid spacing. Sample plots are provided in Figure 2-5, Figure 2-6, and Figure 2-7. Some cities' data followed a linear trend line while others followed a polynomial, or even logarithmic, trend line. In each case, a reasonable best-fit curve or line was used to determine optimum grid spacing. Some of the cities selected for this study, particularly those with low *PGA* values, did not reach a maximum absolute error of 0.0015 even when the grid spacing was increased to 50 km (31.07 mi) or more. To avoid extrapolation, a maximum grid spacing threshold of 50 km was set, regardless of how low the error was. A description of the final correlation between *PGA* and optimum grid spacing is included in the following section.

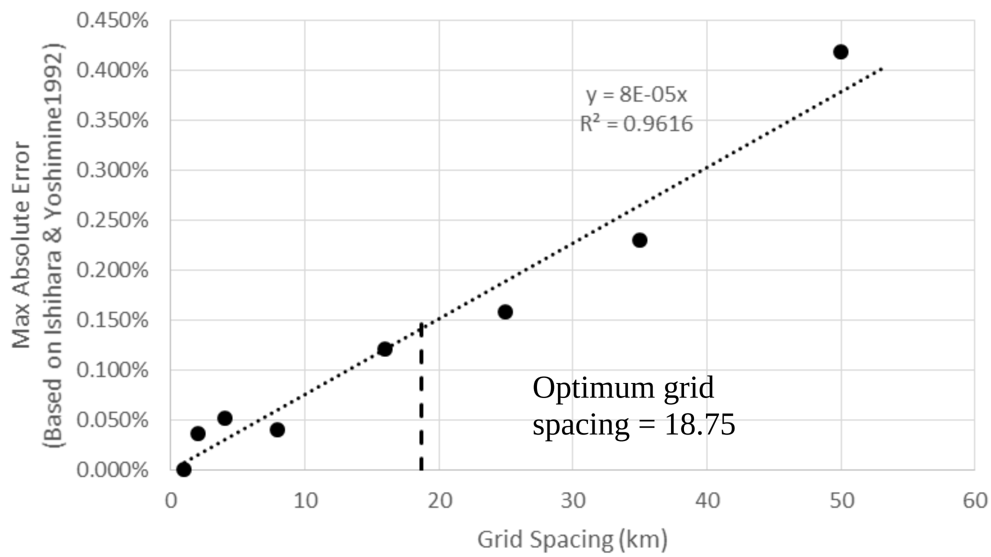

Figure 2-5 Variation of maximum percent error (based on Ishihara & Yoshimine 1992) with increasing distance between grid points for Eureka, CA. (Pink zone, *PGA* = 1.4004)

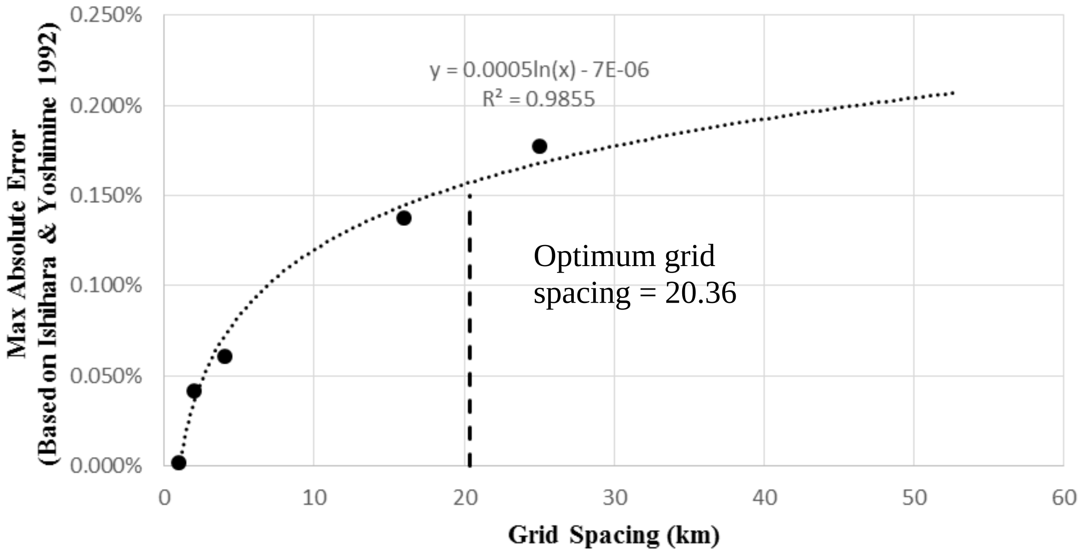

Figure 2-6 Variation of maximum percent error (based on Ishihara & Yoshimine 1992) with increasing distance between grid points for Portland, OR. (Orange zone, *PGA* = 0.4366)

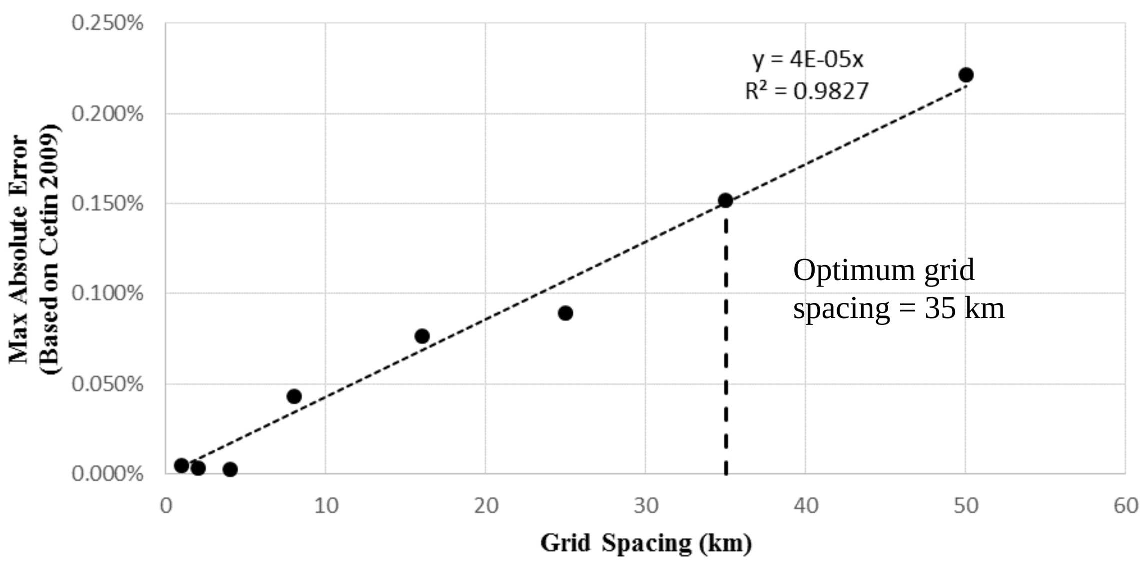

Figure 2-7 Variation of maximum percent error (based on Cetin 2009) with increasing distance between grid points for Butte, MT. (Yellow zone, *PGA* = 0.1785)

2.2.3 *PGA* Correlation

As described in the previous section, optimum grid spacing was determined for each city included in the study that reached at least a maximum absolute error of 0.0015 based on either reference strain (Cetin 2009 or Ishihara and Yoshimine 1992). Optimum grid spacing was then plotted against *PGA* as shown in Figure 2-8. The vertical dashed lines indicate the boundaries between *PGA* bins as defined in the USGS 2008 *PGA* hazard map. The general trend of the points supports the hypothesis that as *PGA* increases the optimum grid spacing decreases. A hand-drawn lower bound was used to determine the optimum grid spacing based on *PGA*. The lower bound line was chosen as a conservative estimate of optimum grid spacing.

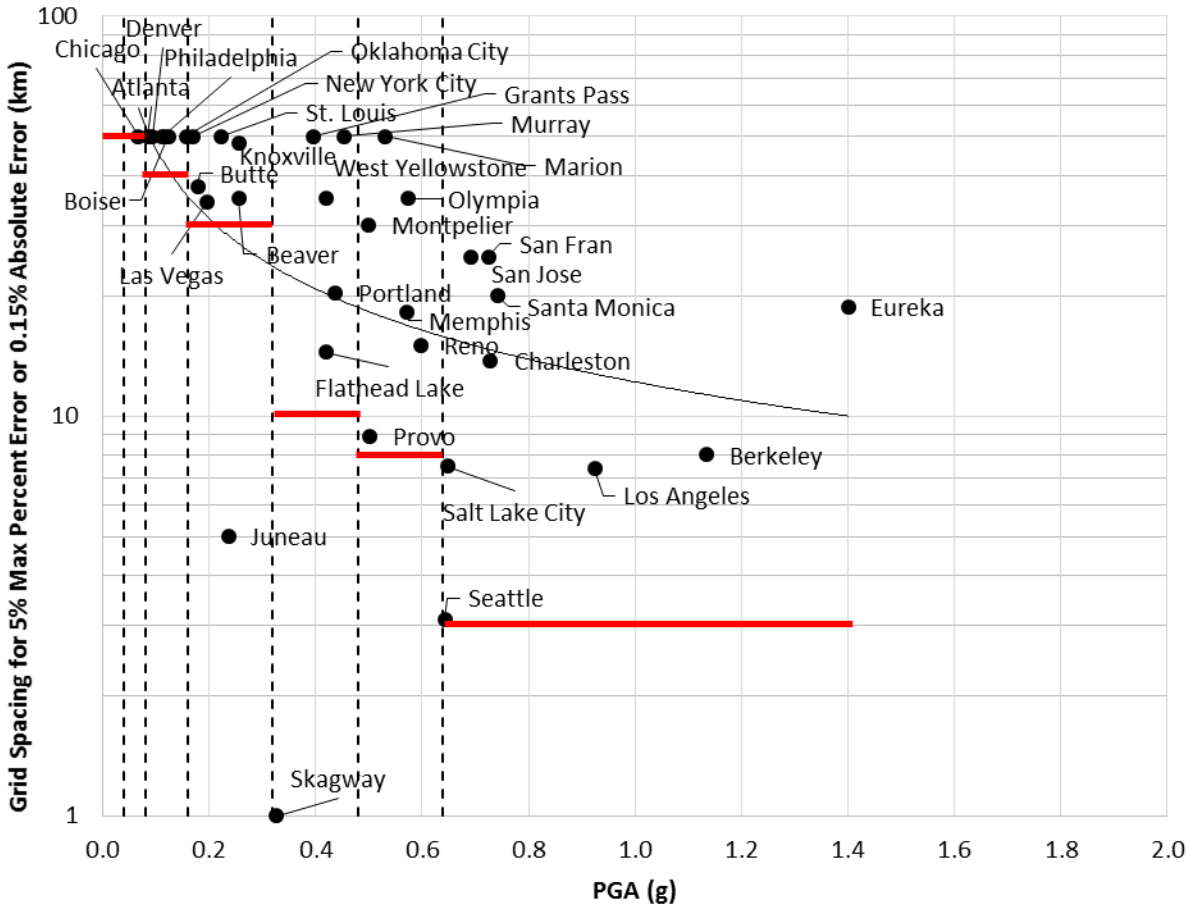

Figure 2-8 Correlation between *PGA* and optimum grid spacing to achieve 0.0015 maximum absolute error (based on minimum grid spacing between Cetin 2009 and Ishihara & Yoshimine 1992)

The hand-drawn lower bound shown in Figure 2-8 was used to determine the set of rules for selecting grid spacing in the mapping procedure. Within each *PGA* bin, a lower-bound value for optimum grid spacing was selected. The set of rules includes one optimum grid spacing distance for each *PGA* bin included in the study. Table 2-1 summarizes this set of rules.

Table 2-1 Proposed Set of Rules to Determine Optimum Grid Spacing within a *PGA* Range

PGA	Color	Spacing (km)	Spacing (mi)
0 - 0.04	Gray	50	31.1
0.04 - 0.08	Blue	50	31.1
0.08 - 0.16	Green	40	24.9
0.16 - 0.32	Yellow	30	18.6
0.32 - 0.48	Orange	10	6.21
0.48 - 0.64	Red	8	4.97
0.64+	Pink	3	1.86

In summary, the correlation determined in this study provided a set of rules to use when creating liquefaction parameter maps for $\varepsilon_{Cetin}^{ref}$ and $\varepsilon_{IshiharaYoshi\min e}^{ref}$

2.3 Seismic Slope Displacement Model

This section will describe the methods used to derive the optimum grid spacing to ensure accuracy of interpolated points determined by the simplified performance-based seismic slope displacement evaluation. To ensure accuracy of the maps, interpolation between grid points must result in values reasonably close to the results of an actual analysis at the same location. A common way to ensure that the mean value will be within a range is that of a 95% confidence interval, or a corresponding 5% error. For this study, it was determined that if the interpolated result was within 5% of an actual value computed at that site, then the result was acceptable. A few cities were analyzed using the absolute difference instead of the 5% error as it will be discussed in the following section because as a percentage these did not meet the criteria. When looking at the absolute difference between the interpolated value and the actual value at the anchor point corresponding optimum grid spacings to displacements, no greater than 5cm were recommended for the specific cities.

2.3.1 Methodology for Grid Spacing Study

The methodology used to derive the optimum grid spacing for the simplified seismic slope displacement model was the same as described in the previously addressed lateral spread displacement model. Using the USGS 1996 and 2008 Deaggregation websites the PGA at each site was determined for the 2475 year return period. The hazard level at each site as well as the hazard range for each state was found based on the same representation seen in the USGS 2008 PGA hazard map for the 2475 year return period shown in Figure 2-3

The grid spacing for the corresponding hazard zone was determined by calculating seismic slope displacements on a grid as seen in Figure 2-2. This process was repeated at 2 km, 4 km, 8 km, 16 km, 25 km, 35 km, and 50 km grid spacing, and the % error was calculated as shown in Equation (2) . A plot of each city and simplified seismic slope displacement method was generated and using best fit lines the optimum grid spacing corresponding to 5 % error was identified as shown in the figures below.

$$PercentError = \frac{|InterpolatedValue - ActualValue|}{ActualValue} \times 100\% \qquad (2)$$

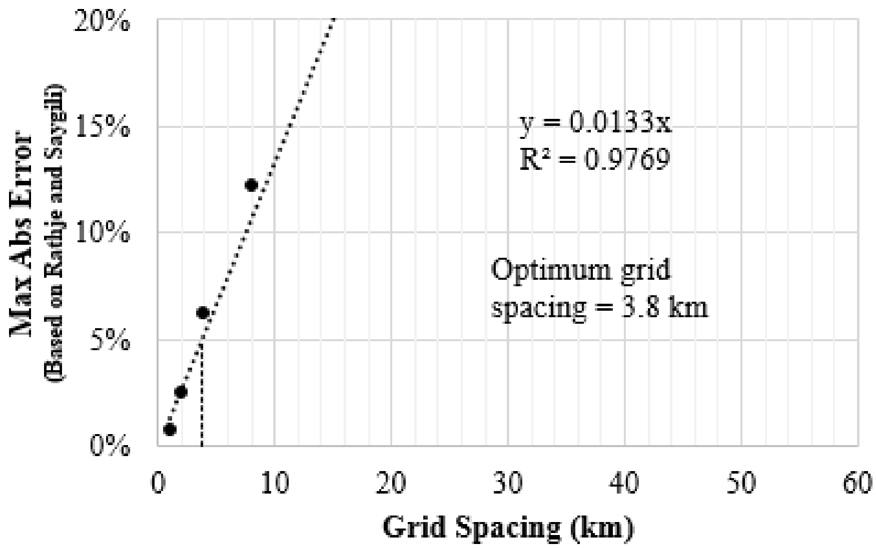

Figure 2-9 Variation of maximum percent error (based on Rathje & Saygili 2009) with increasing distance between grid points for Eureka, CA. (Pink zone, PGA = 1.4004)

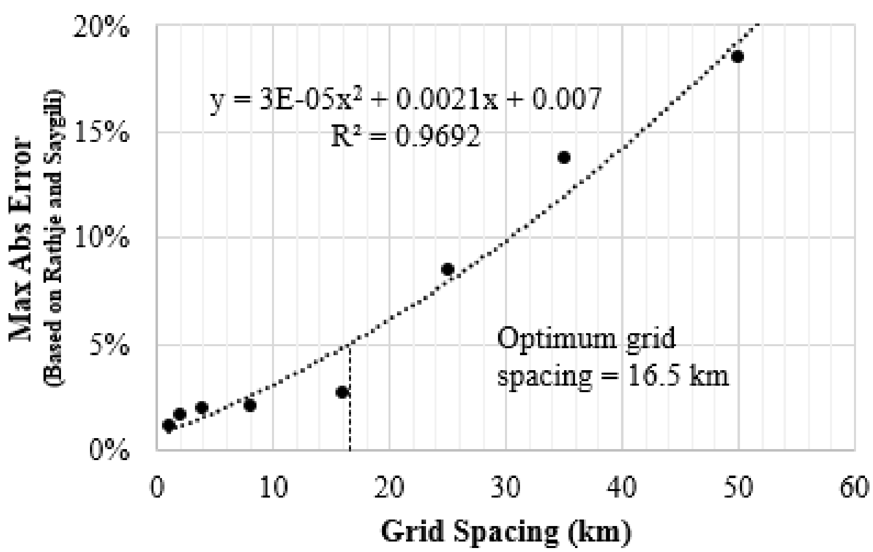

Figure 2-10 Variation of maximum percent error (based on Rathje & Saygili 2009) with increasing distance between grid points for Portland, OR. (Orange zone, *PGA* = 0.4366)

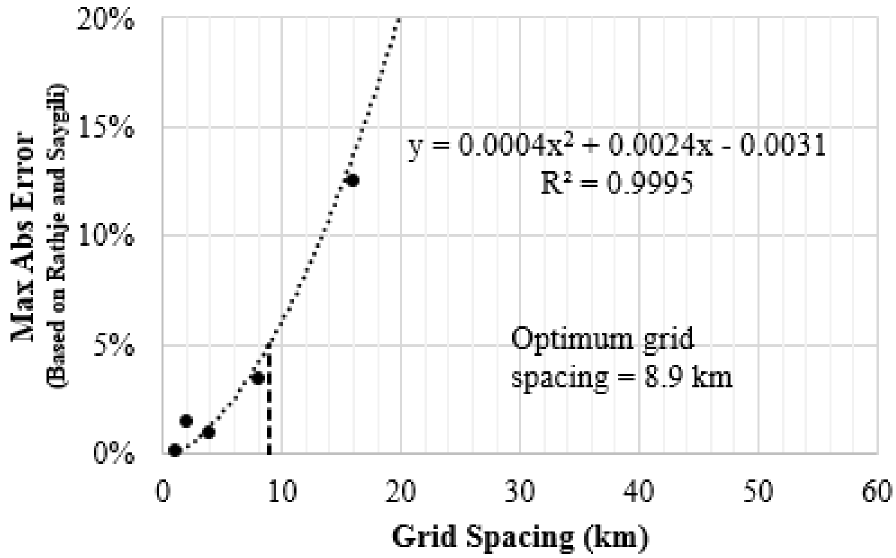

Figure 2-11 Variation of maximum percent error (based on Rathje & Saygili 2009) with increasing distance between grid points for Butte, MT. (Yellow zone, *PGA* = 0.1785)

This process was repeated for each city shown in Figure 2-1. The grid spacing, where the absolute difference was 5 cm or less, was plotted against *PGA* to get an idea of how the grid spacing differs from site to site. This plot can be seen in Figure 2-12 below.

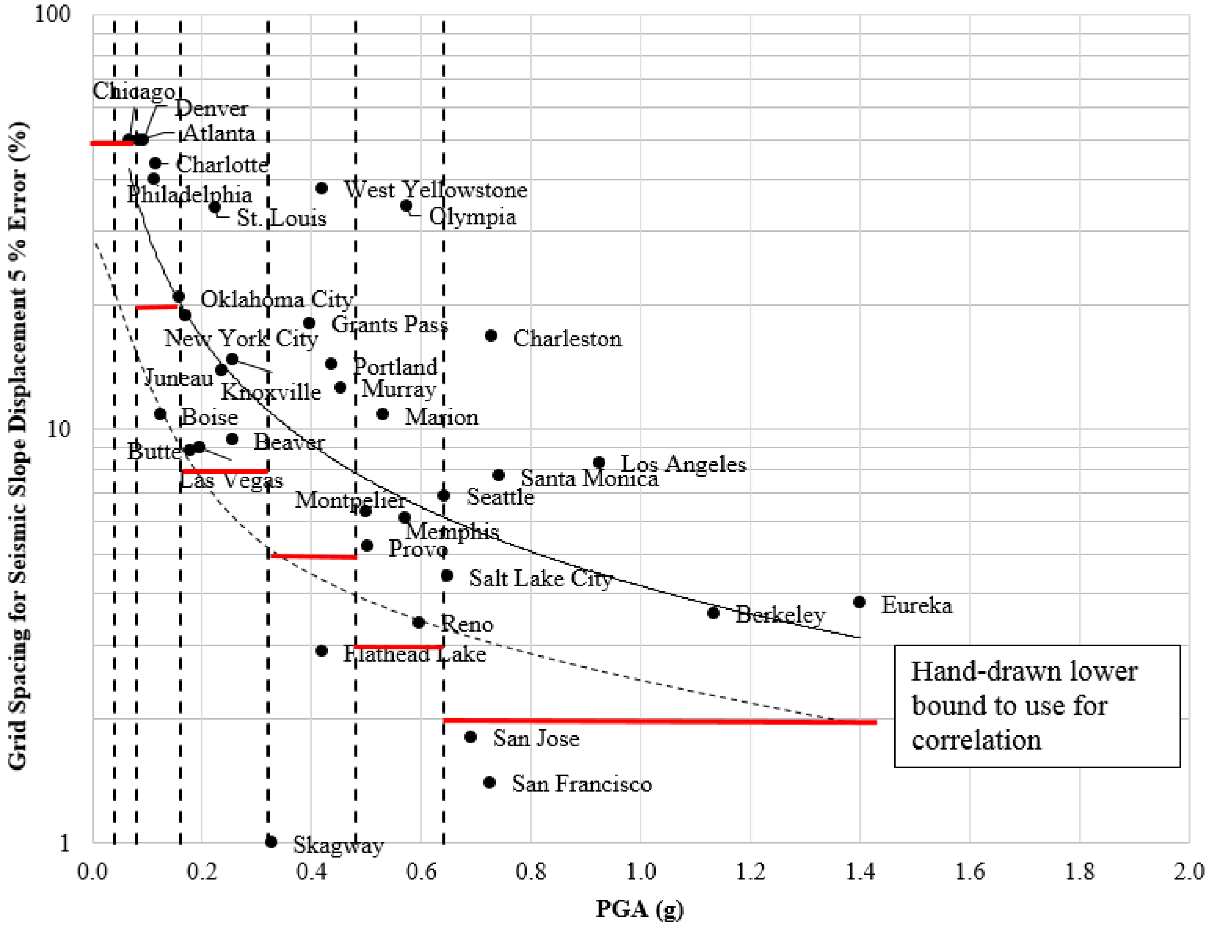

Figure 2-12 Grid spacing based on 5% Error plotted against PGA for all sites.

Figure 2-12 shows significant scatter of the results. The seismic loading at the different locations seems to be a factor affecting the seismic slope displacement analysis' results. A way to address the uncertainty is with the use of a best fit line to identify a trend in the data's behavior and then draw a dashed line just below it as the lower bound to identify the recommended grid spacing for the cities analyzed. The proposed grid spacing for each PGA interval was hand drawn with the red lines.

Five out of the thirty five cities used in the study did not meet the criteria of 5% error. These cities were Skagway (AK), Flathead (MT), Salt Lake City (UT), San Jose (CA), and San Francisco (CA). After this observation, the absolute difference in centimeters was calculated for these cities. The criteria was to use 5 cm as the maximum allowable difference between the actual value and the interpolated value and the proposed spacing the cities not meeting the 5% error criteria. Once a grid spacing was assigned to the cities not meeting the criteria, an overall grid spacing was proposed as shown below in Table 2-2.

Table 2-2 Proposed Grid Spacing for Seismic Slope Displacement Analysis

PGA	Color	Spacing (km)	Spacing (mi)
0 - 0.04	Gray	50	31.1
0.04 - 0.08	Blue	50	31.1
0.08 - 0.16	Green	20	12.4
0.16 - 0.32	Yellow	8	5.0
0.32 - 0.48	Orange	5	3.1
0.48 - 0.64	Red	3	1.9
0.64+	Pink	2	1.2

2.4 Summary

Based on the analysis outlined here, the grid spacing necessary to maintain accuracy in the interpolated results was found. For post liquefaction settlement, the grid spacing should result on an absolute difference of 0.0015 between an interpolated value and the result if an analysis were performed at the same site. For seismic slope displacement, the grid spacings should result on average 5% difference between an interpolated value and the result if an analysis were performed at the same site. These grid spacings will be very important in creating the grid of points that will be used in the analysis.

3.0 MAP DEVELOPMENT

3.1 Overview

Now that the optimum grid spacing between points has been determined, the grid points used in the analysis need to be determined, then those points need to be analyzed and the hazard parameters calculated. Once the analysis has been conducted for each grid, then those points will be used to create the post-liquefaction settlement and seismic slope displacement parameter maps for the target return periods.

This process required the use of several specialized software programs. To create the grid spacing and the maps, the Geographic Information System (GIS) software ArcMap, developed by ESRI Incorporated, was used extensively. To obtain the full performance-based strain and seismic slope displacement values, the software PBLiquefY, developed in house at BYU, was utilized.

3.2 Creating the Grid Points

The process was started by dividing each state into sections based on the USGS 2008 *PGA* hazard map. This was done creating GIS shapefiles developed from downloaded data from the USGS website representing the 2008 hazard map. Each *PGA* hazard zone was assigned a grid spacing based on the suggested grid spacing from the previous section. Then using ArcMap, a grid of points with latitude and longitude was generated for each hazard zone at the specified grid spacing. PBLiquefY (2014) has the capability of calculating liquefaction settlements and seismic slope displacements simultaneously for a given geographic coordinate; therefore, in order to limit the number of performance based analysis runs, the governing (finer) grid spacing was run for both liquefaction settlement and slope displacement. The governing grid spacing in all PGA zones was seismic slope displacement. All the zones were then combined into one general grid for the state. An example of the subdivision and the overall grid of points for Utah can be seen in Figure 3-1.

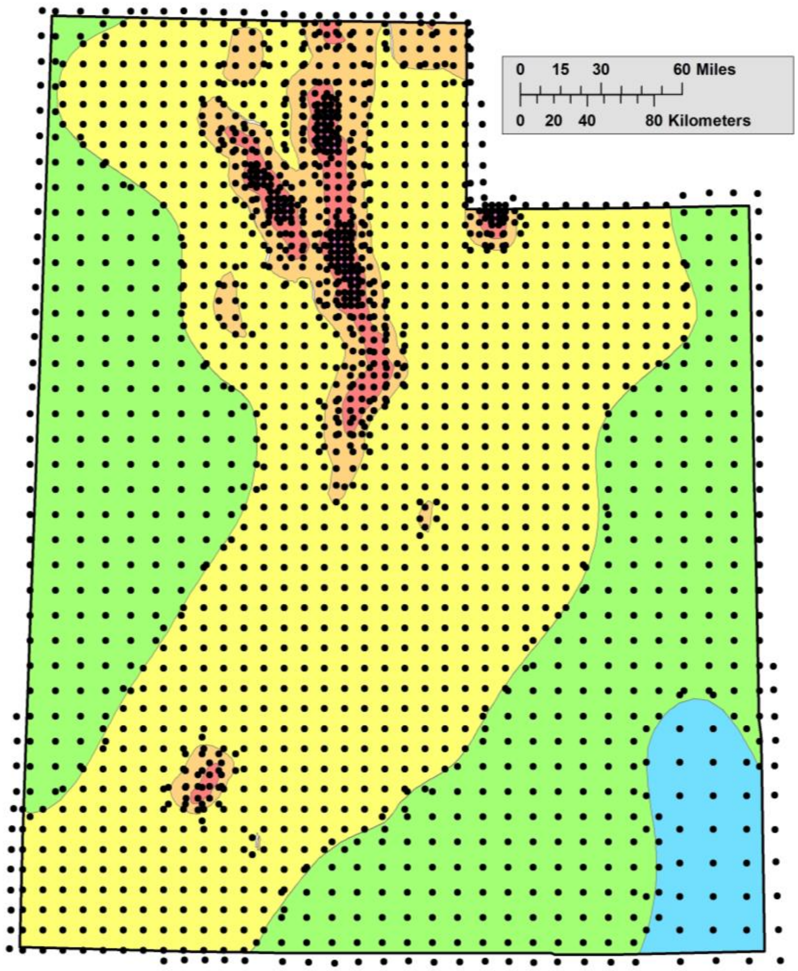

Figure 3-1 Grid points for Utah combined with USGS 2008 PGA hazard map.

3.3 Analysis of the Grid Points

Once the grid points were developed for all the states, the location of each of the points was evaluated for post-liquefaction settlement and seismic slope displacement using the reference soil profiles discussed in the previous report. Each point was analyzed for the 475, 1033, and 2475 year return periods. Once all of the points for a particular state were successfully run, the results were compiled and then imported back into ArcMap to begin the process of making the parameter maps.

3.3.1 Analysis of the Liquefaction Initiation Model Grid Points

The grid points used in the liquefaction hazard analysis were analyzed using the USGS 2008 deaggregations for Connecticut, Idaho, Montana, South Carolina, and Utah while the USGS 1996 deaggregations were used for Alaska. The maps for Alaska are not included in this report because the 1996 deaggregations are not accessible from the USGS website at the moment. As soon as the data is available an addendum to this report will be made including those maps. The process utilized the ability of PBLiquefY (2014) to run multiple sites sequentially.

3.4 Creation of the Maps

Once the analyzed grid points were imported back into ArcMap the points needed to be turned into a contour map. This was done by converting the individual points into a surface raster using the Kriging tool. This tool interpolates between each point and makes a surface with a value at every point. In order to ensure that the contours of each state run all the way to the border, the state shape is buffered slightly. The Kriging raster is created based on this buffered shape. Once the Kriging raster is made, the raster surface needs to be converted into a contour.

To make the contour from the Kriging, first the spacing of the contours needs to be determined. It is important that the contour spacing be fine enough that the detail of the map can be read, but far enough apart that the contours can be read. The spacing will vary from map to map based on this process. An example of a Kriging raster and contour for the state of Utah can be seen in Figure 3-2.

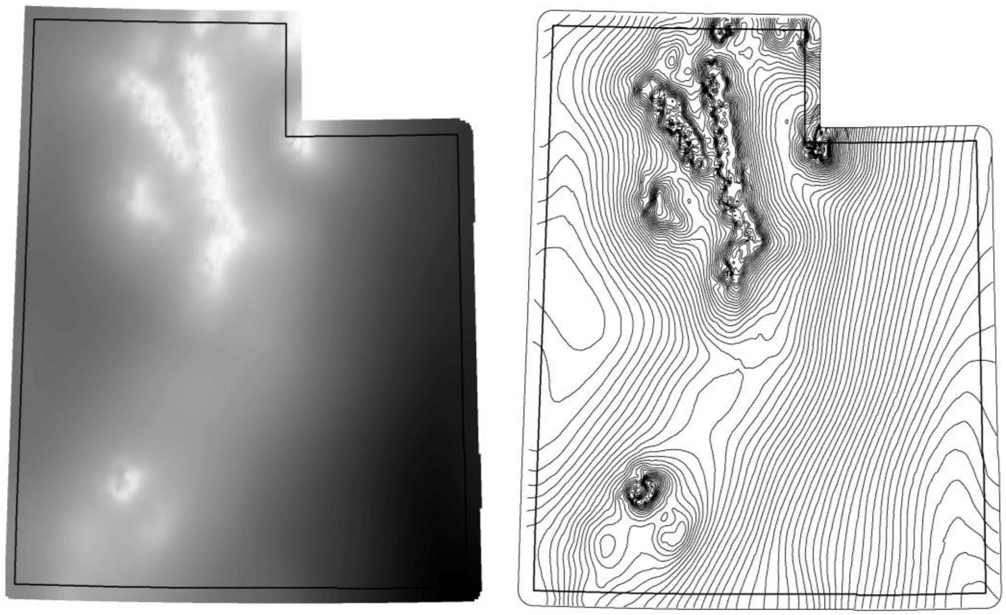

a) b)

Figure 3-2 a) Kriging raster and b) contours for Utah (T_r = 2475 yrs).

Once the proper contour spacing is determined for each map, the contour is labeled and clipped to fit the state shapefile. Then a basemap and reference features are added to provide more detail about the topography to the parameter maps. An example of a completed reference parameter map can be seen in Figure 3-3.

Each model has different parameters represented by the contours on the map. Post-liquefaction settlement and seismic slope displacement have two different models used in this study and therefore two different maps associated with each return period. For post-liquefaction settlement the first parameter is the reference value of strain, $\varepsilon_{Cetin}^{ref}$, as calculated using the Cetin (2009) model. Strain is usually given as a decimal but was changed to a percent to make reading the maps easier. The second parameter is the reference value for strain, $\varepsilon_{IshiharaYoshi\min e}^{ref}$, as calculated using the Ishihara & Yoshimine (1992) model and is also as a percent. The seismic slope displacement parameter maps seismic slope displacement for the Rathje and Saygili (2009) model ($D_{Rathje\&Saygili}^{ref}$) in centimeters, and Bray and Travasarou (2007) model ($D_{Bray\&Travasarou}^{ref}$) also in centimeters. Careful attention needs to be given to the labeling of each map to ensure that map has the correct parameter and that the reference value used in the later steps of the simplified method are accurately read from the contours.

For this report, maps of $\varepsilon^{ref}_{Cetin}$, $\varepsilon^{ref}_{IshiharaYoshi\min e}$, $D^{ref}_{Rathje\&Saygili}$ and $D^{ref}_{Bray\&Travasarou}$ were made for each state at the 475, 1033, and 2475 year return periods with the exception of Alaska as indicated before. These maps can be viewed in the Appendix: post-liquefaction settlement in Appendix A and seismic slope displacement maps in Appendix B. The contours were adjusted for each map to make reading it as user friendly as possible.

These maps were provided to show the potential types of parameter maps that can be created. Using the Kriging rasters that will be provided at the culmination of this research, each state can create maps of any area in their state and determine the contour spacing and scale.

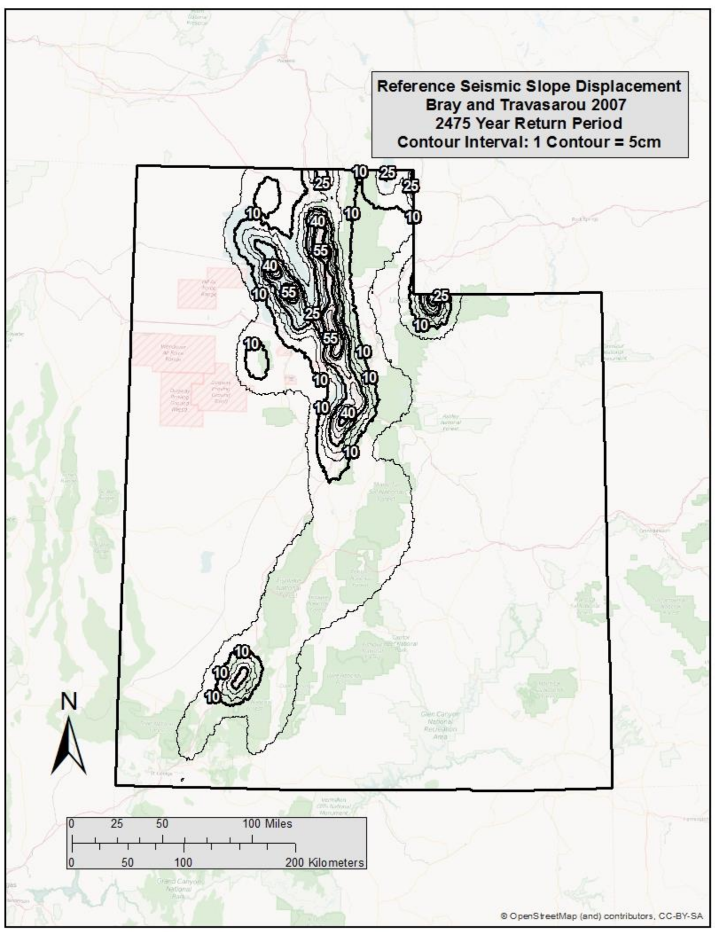

Figure 3-3 D^{ref} for Utah (T_r = 2475 years).

3.5 Summary

To create the parameter and hazard maps, the state is subdivided into zones and a grid spacing for each zone is assigned. A grid of points is generated in ArcMap based on this grid spacing. Then the points are analyzed using the specified performance-based analytical software (i.e. PBLiquefY). These points are then imported into ArcMap and converted to a Kriging raster that is then used to create a contour of the reference parameter. Sample maps for the states participating in this research study can be seen in the Appendix.

4.0 CONCLUSIONS

4.1 Summary

The purpose of the research being performed is to provide the benefit of the full performance-based probabilistic earthquake hazard analysis, without requiring special software, training, and experience. To do this, simplified models of post-liquefaction settlement and seismic slope displacement were developed in the Year 2 Quarter 1 update report that approximate the results of the full probabilistic analysis. These simplified methods require liquefaction parameter maps. This quarterly report addresses proper grid spacing of the points used for analysis and the process of creating parameter maps.

4.2 Findings

4.2.1 Evaluation of Grid Spacing

To create maps appropriate for the simplified performance-based procedures used in this research, it was necessary to define a set of rules for proper grid spacing which would keep error due to interpolation within a reasonable amount. As shown in this report, such a set of rules was derived. Assuming that these rules are followed, the difference between an interpolated value and the value that would have been produced if a full analysis were performed at that location, the grid spacings should result in an absolute error no greater than 0.0015 or 5 % error for post-liquefaction strain or seismic slope displacements, respectively. The appropriate set of grid spacing rules for each model type (i.e. post-liquefaction strain or seismic slope displacement) were used in creating the grid of points used for map making.

4.2.2 Map Development

Using the set of rules developed in the grid spacing study, a set of points was determined for each state to be used in analysis. A full performance-based analysis was performed at each point for three return periods (475, 1033, and 2475 years) yielding three different values for each return period: ε^{ref} for the Cetin (2009) model, ε^{ref} for the Ishihara & Yoshimine (1992) model,

D^{ref} for Rathje & Saygili (2009) model, and D^{ref} for Bray & Travasarou (2007). These values were calculated based on the reference soil profile introduced in the Year 2 Quarter 1 update report, not based on site-specific soil characteristics. The values at each point were used to create a surface raster file in ArcMap using Kriging-style interpolation. This raster was then used to create contour maps for each parameter in each state. These contour maps can be re-formatted as desired from the raster file in ArcMap. Sample contour maps created by the research team can be found in the Appendix of this report.

4.3 Limitations and Challenges

These liquefaction parameter maps do not include site-specific soil information. Instead, these maps are based on a reference soil profile (introduced in the Year 2 Quarter 1 update report) and as such provide *reference* values to be inserted into the simplified performance-based procedure derived in the Year 2 Quarter 1 update report. These specific maps created for this report should not be used in any other way. Also, the values on these parameter maps should not be viewed as the actual hazard at a given site. Again, these are reference values which do not include site-specific soil characteristics.

As these maps are used, keep in mind the limitations of the liquefaction evaluation models used to calculate the reference values. Please refer to the proper liquefaction evaluation models (Cetin, 2009; Ishihara & Yoshimine, 1992; Rathje & Saygili, 2009; and Bray & Travasarou, 2007) for detailed descriptions of these models' limitations. While the reference maps were created using appropriate model inputs, it is possible that site-specific properties will use values outside of recommended limits stated in the models. These limitations should be carefully considered before accepting the results of this simplified procedure.

The reference values displayed on these parameter maps were calculated based on data from available seismic models. The 2008 USGS deaggregations were used for Connecticut, Idaho, Montana, South Carolina, and Utah; the 1996 deaggregations were used for Alaska. Therefore, the results displayed on these parameter maps are only as accurate as the seismic models used to create them. Any inaccuracies which may exist in these models may affect the accuracy of the simplified methods developed as part of this research.

REFERENCES

Boulanger, R., & and Idriss, I. (2012). Probabilistic Standard-Penetration Test-Based Liquefaction-Triggering Procedure. *Journal of Geotechnical and Geoevironmental Engineering*, 1185-1195.

Bray, J. D., ASCE, F., & Travasarou, T. (2007, April). Simplified Procedure for Estimating Earthquake-Induced Deviatoric Slope Displacements. *Journal of Geotechnical and Geoenvironmental Engineering*, 381-392.

Cetin, K. O., & al., e. (2009, March). Probabilistic Model for the Assessment of Cyclical Induced Reconsolidation (Volumetric) Settlements. *Journal of Geotechnical and Geoenvironmental Engineering*, 387-396.

Cetin, K. O., Seed, R. B., Kiureghian, A. D., Tokimatsu, K., Harder Jr., L. F., Kayen, R. E., & Moss, R. E. (2004, December). Standard Penetration Test-Based Probabilistic and Deterministic Assessment of Seismic Soil Liquefaction Potential. *Journal of Geotechnical and Geoenvironmental Engineering*, 1314-1340.

Franke, K., Mayfield, R., & and Wright, A. (2014d). Simplified uniform hazard analysis for bridges. *Transportation Research Record.* Washington D.C.

Franke, K., Wright, A., & Hatch, C. (2014c). PBLiquefY: A new analysis tool for the performance-based evaluation of liquefaction triggering. *Proceedings, 10th National Conference on Earthquake Engineering.* Oakland, CA: EERI.

Huang, Y.-M. (2008). *Performance-based design and evaluation for liquefaction-related seimic hazards.* Seattle, Washington: University of Washington.

Idriss, I., & Boulanger, R. (2008). Soil liquefaction during earthquakes. *Monograph MNO-12* (p. 261 pp). Oakland, CA: Earthquake Engineering Research Institute.

Ishihara, K., & Yoshimine, M. (1992). Evaluation of settlements in sand deposits following liquefaction during earthquakes. *Soils Found., 32*, 173-188.

Kramer, S. L. (2008). *Evaluation of liquefaction hazards in Washington State.* Seattle: WSDOT Report.

Kramer, S. L. (2014). Performance-based design methodologies for geotechnical earthquake engineering. *Bull Earthquake Engineering*, 1049-1070.

Mayfield, R. T., Kramer, S. L., & Huang, Y.-M. (2010, January). Simplified Approximation Procedure for Perfomance-Based Evaluation on Liquefaction Potential. *Journal of Geotechnical and Geoenvironmental Engineering*, 140-150.

Rathje, E. M., & Saygili, G. (2009, March). Probabilistic Assesment of Earthquake-Induced Sliding Displacements of Natural Slopes. *Bulletin of the New Zeland Society of Earthquake Engineering, 42*(1), 18-27.

Shamoto, Y., Zhang, J.-M., & Tokimatsu, K. (1998). New charts for predicting large residual post-liquefaction ground deformation. *Soil Dynamics and Earthquake Engineering*, 427-438.

Tokimatsu, K., & Seed, B. H. (1987). Evaluation of settlements in sand due to earthquake shaking. *Journal of Geotechnical and Geoenvironmental Engineering*, 861-878.

USGS. (2013, May 17). *2008 Interactive Deaggregations*. Retrieved June 2015, from Geologic Hazards Science Center: http://geohazards.usgs.gov/deaggint/2008/

Wu, J., & Seed, R. B. (2004). Estimating liquefaction-induced ground settlement (case studies). *5th International Conf. on Case Histories in Geotechnical Engineering.*

Youd, T., Hansen, C., & Bartlett, S. (2002). Revised multilinear regression equations for prediction of lateral spread displacement. *Journal of Geotechnical and Geoenvironmental Engineering*, 128(12), 1007-1017.

APPENDIX A: Sample Post-Liquefaction Settlement Maps

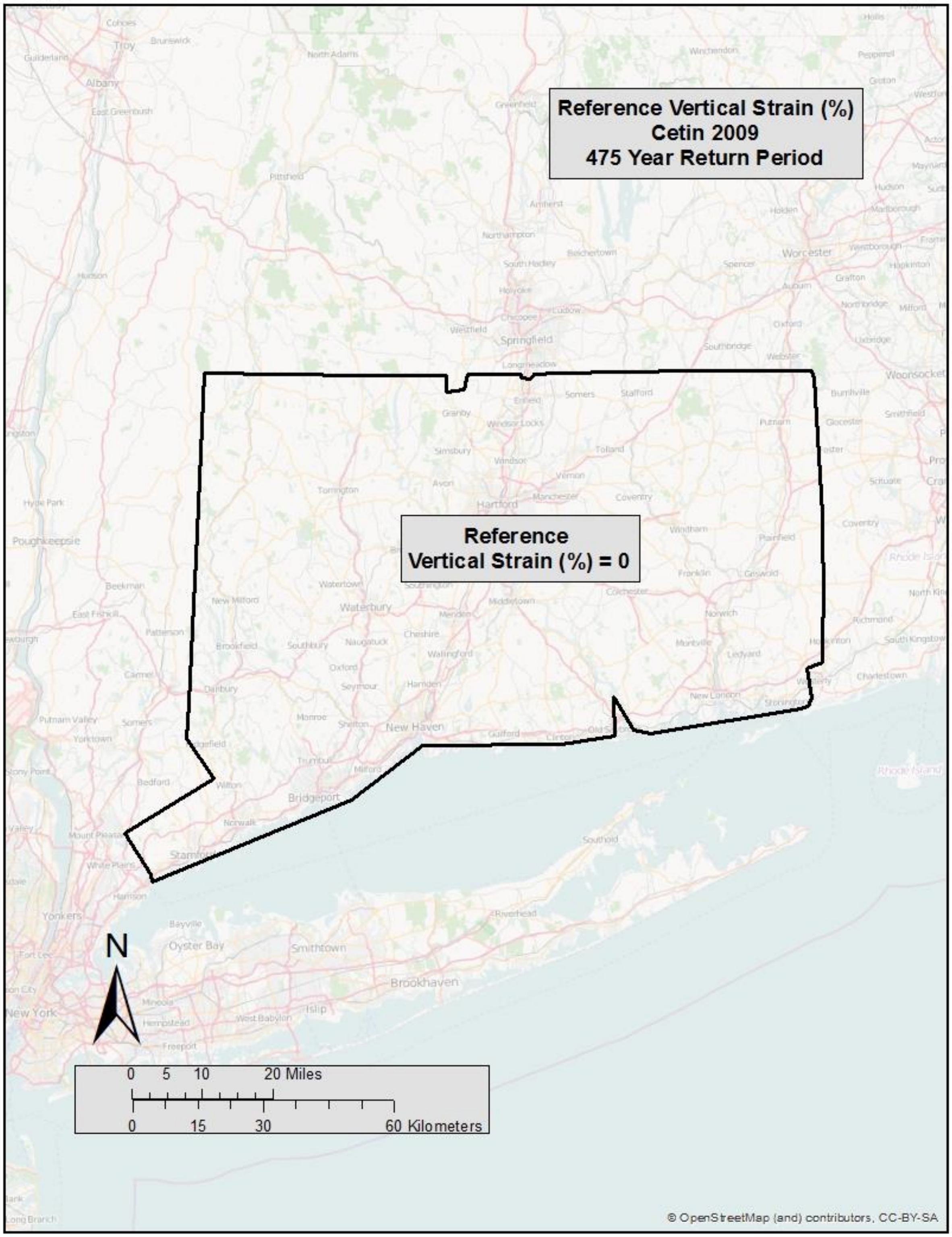

Figure A- 1 Cetin et al. (2009) Post-Liquefaction Settlement (ε^{ref}) Map for Connecticut (Tr=475)

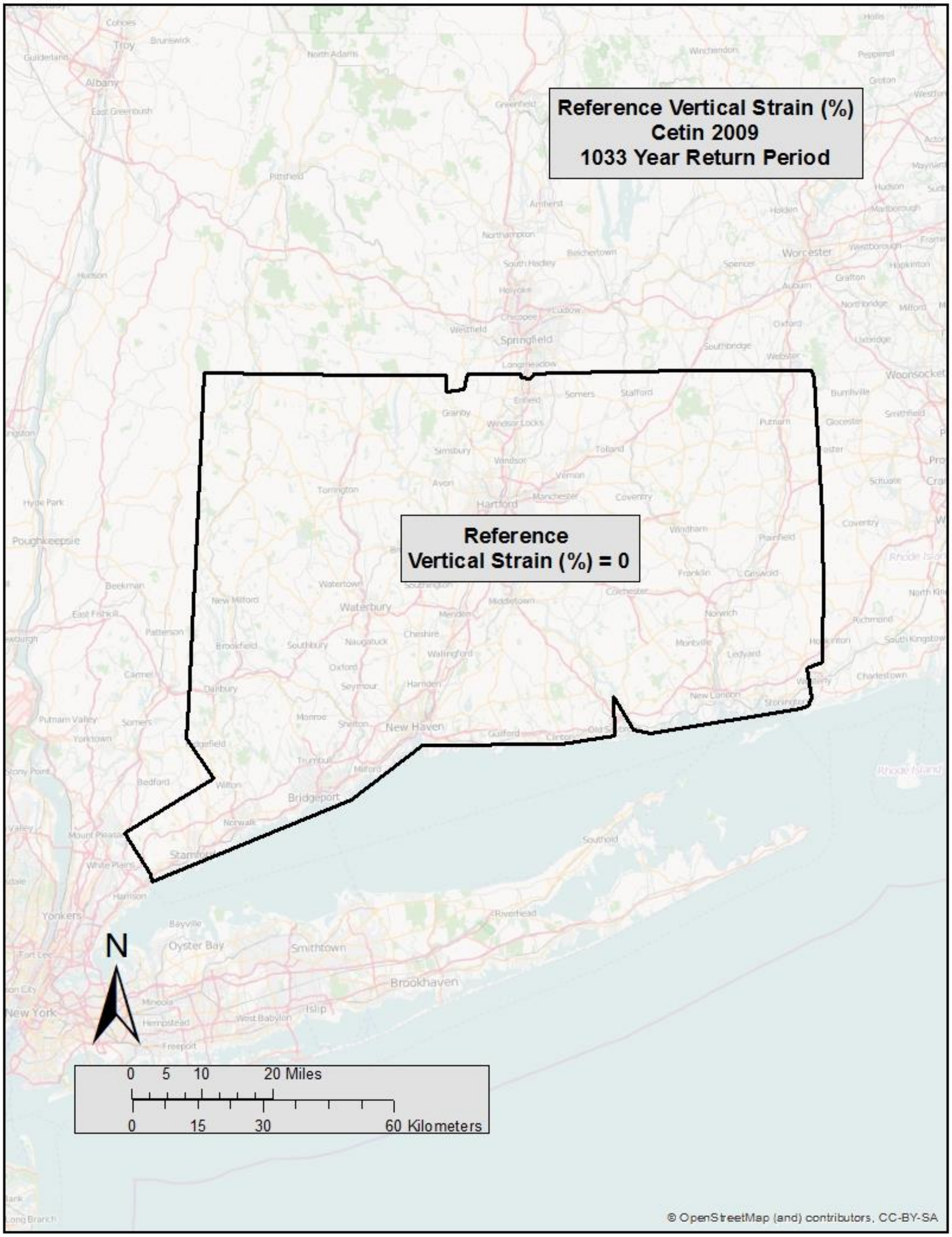

Figure A- 2 Cetin et al. (2009) Post-Liquefaction Settlement *(ε^{ref})* Map for Connecticut (Tr= 1,033)

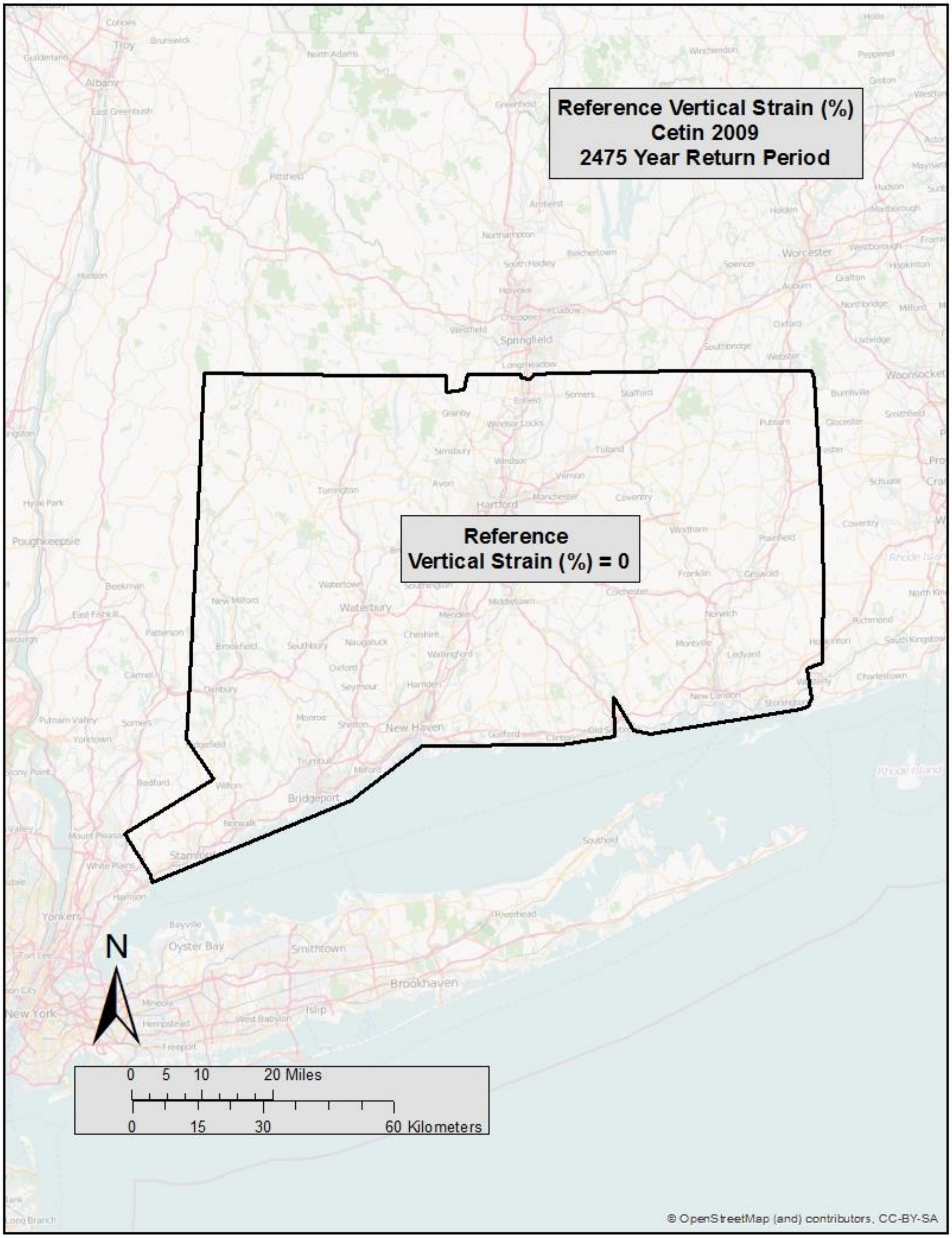

Figure A- 3 Cetin et al. (2009) Post-Liquefaction Settlement *(ε^{ref})* Map for Connecticut (Tr=2,475)

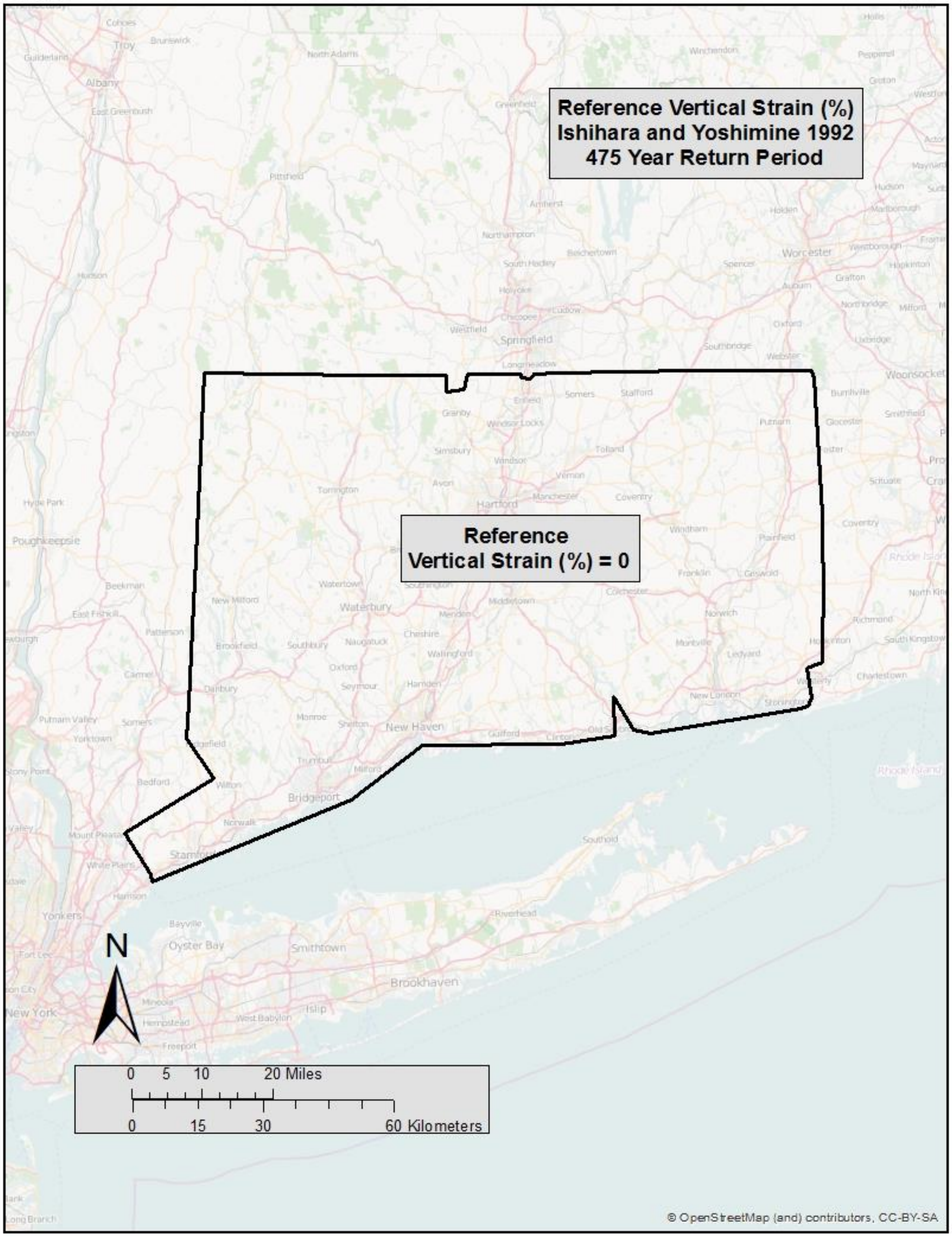

Figure A- 4 Ishihara and Yoshimine (1992) Post-Liquefaction Settlement (ε^{ref}) Map for Connecticut (Tr = 475)

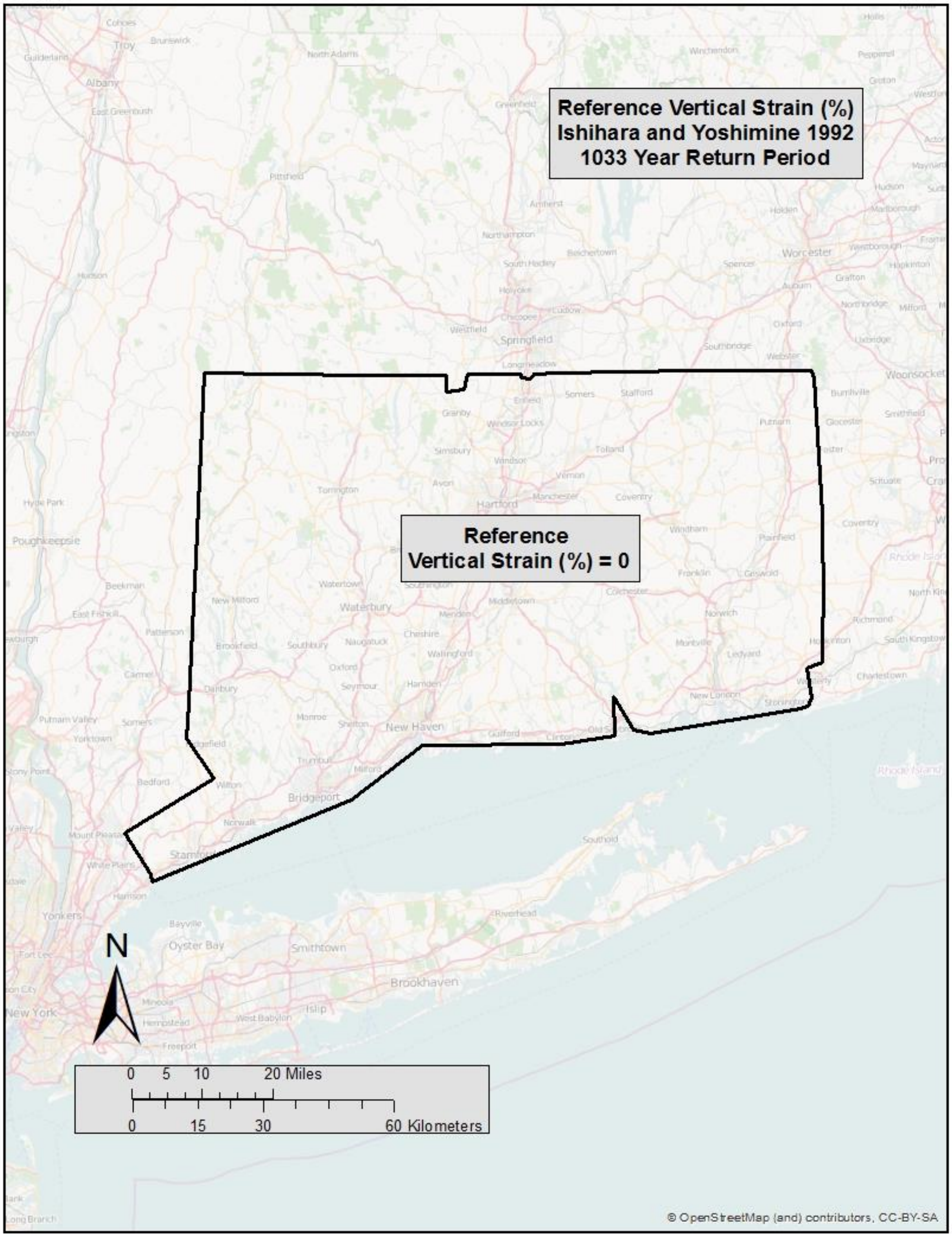

Figure A- 5 Ishihara and Yoshimine (1992) Post-Liquefaction Settlement *(ε^{ref})* Map for Connecticut (Tr = 1,033)

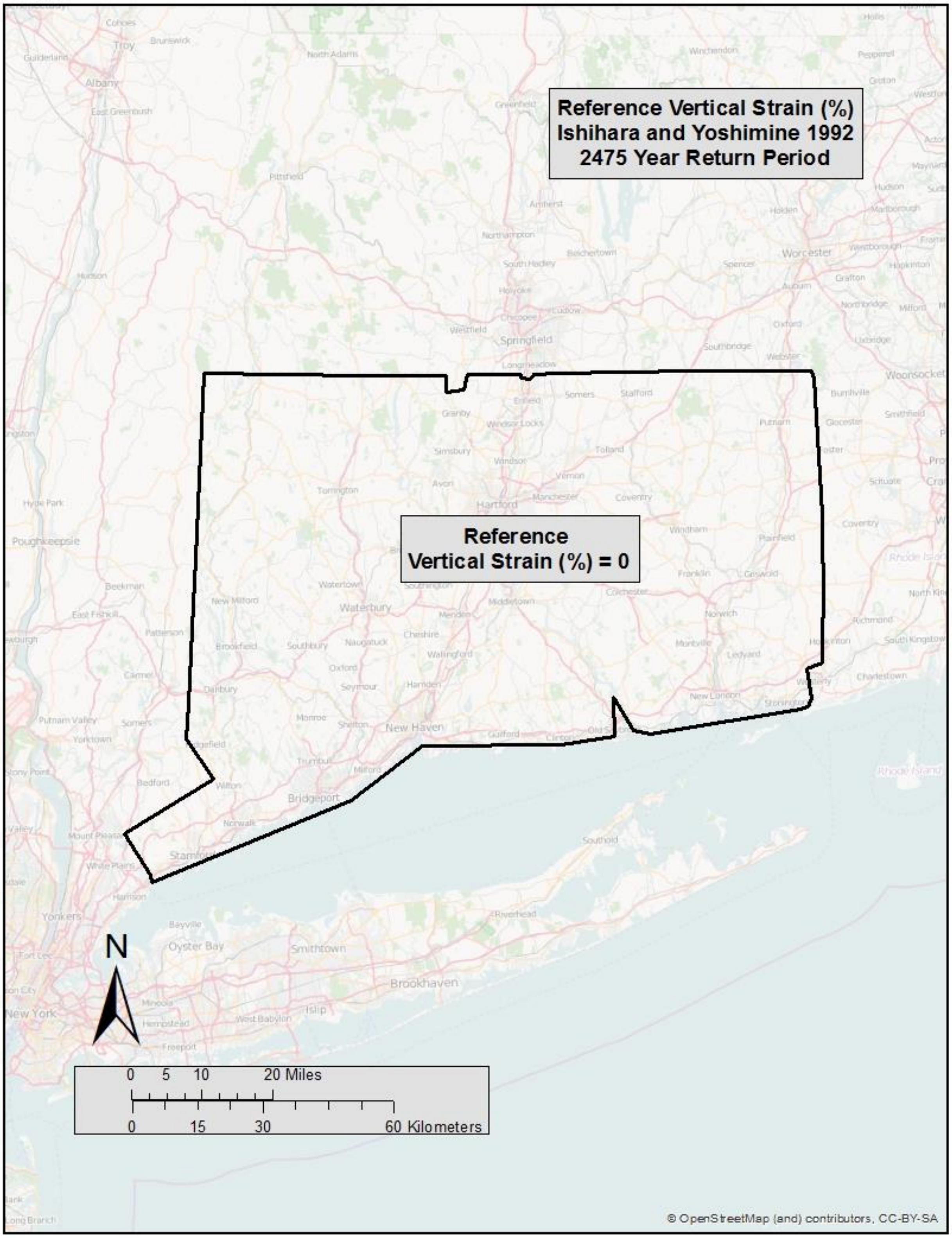

Figure A- 6 Ishihara and Yoshimine (1992) Post-Liquefaction Settlement (ε^{ref}) Map for Connecticut (Tr = 2,475)

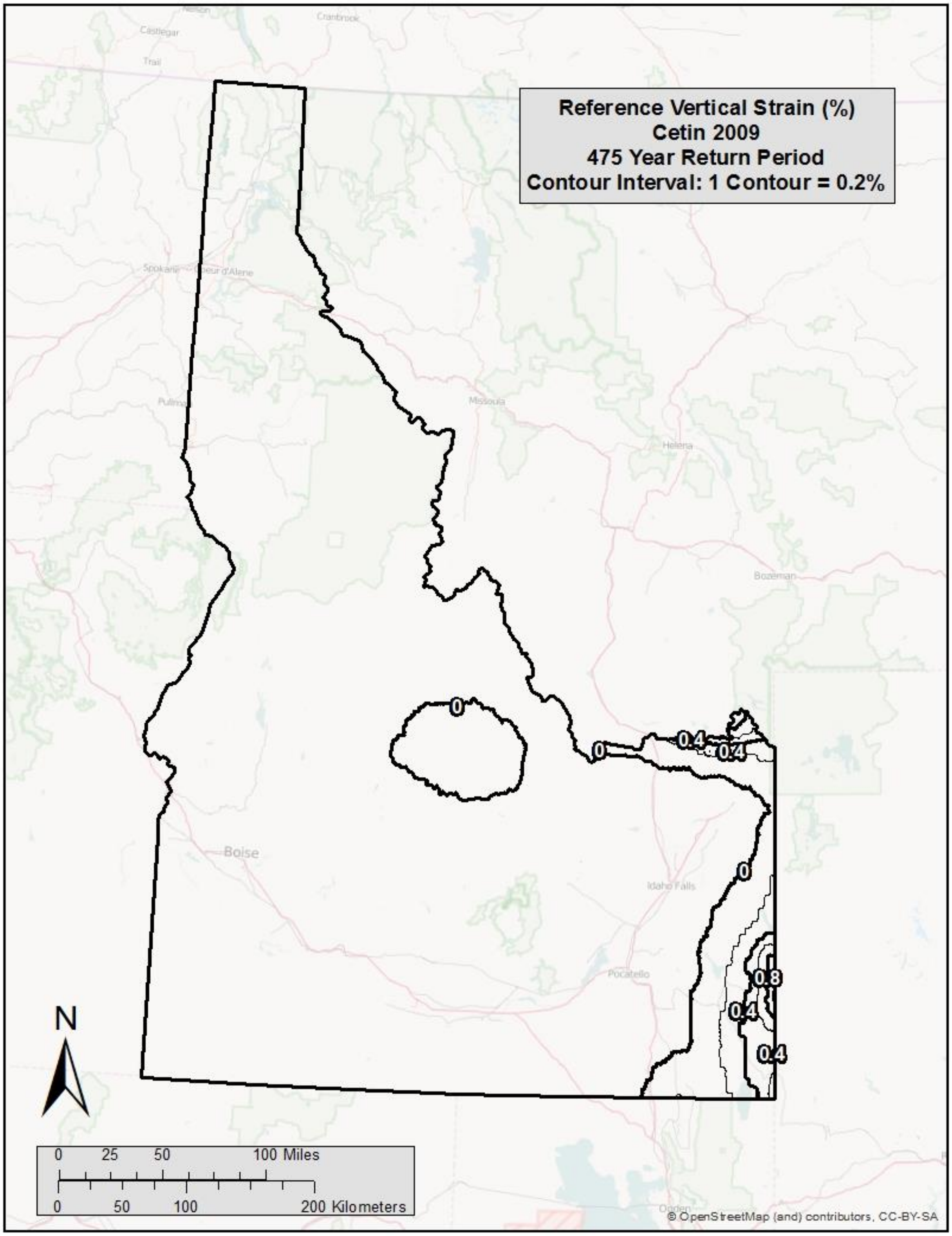

Figure A- 7 Cetin et al. (2009) Post-Liquefaction Settlement *(ε^{ref})* Map for Idaho (Tr = 475)

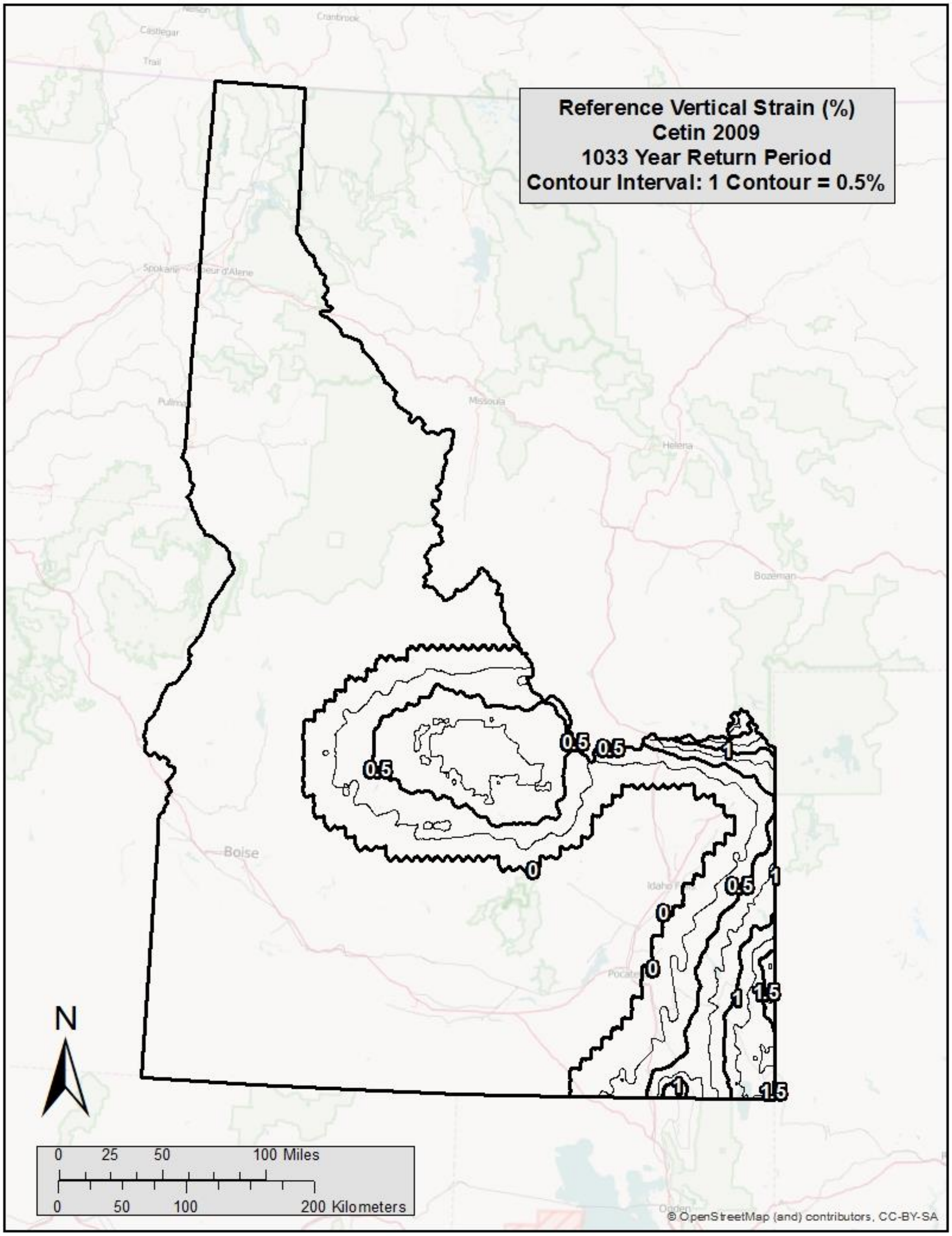

Figure A- 8 Cetin et al. (2009) Post-Liquefaction Settlement (ε^{ref}) **Map for Idaho (Tr=1,033)**

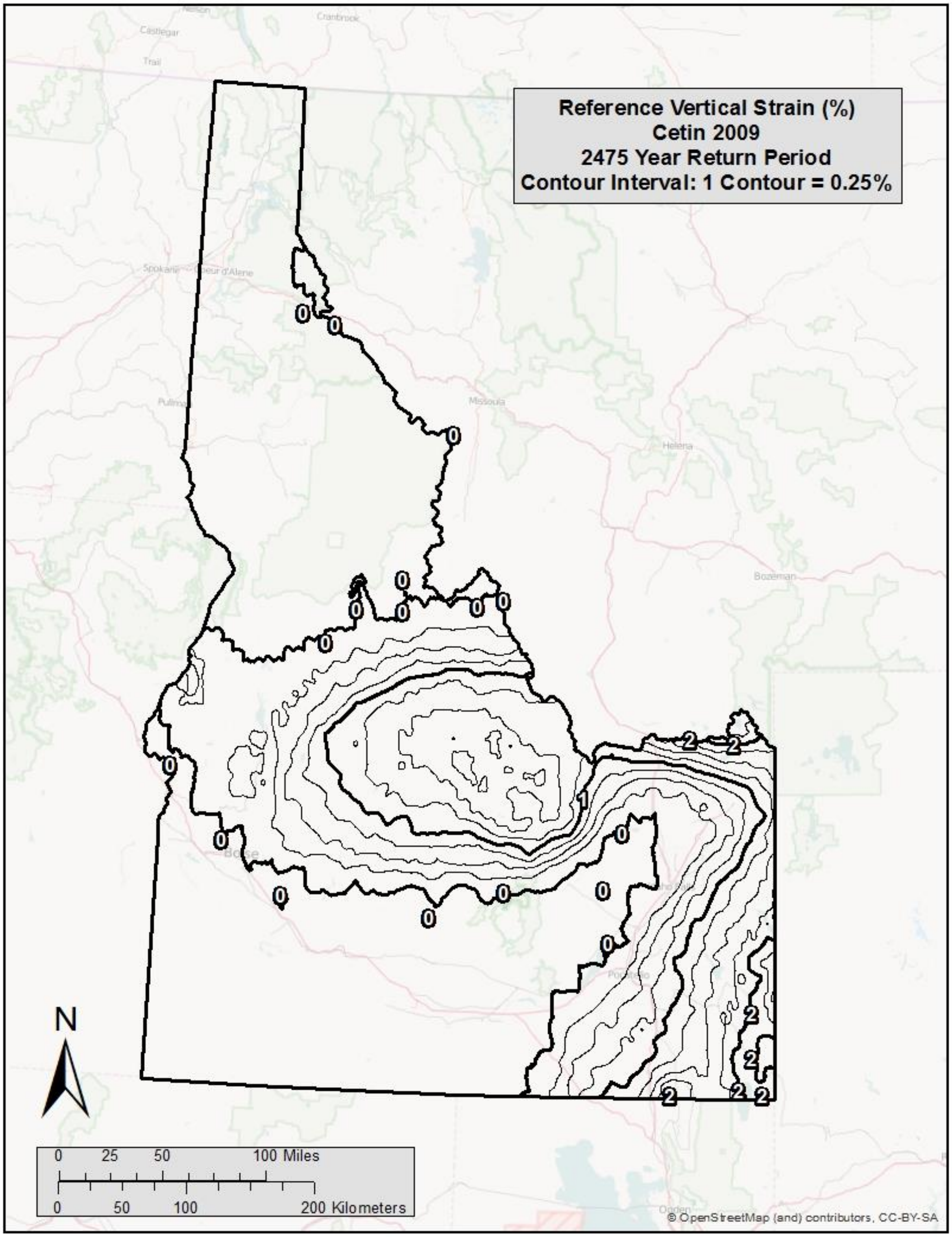

Figure A- 9 Cetin et al. (2009) Post-Liquefaction Settlement *(ε^{ref})* Map for Idaho (Tr=2,475)

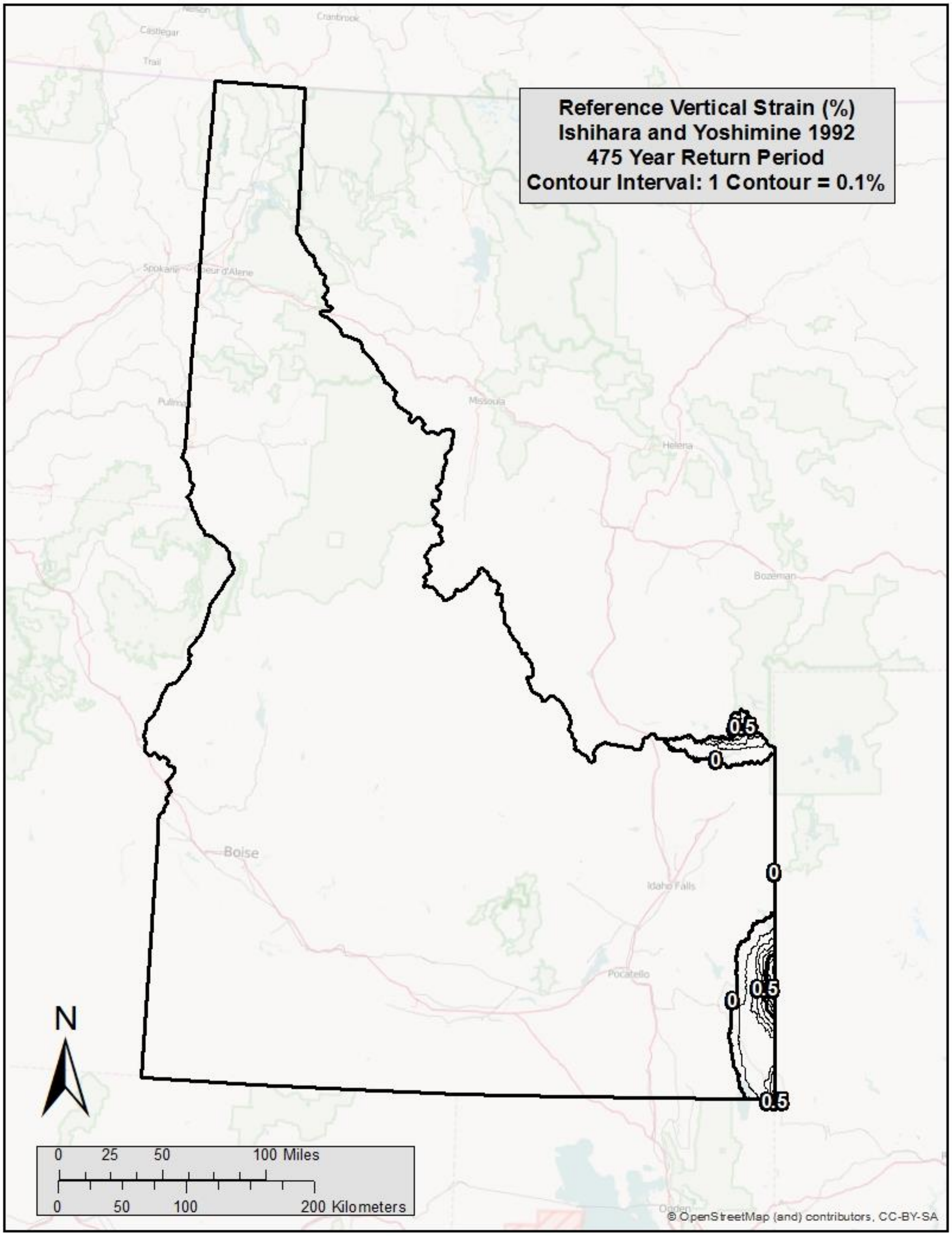

Figure A- 10 Ishihara and Yoshimine (1992) Post-Liquefaction Settlement *(ε^{ref})* Map for Idaho (Tr = 475)

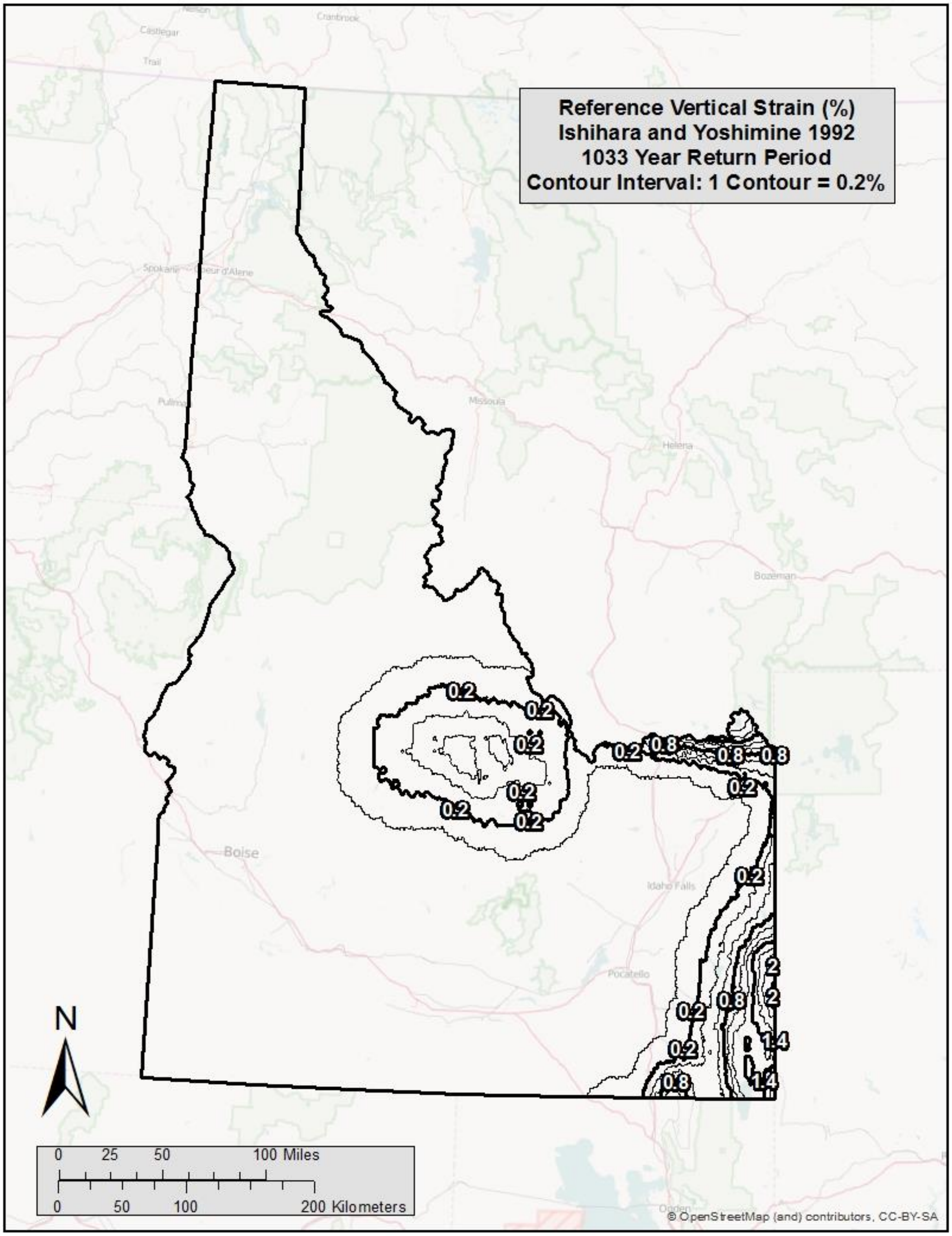

Figure A- 11 Ishihara and Yoshimine (1992) Post-Liquefaction Settlement *(ε^{ref})* Map for Idaho (Tr = 1,033)

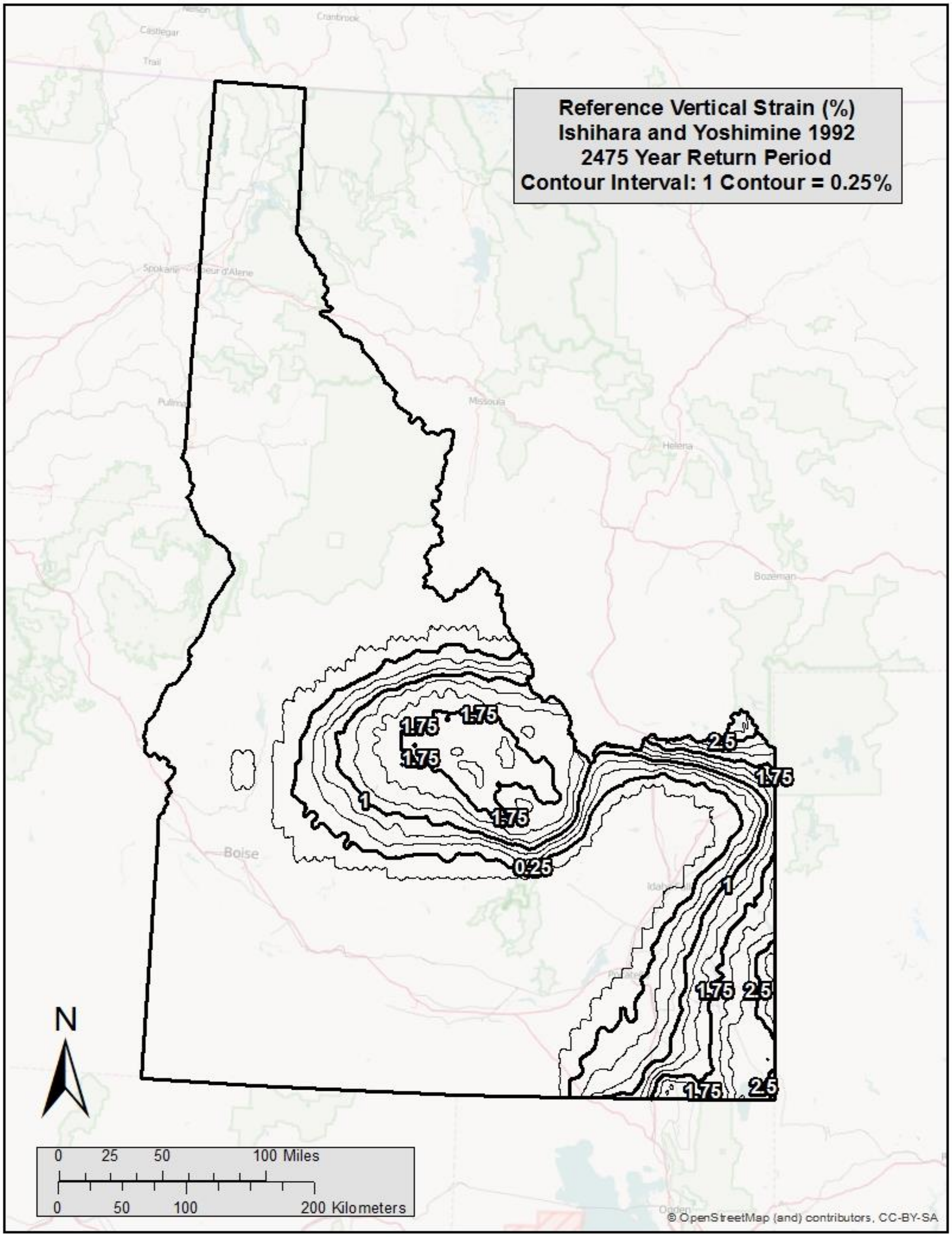

Figure A- 12 Ishihara and Yoshimine (1992) Post-Liquefaction Settlement *(ε^{ref})* Map for Idaho (Tr = 2,475)

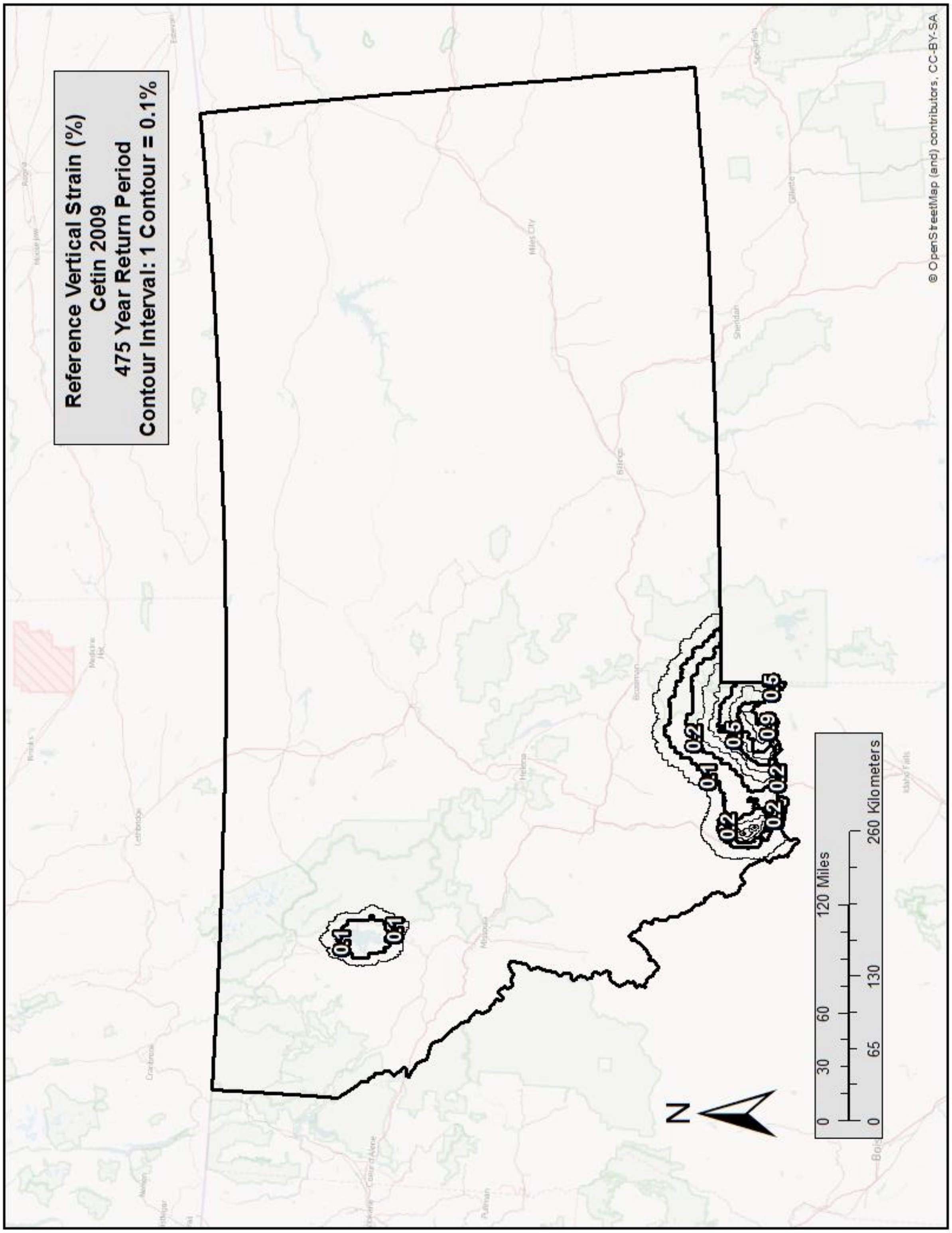

Figure A- 13 Cetin et al. (2009) Post-Liquefaction Settlement *(ε^{ref})* Map for Montana (Tr=475)

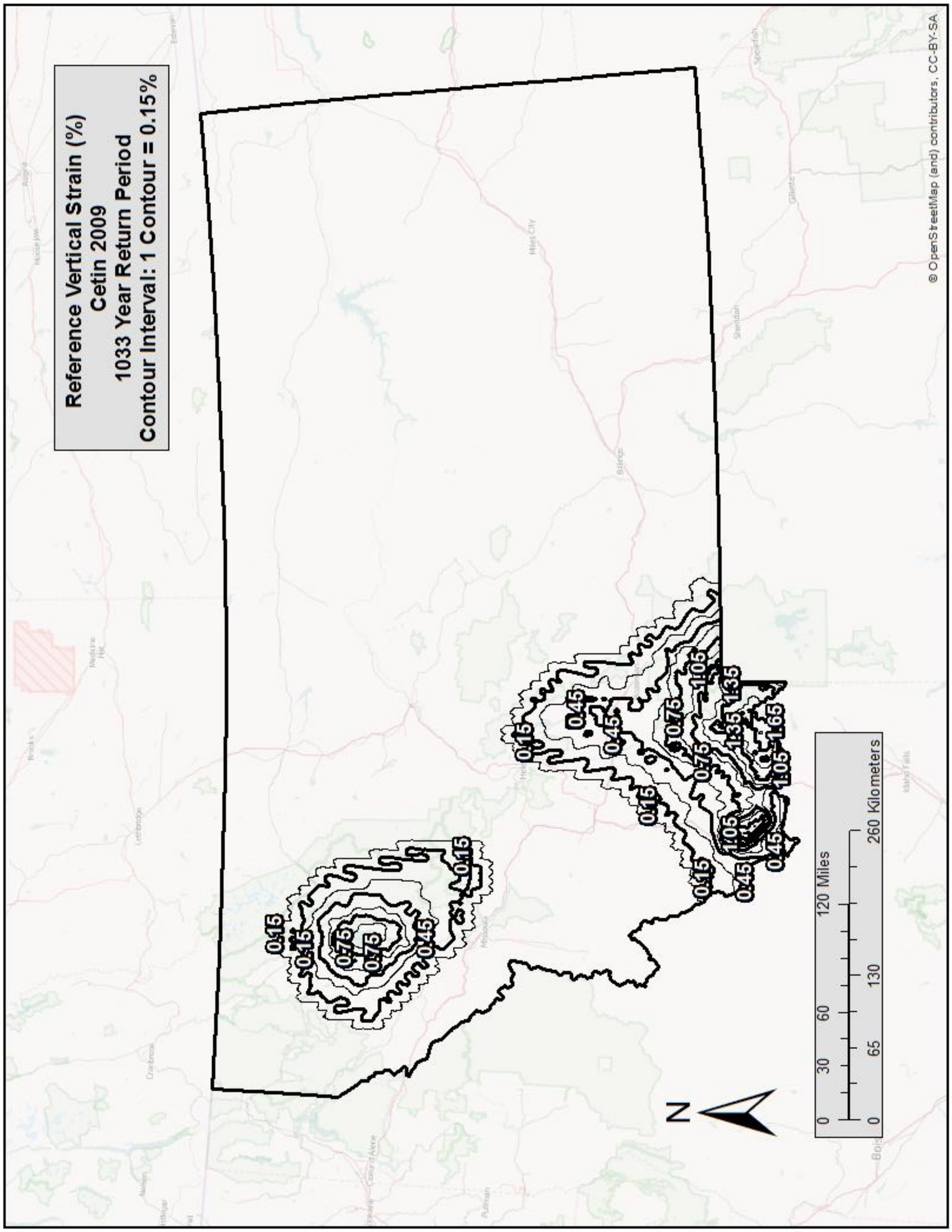

Figure A- 14 Cetin et al. (2009) Post-Liquefaction Settlement *(ε^{ref})* Map for Montana (Tr=1,033)

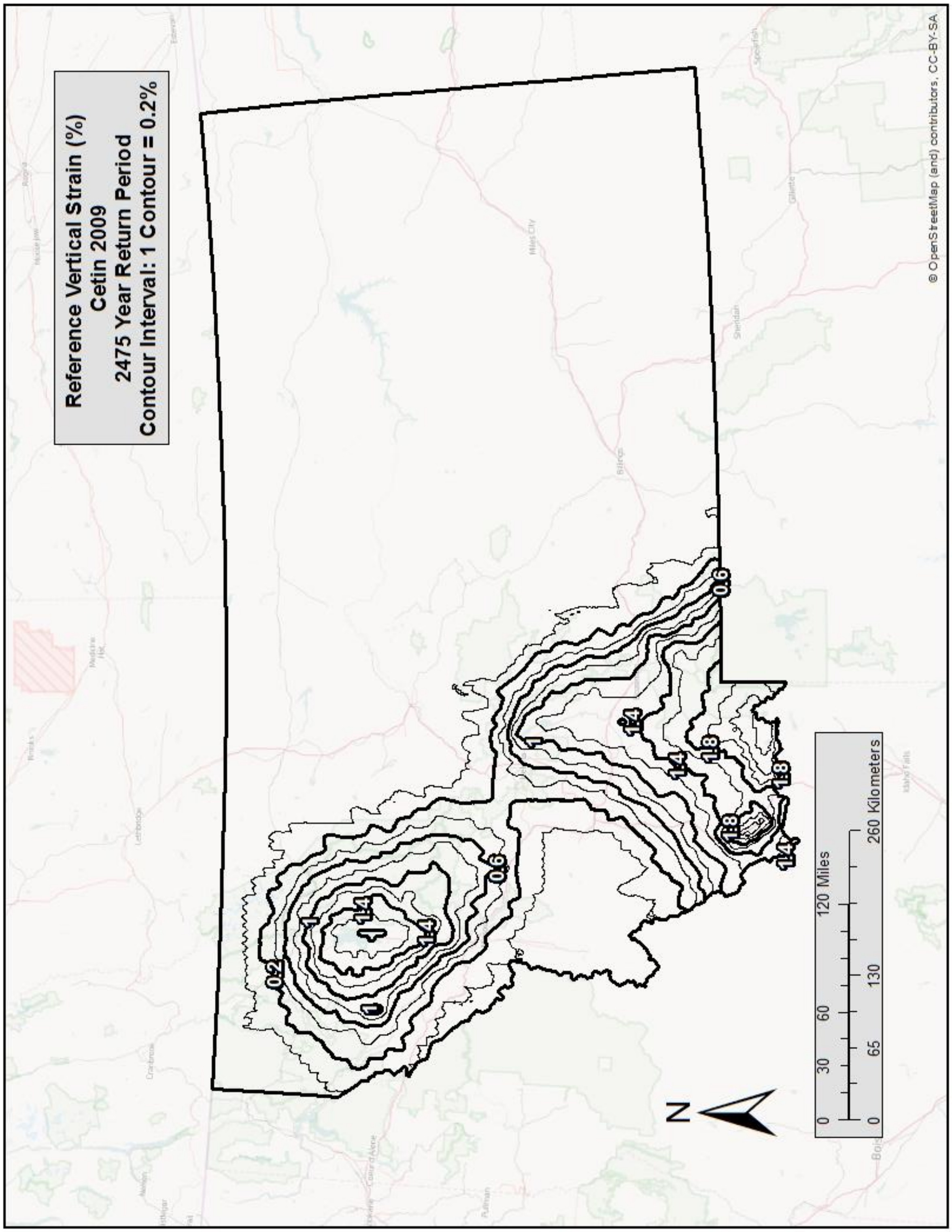

Figure A- 15 Cetin et al. (2009) Post-Liquefaction Settlement (ε^{ref}) **Map for Montana (Tr=2,475)**

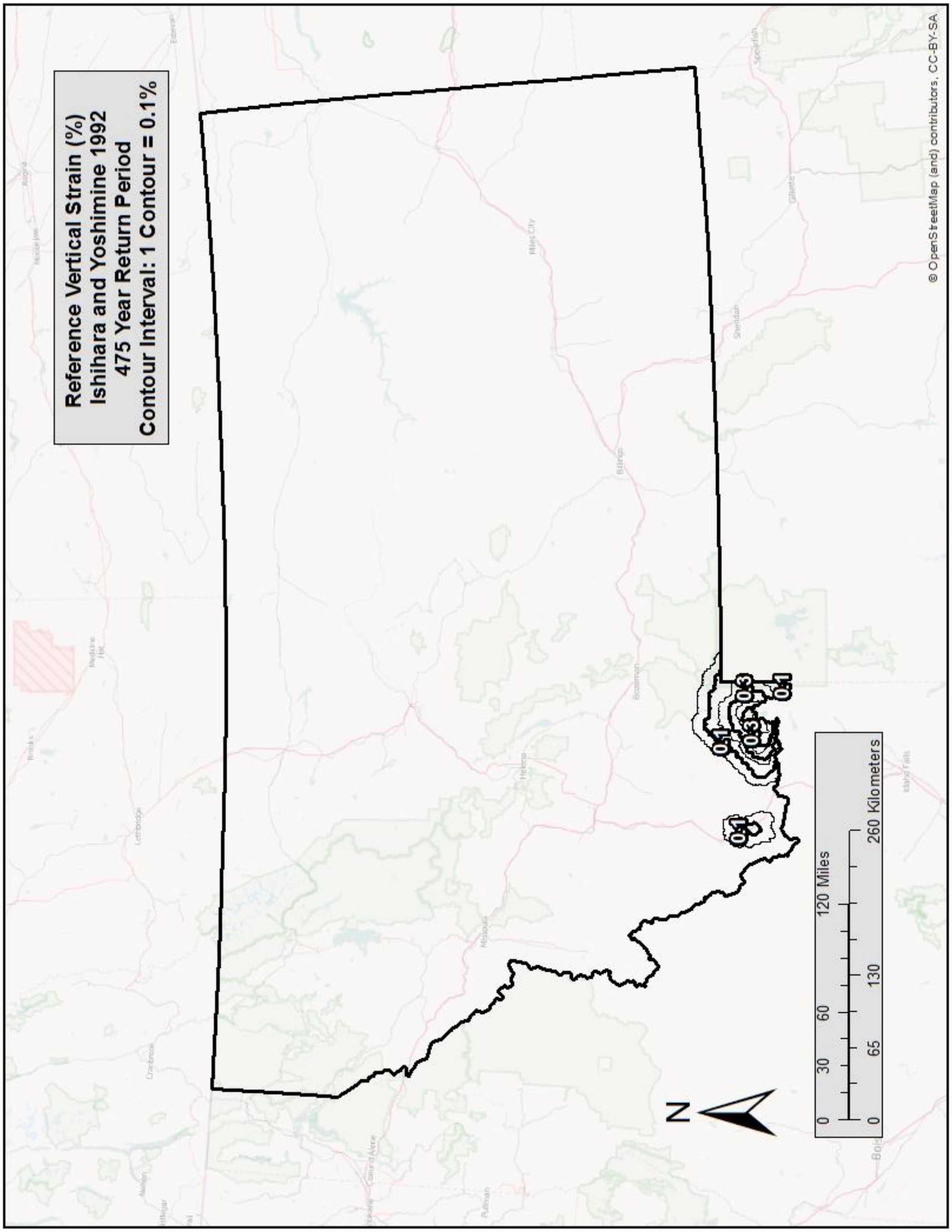

Figure A- 16 Ishihara and Yoshimine (1992) Post-Liquefaction Settlement *(ε^{ref})* Map for Montana (Tr = 475)

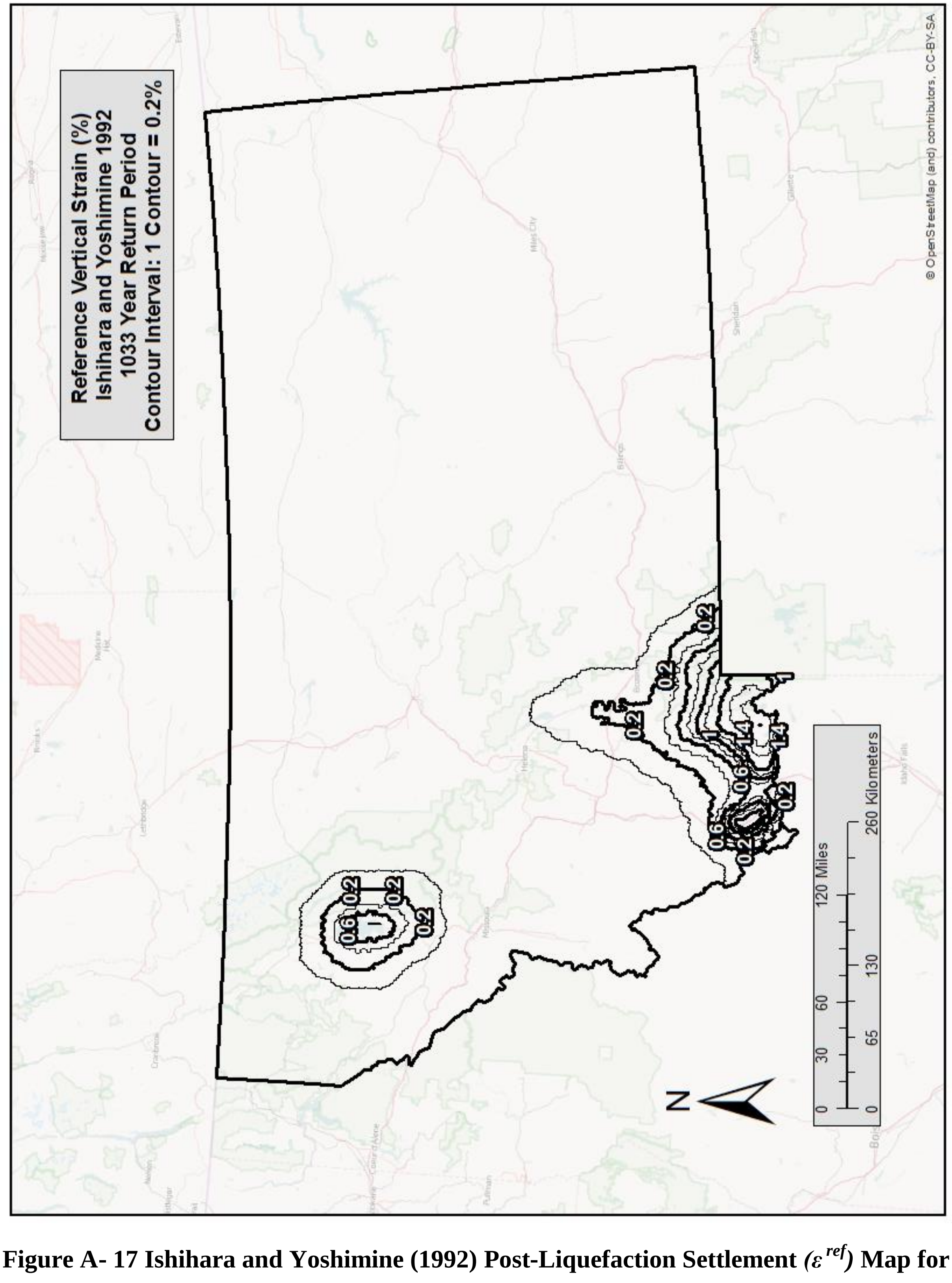

Figure A- 17 Ishihara and Yoshimine (1992) Post-Liquefaction Settlement *(ε^{ref})* Map for Montana (Tr = 1,033)

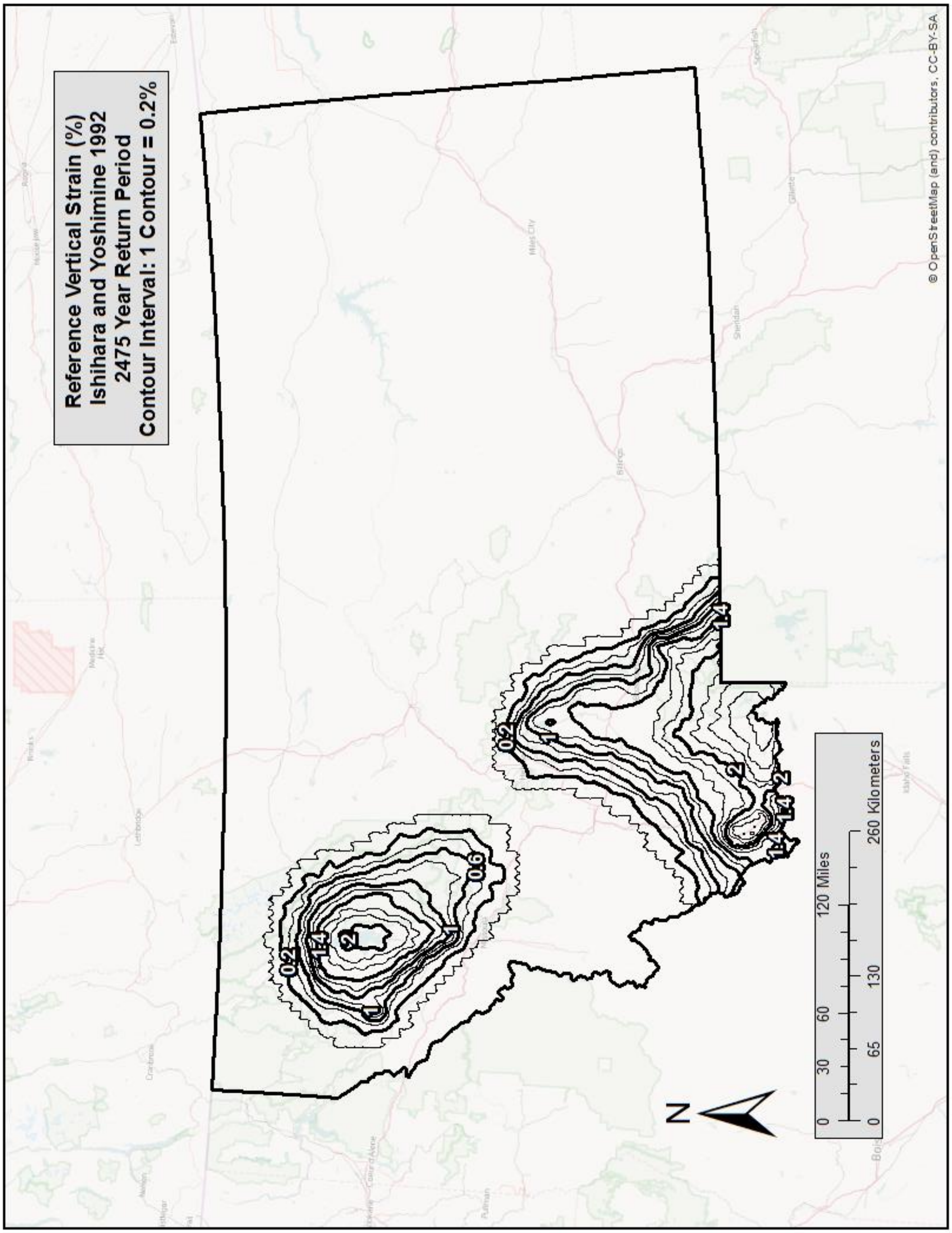

Figure A- 18 Ishihara and Yoshimine (1992) Post-Liquefaction Settlement *(ε^{ref})* Map for Montana (Tr = 2,475)

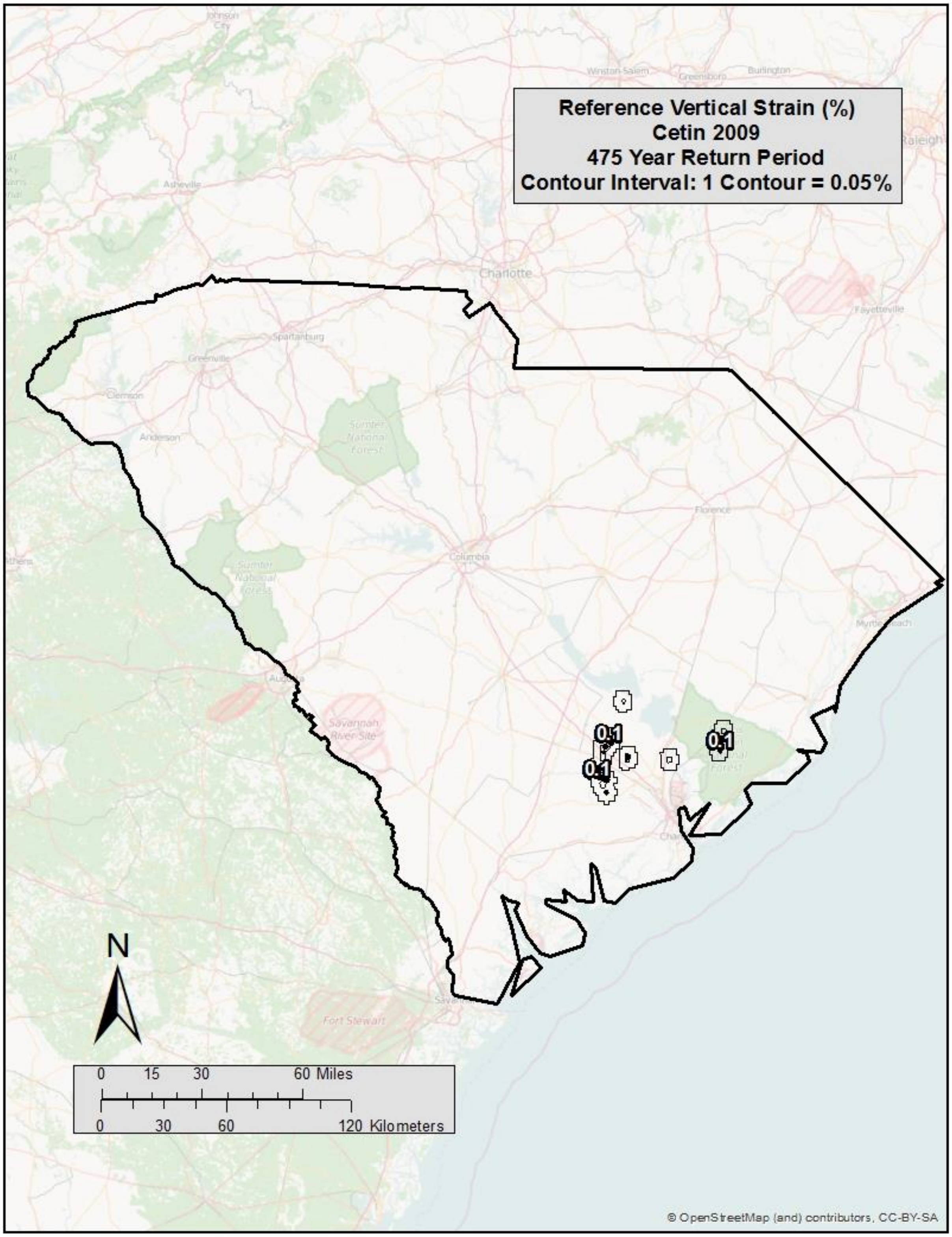

Figure A- 19 Cetin et al. (2009) Post-Liquefaction Settlement *(ε^{ref})* Map for South Carolina (Tr = 475)

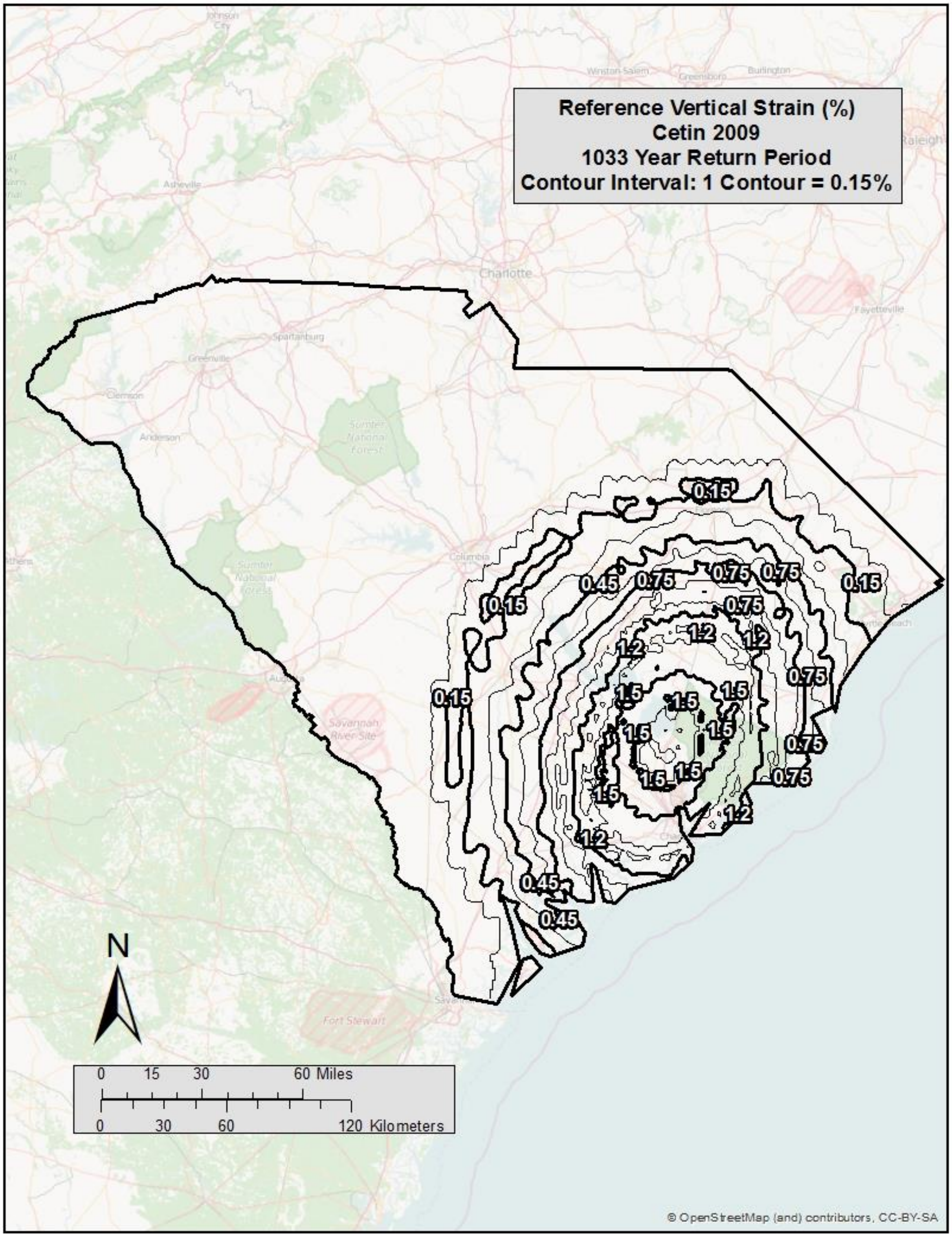

Figure A- 20 Cetin et al. (2009) Post-Liquefaction Settlement *(ε^{ref})* Map for South Carolina (Tr = 1,033)

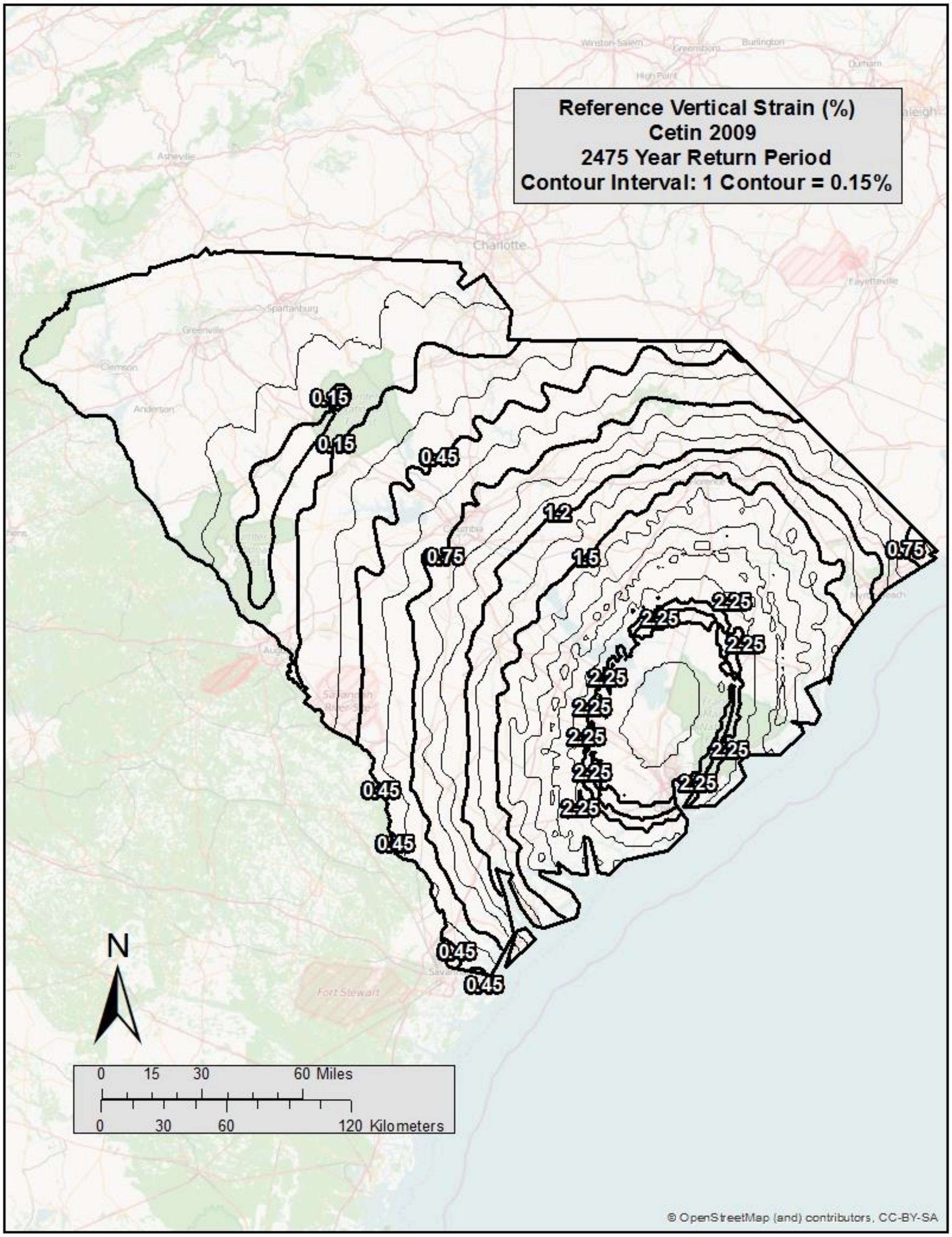

Figure A- 21 Cetin et al. (2009) Post-Liquefaction Settlement (ε^{ref}) Map for South Carolina (Tr = 2,475)

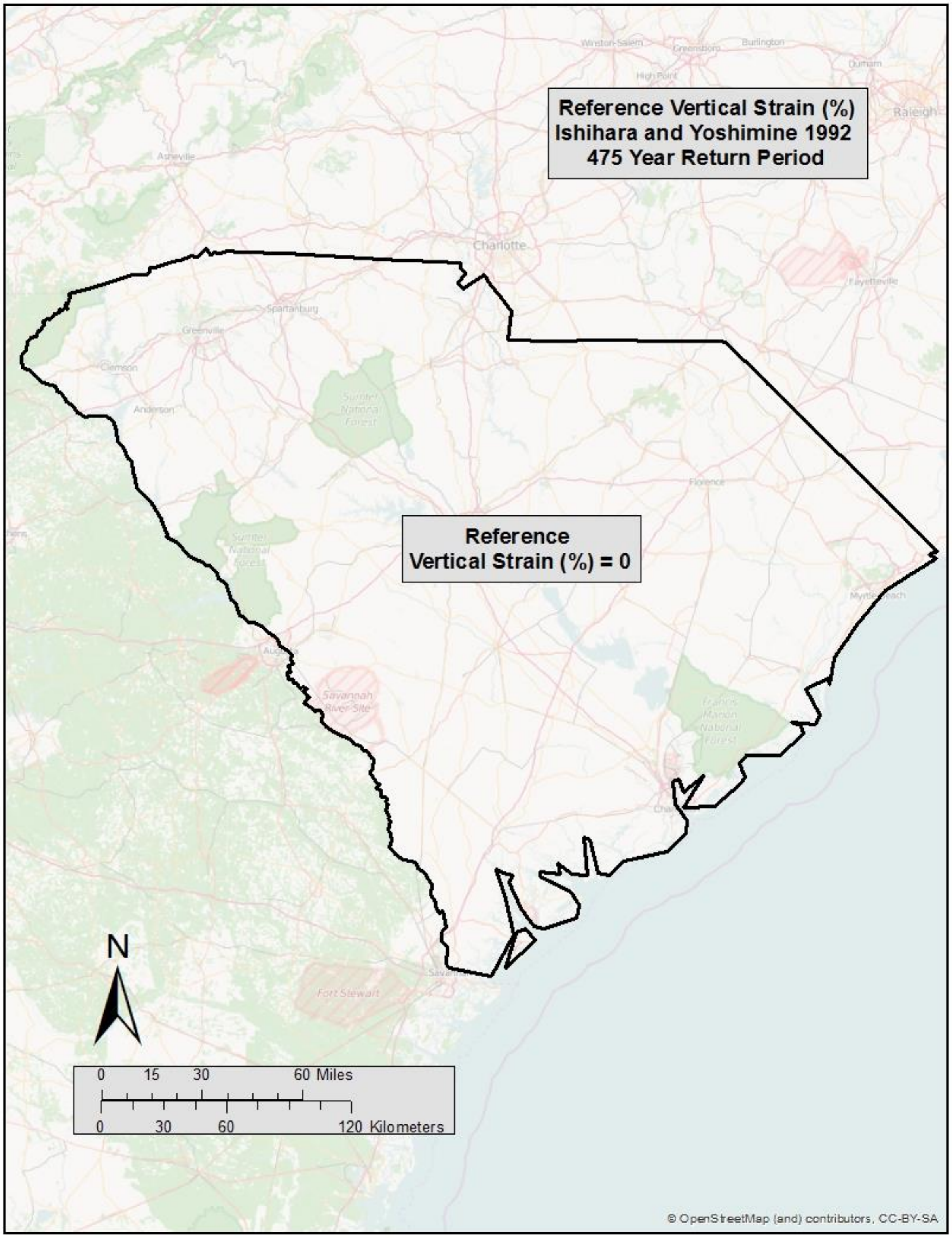

Figure A- 22 Ishihara and Yoshimine (1992) Post-Liquefaction Settlement *(ε^{ref})* Map for South Carolina (Tr = 475)

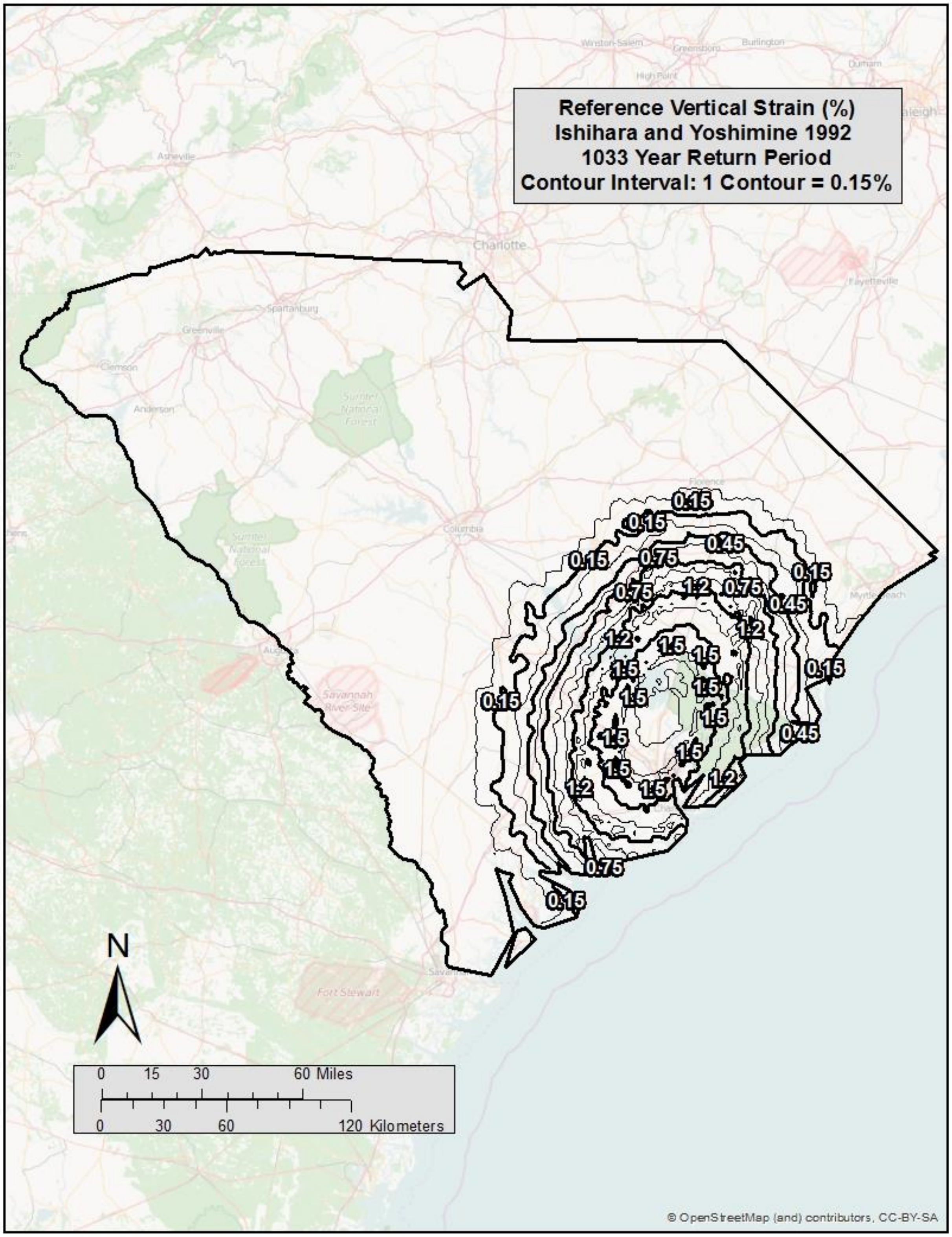

Figure A- 23 Ishihara and Yoshimine (1992) Post-Liquefaction Settlement *(ε^{ref})* Map for South Carolina (Tr = 1,033)

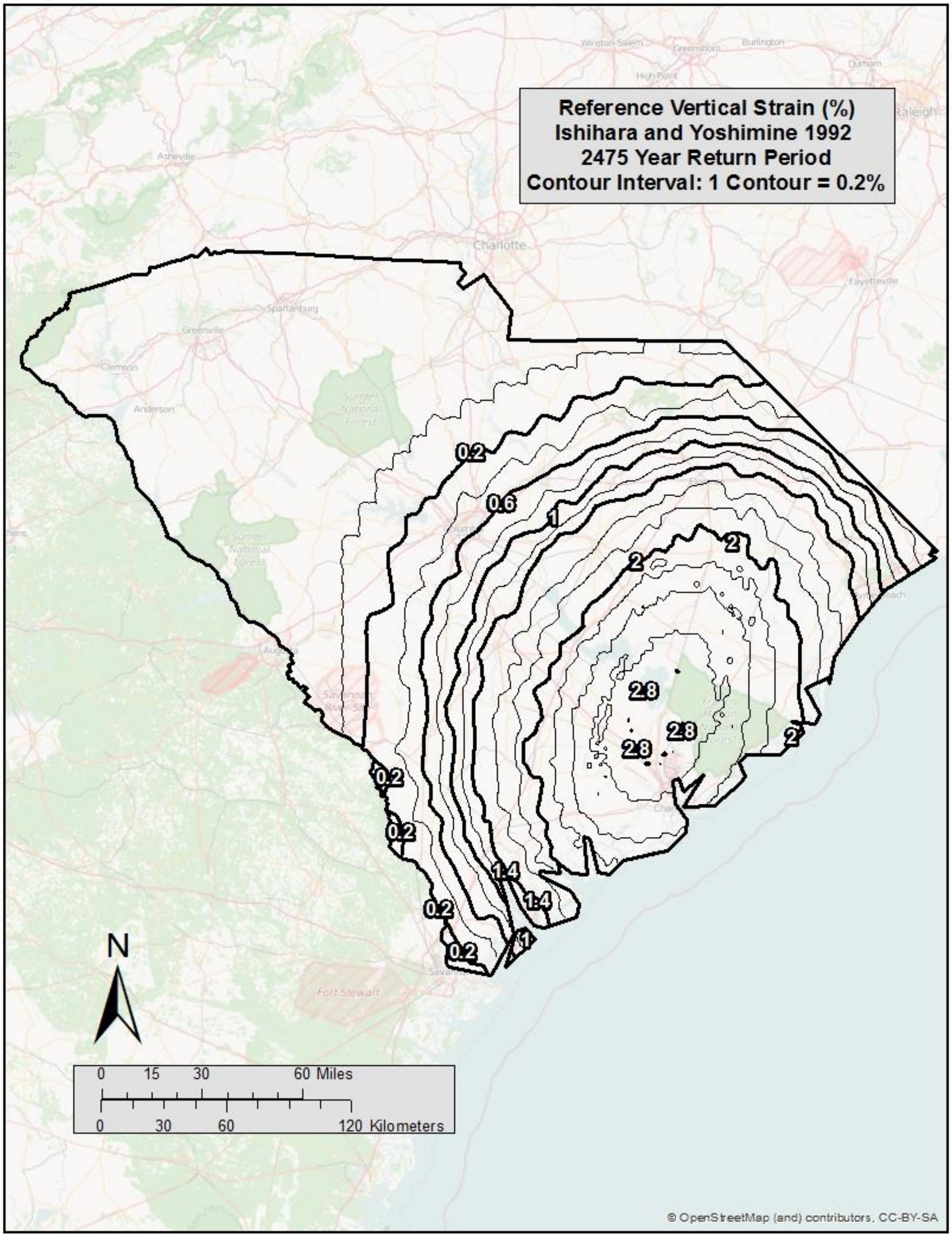

Figure A- 24 Ishihara and Yoshimine (1992) Post-Liquefaction Settlement (ε^{ref}) Map for South Carolina (Tr = 2,475)

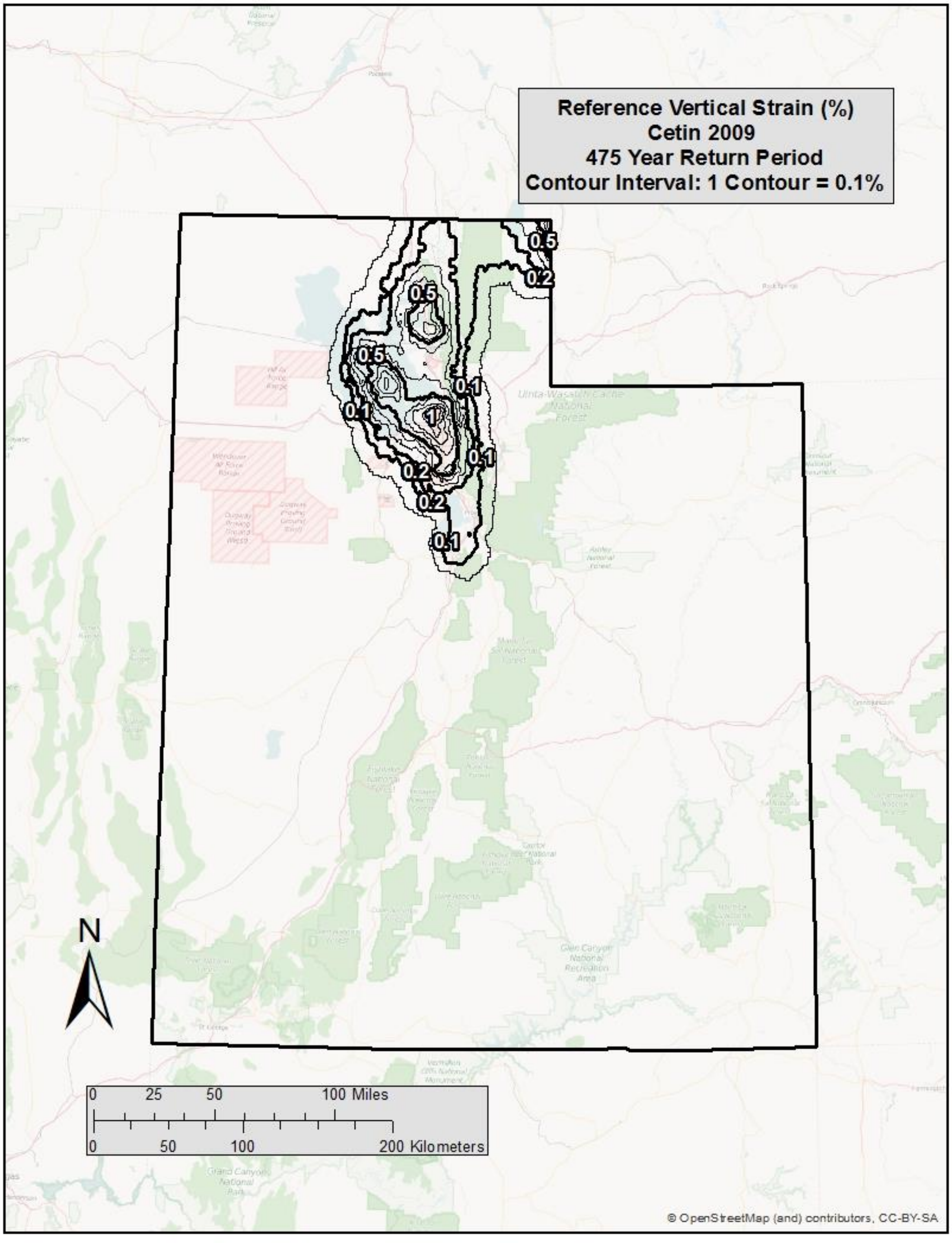

Figure A- 25 Cetin et al. (2009) Post-Liquefaction Settlement *(ε^{ref})* Map for Utah (Tr = 475)

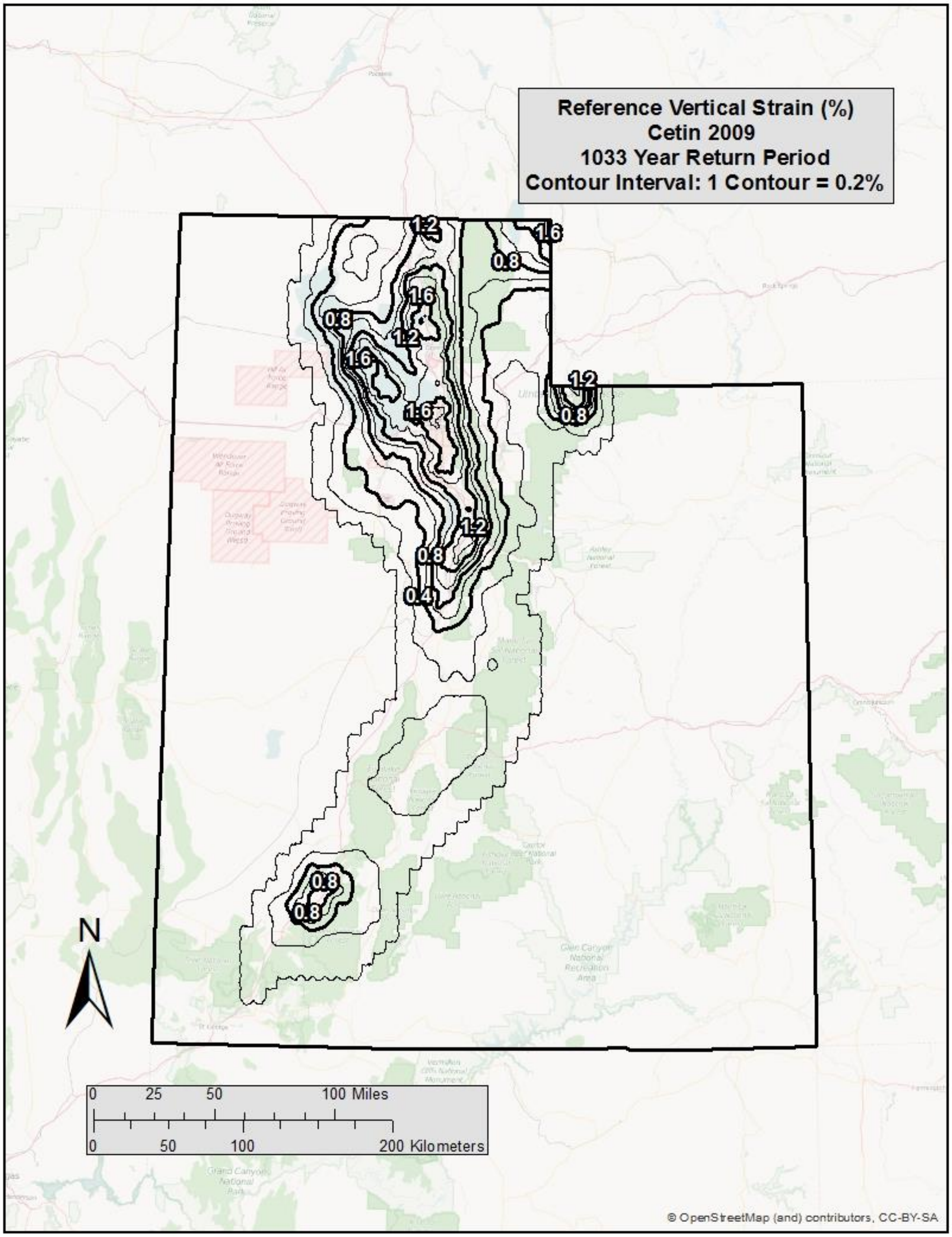

Figure A- 26 Cetin et al. (2009) Post-Liquefaction Settlement *(ε^{ref})* Map for Utah (Tr=1,033)

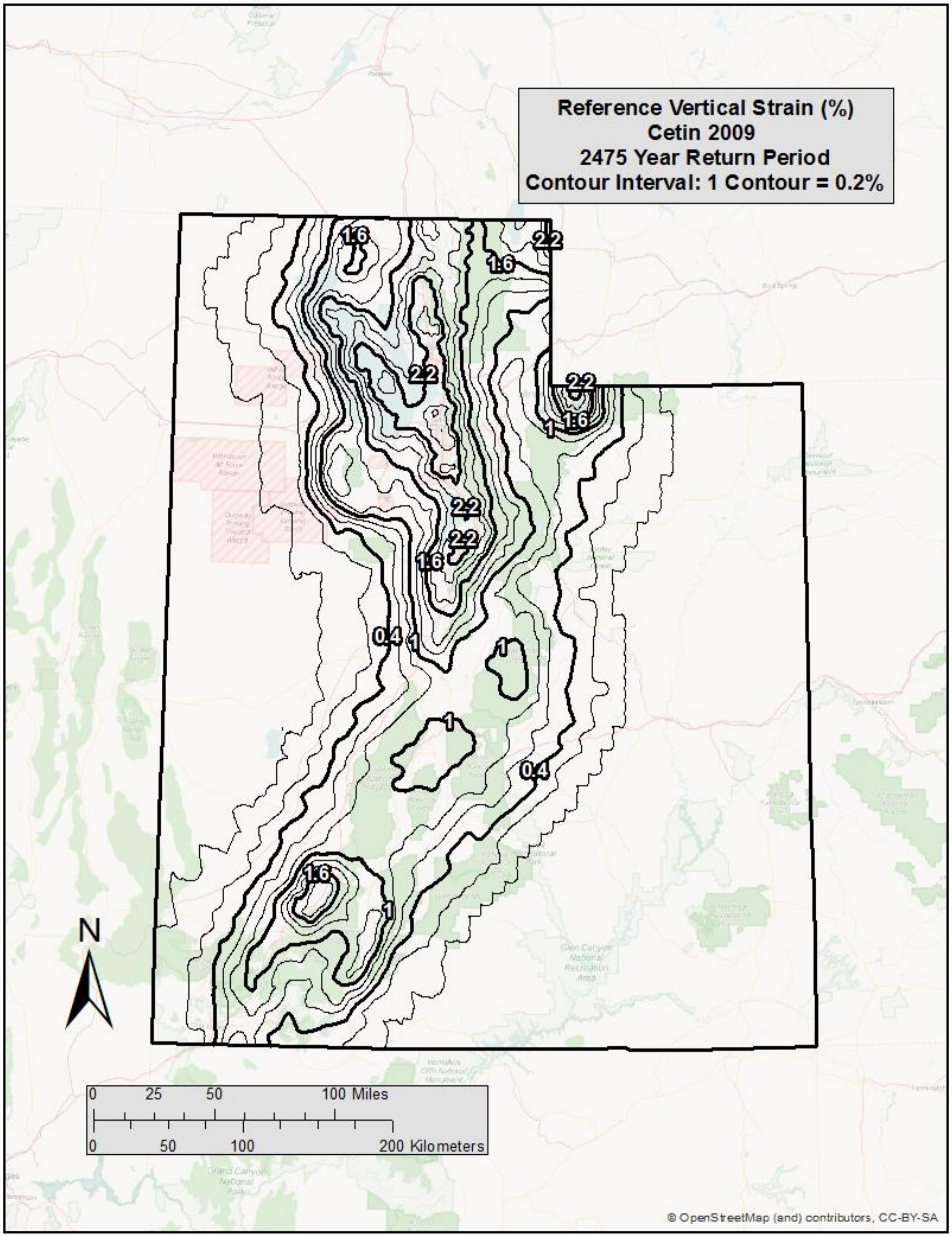

Figure A- 27 Cetin et al. (2009) Post-Liquefaction Settlement *(ε^{ref})* Map for Utah (Tr=2,475)

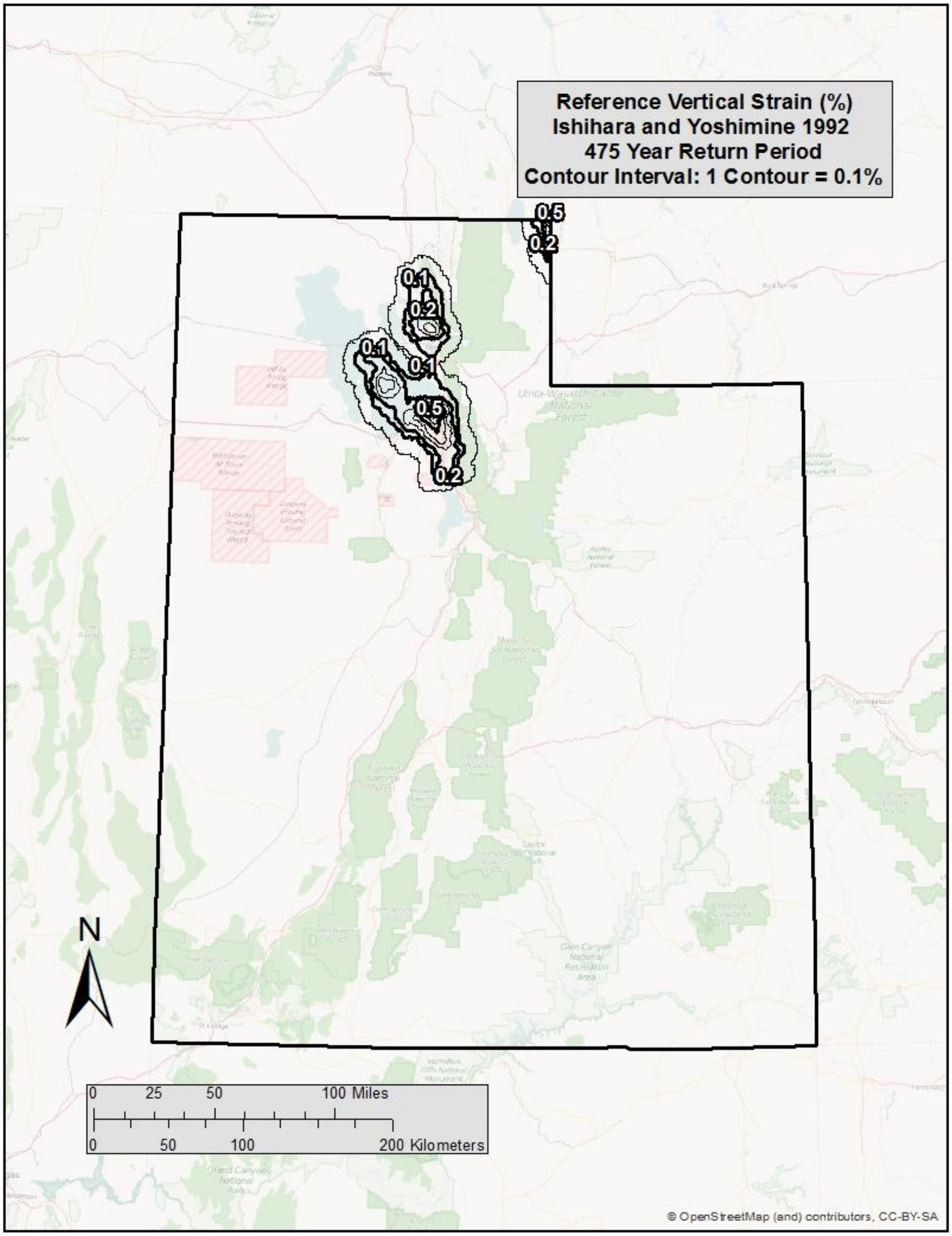

Figure A- 28 Ishihara and Yoshimine (1992) Post-Liquefaction Settlement *(ε^{ref})* Map for Utah (Tr = 475)

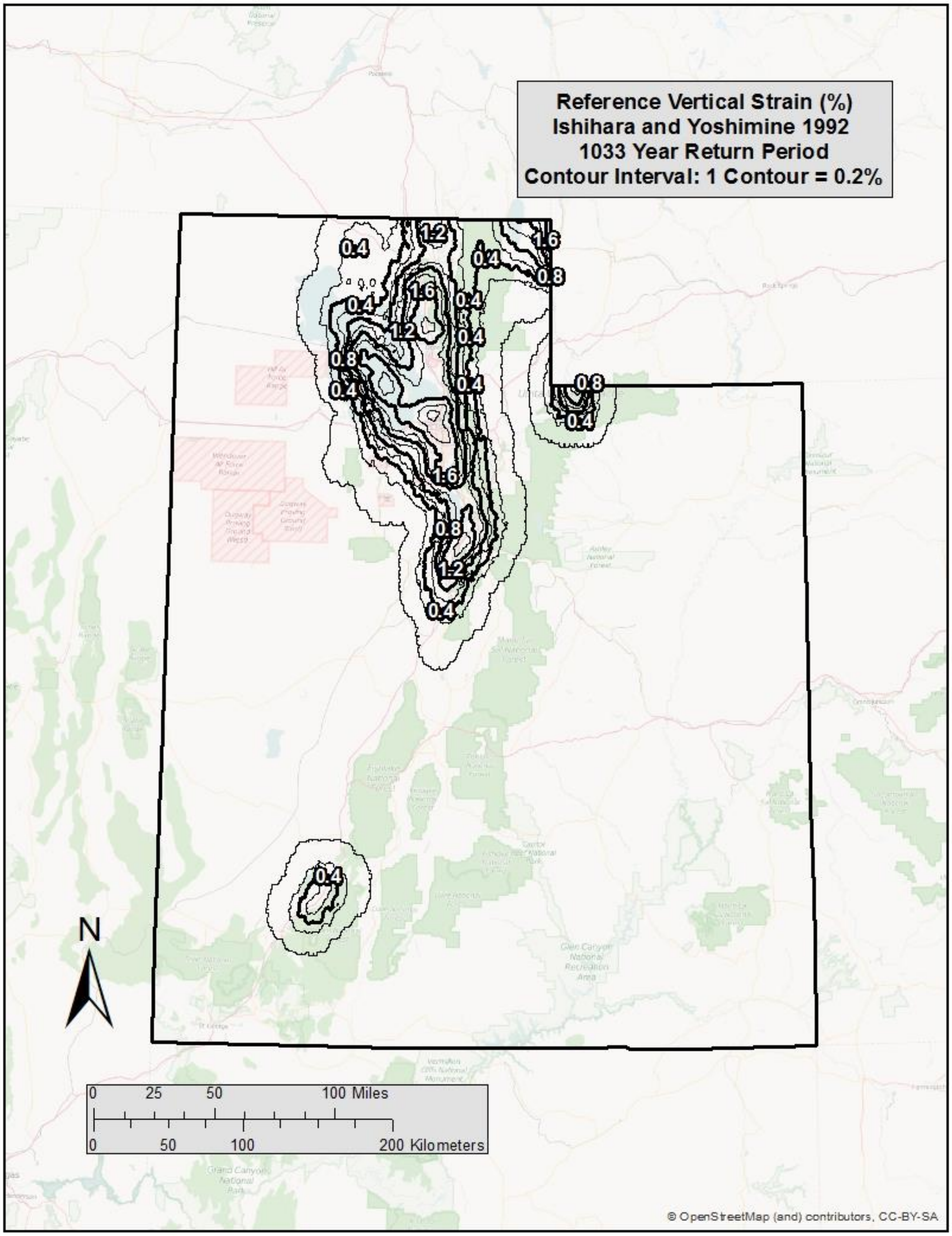

Figure A- 29 Ishihara and Yoshimine (1992) Post-Liquefaction Settlement *(ε^{ref})* Map for Utah (Tr = 1,033)

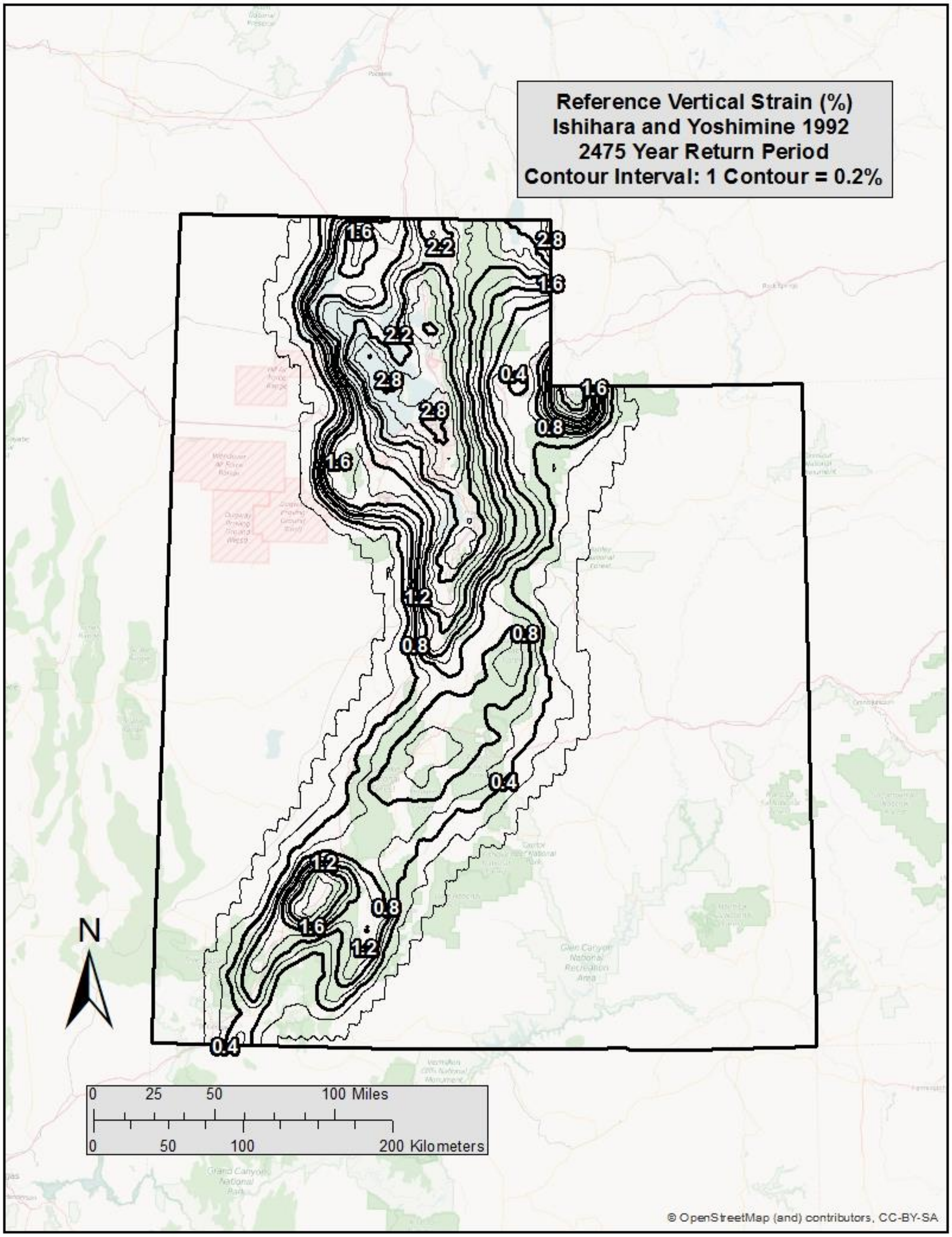

Figure A- 30 Ishihara and Yoshimine (1992) Post-Liquefaction Settlement *(ε^{ref})* Map for Utah (Tr = 2,475)

APPENDIX B: Sample Seismic Slope Displacement Maps

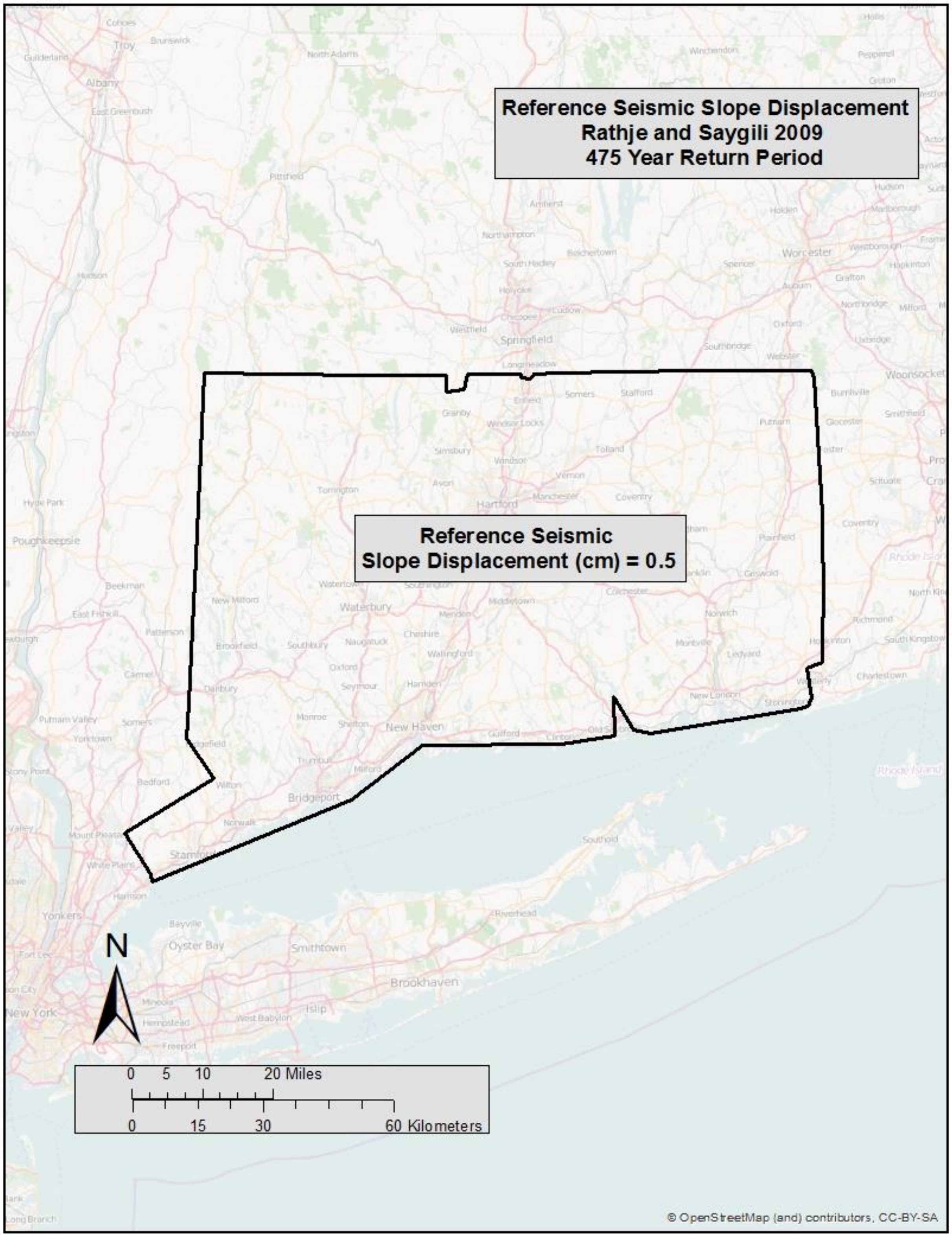

Figure B- 1 Rathje and Saygili (2009) Seismic Slope Displacement *(D^{ref})* Map for Connecticut (Tr = 475)

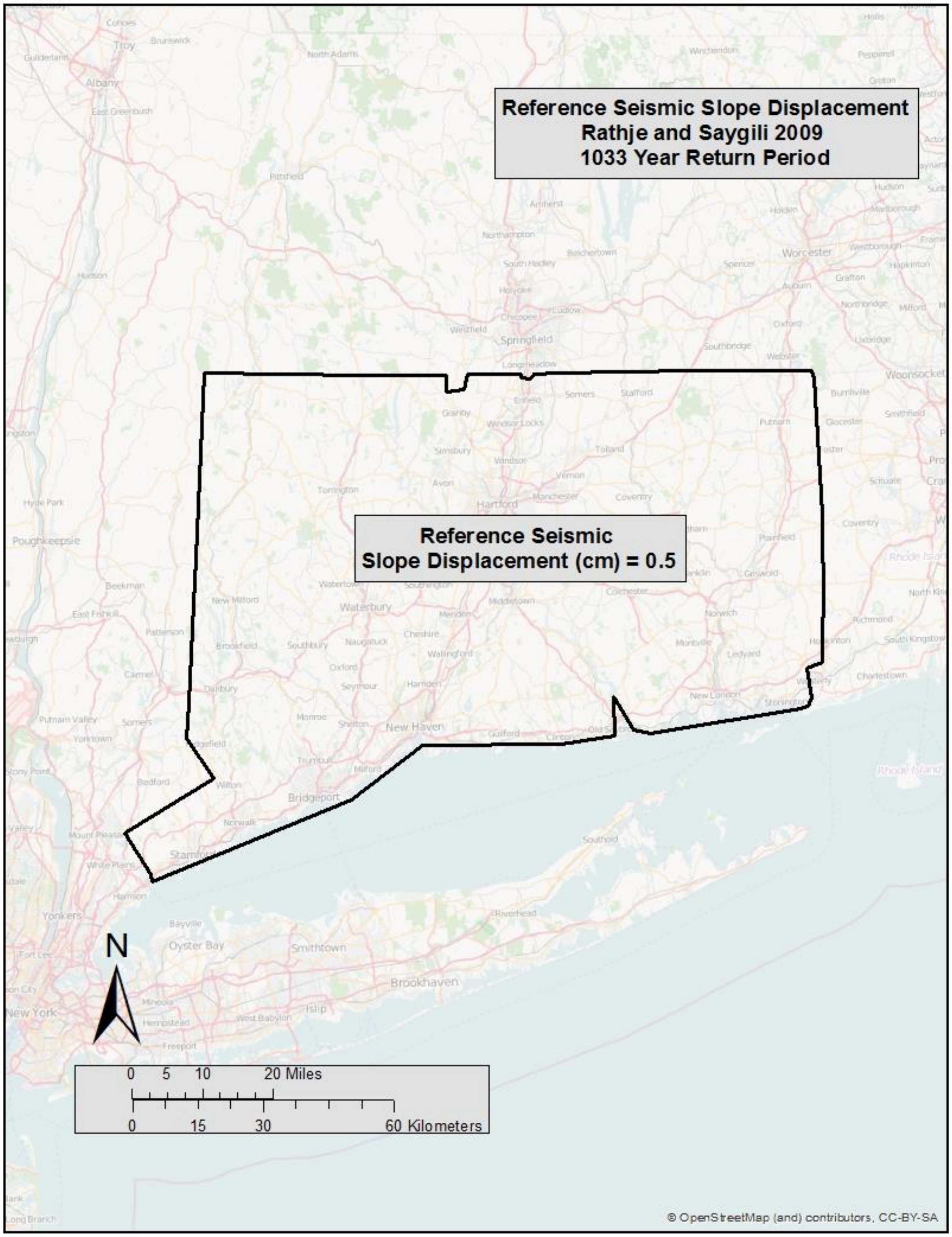

Figure B- 2 Rathje and Saygili (2009) Seismic Slope Displacement *(D^{ref})* Map for Connecticut (Tr = 1,033)

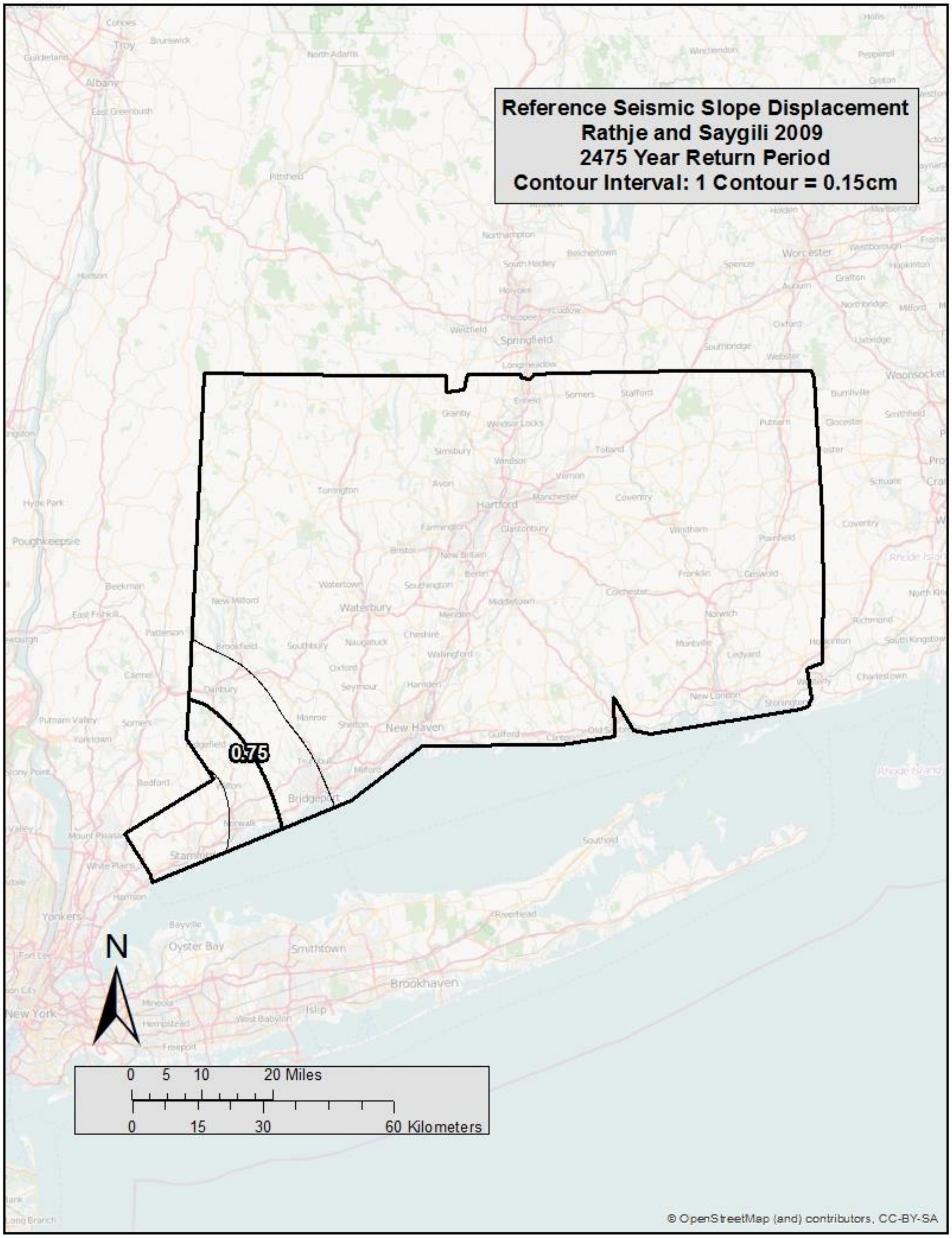

Figure B- 3 Rathje and Saygili (2009) Seismic Slope Displacement *(D^{ref})* Map for Connecticut (Tr = 2,475)

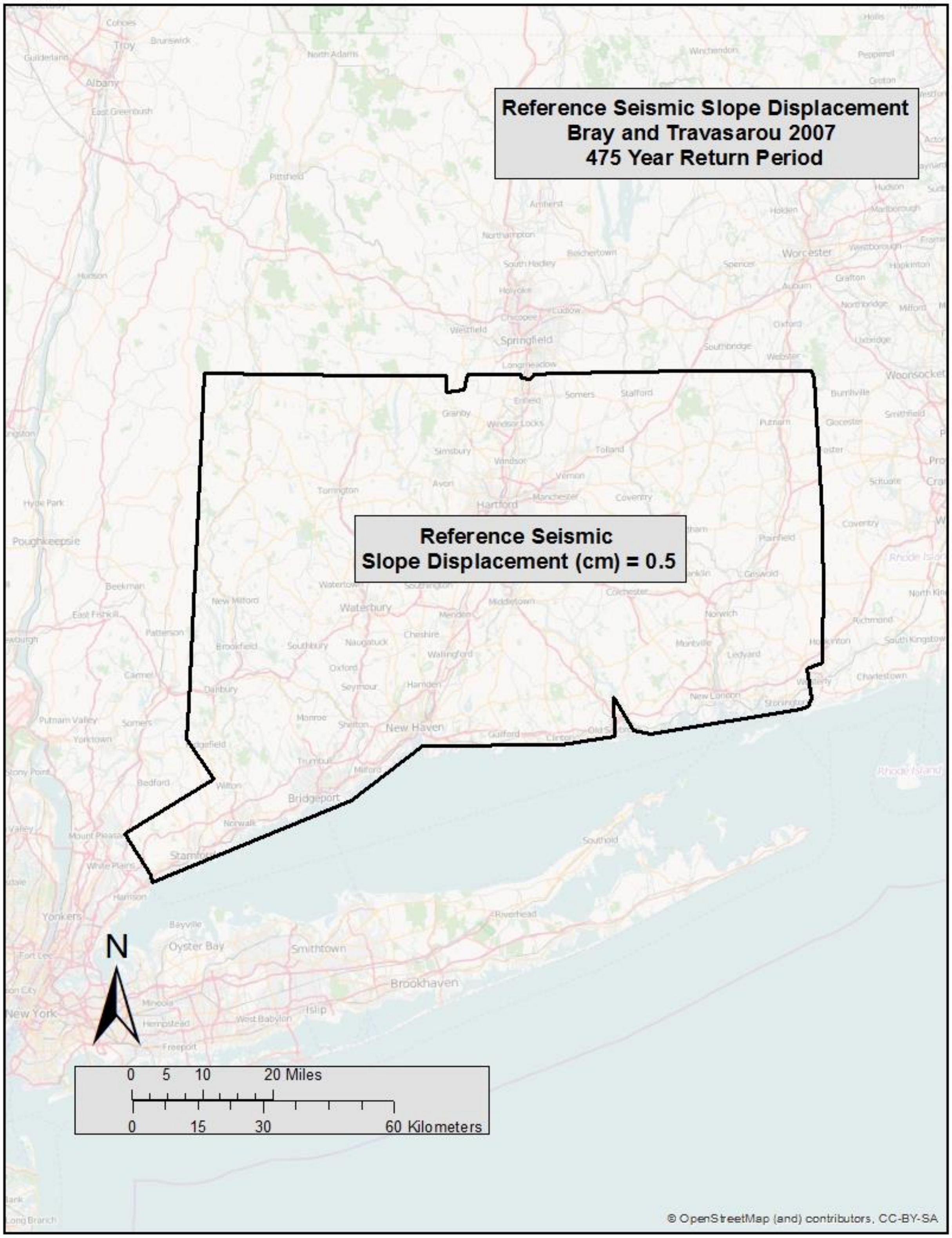

Figure B- 4 Bray and Travasarou (2007) Seismic Slope Displacement *(D^{ref})* Map for Connecticut (Tr = 475)

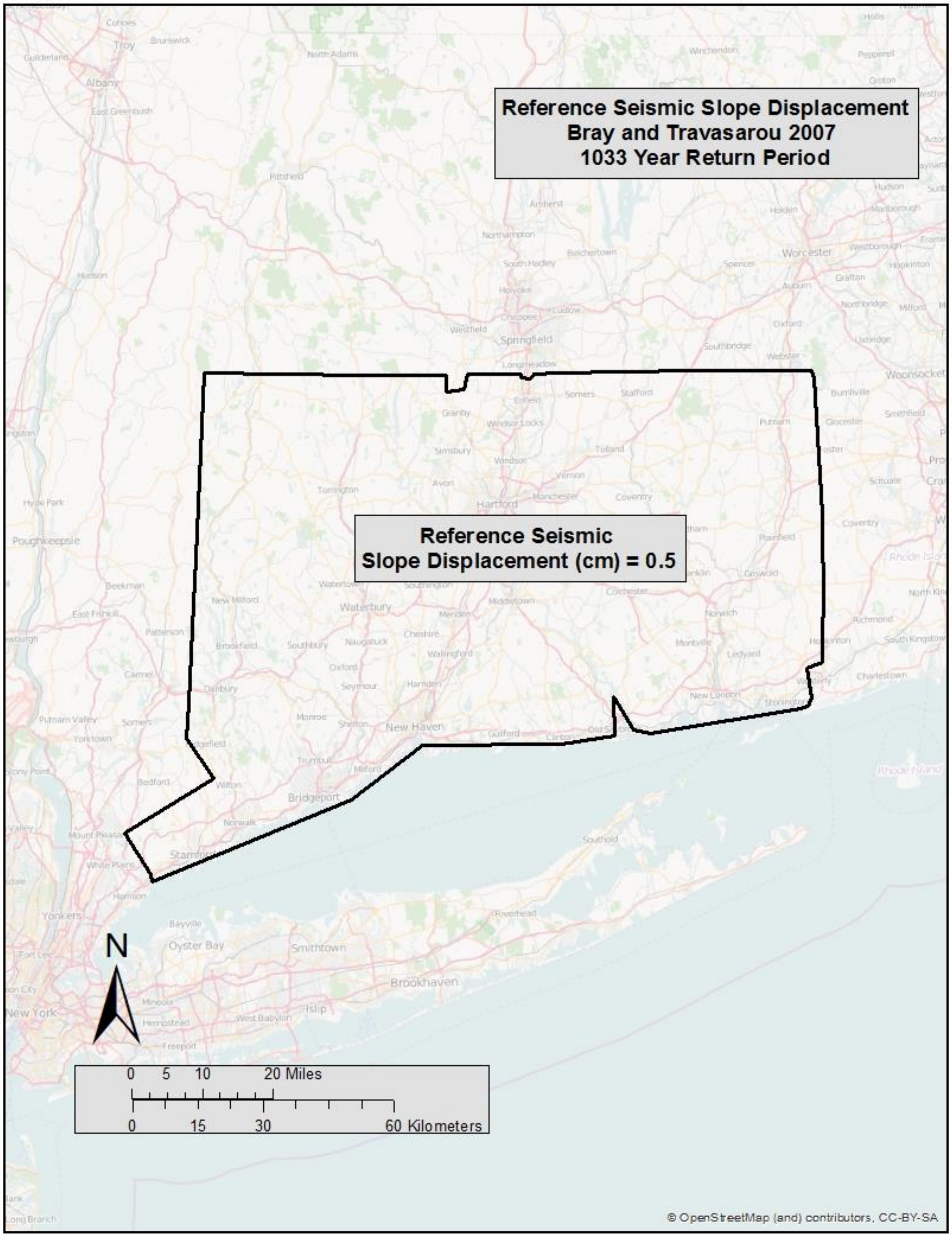

Figure B- 5 Bray and Travasarou (2007) Seismic Slope Displacement *(D^{ref})* Map for Connecticut (Tr = 1,033)

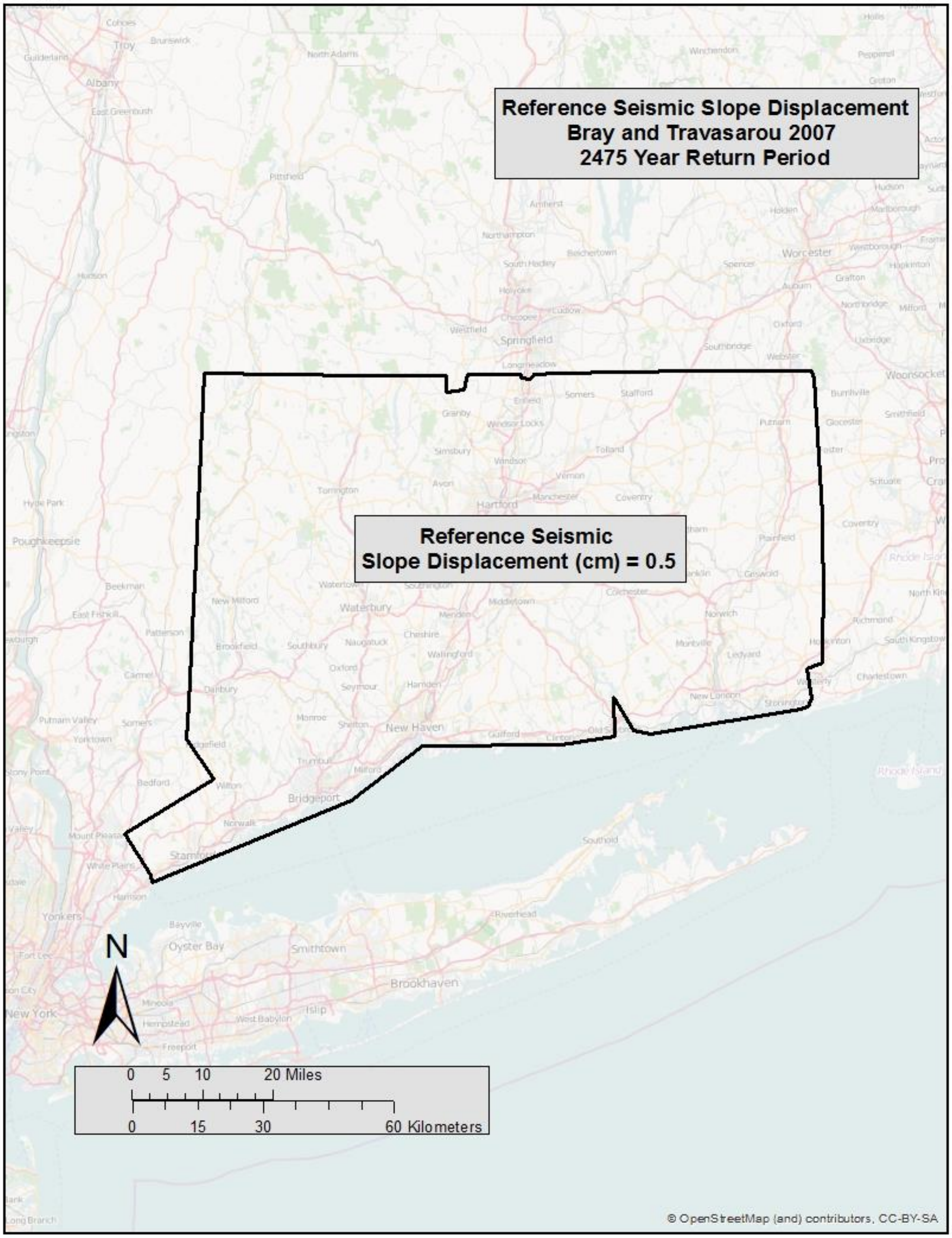

Figure B- 6 Bray and Travasarou (2007) Seismic Slope Displacement *(D^{ref})* Map for Connecticut (Tr = 2,475)

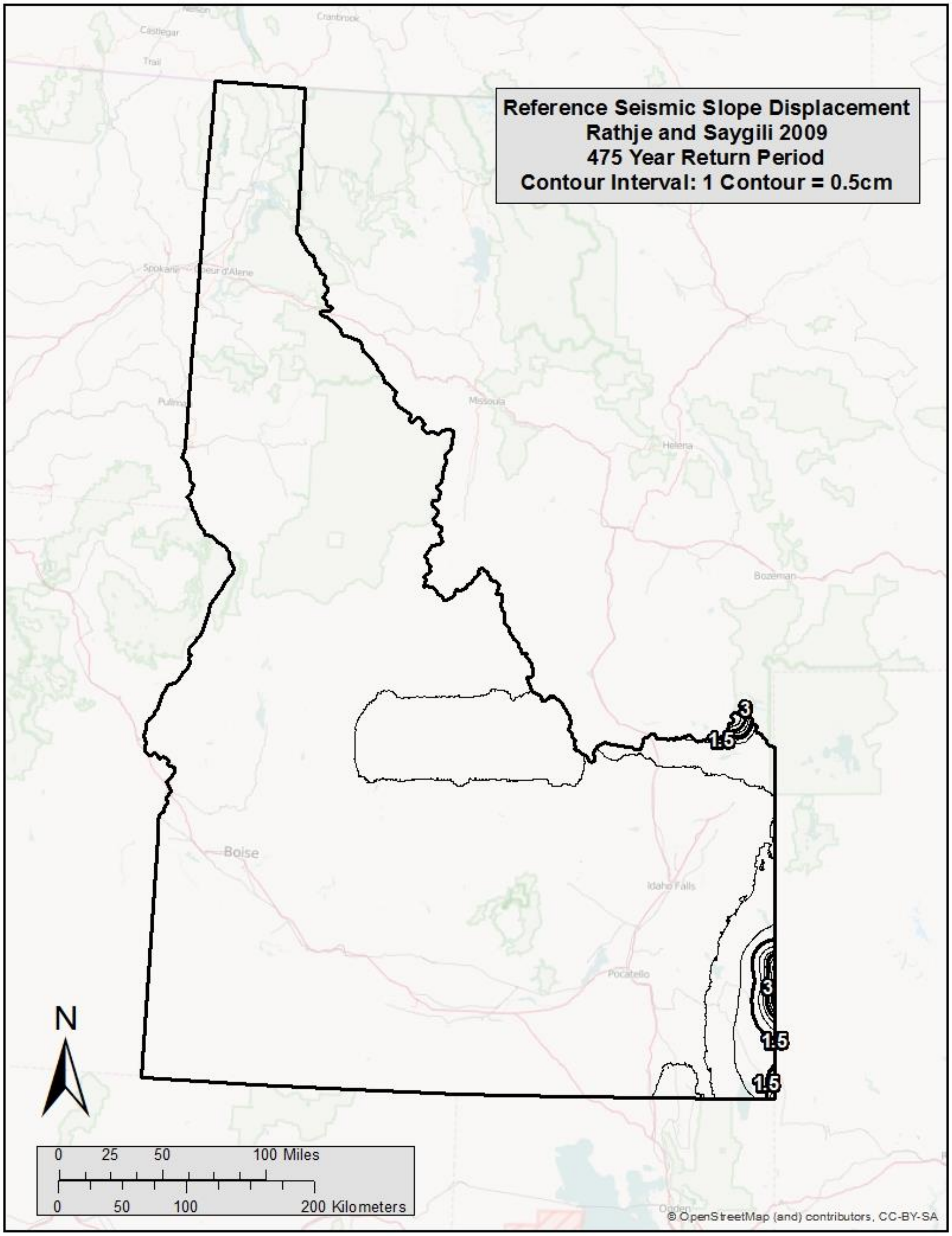

Figure B- 7 Rathje and Saygili (2009) Seismic Slope Displacement *(D^{ref})* Map for Idaho (Tr= 475)

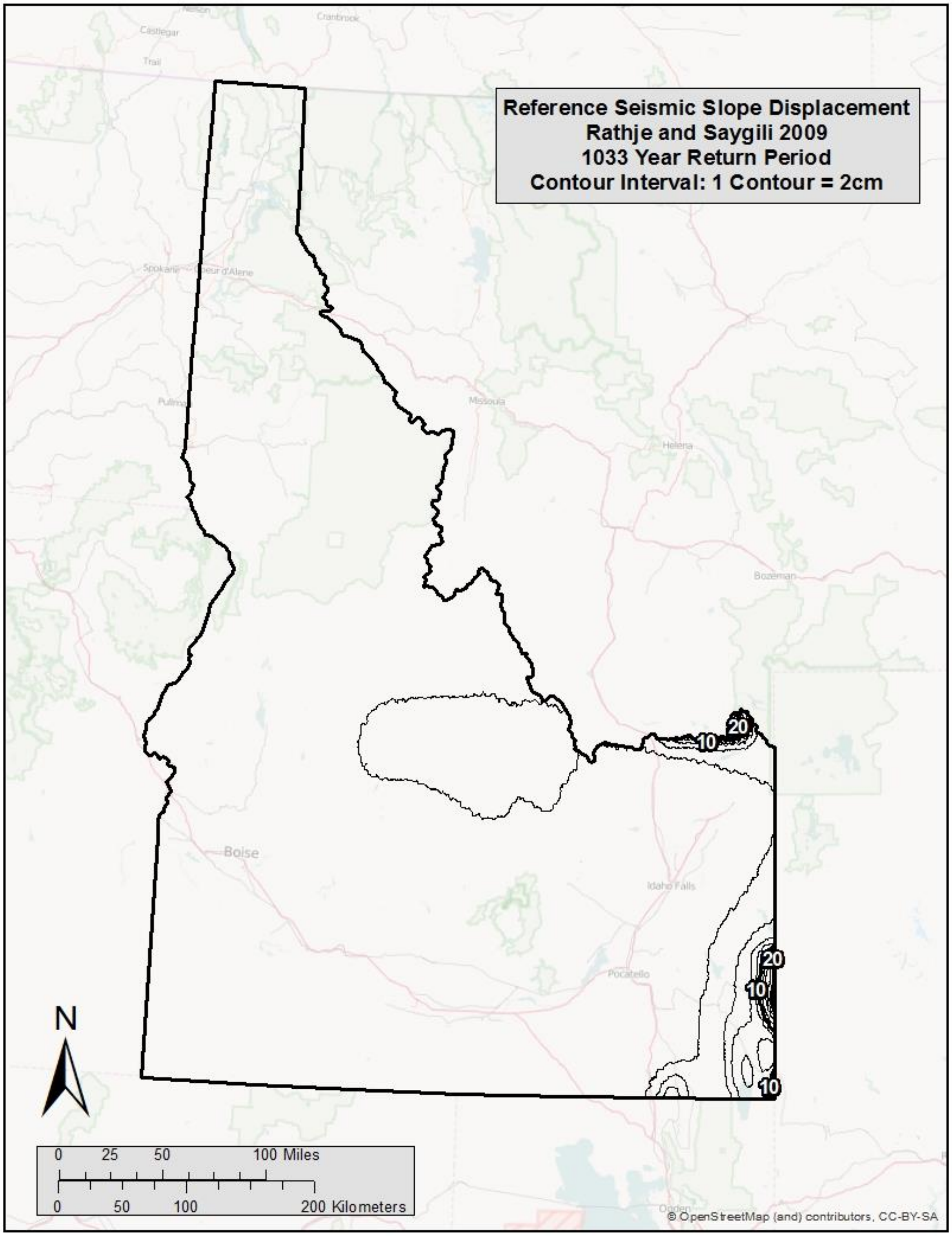

Figure B- 8 Rathje and Saygili (2009) Seismic Slope Displacement *(D^{ref})* Map for Idaho (Tr= 1,033)

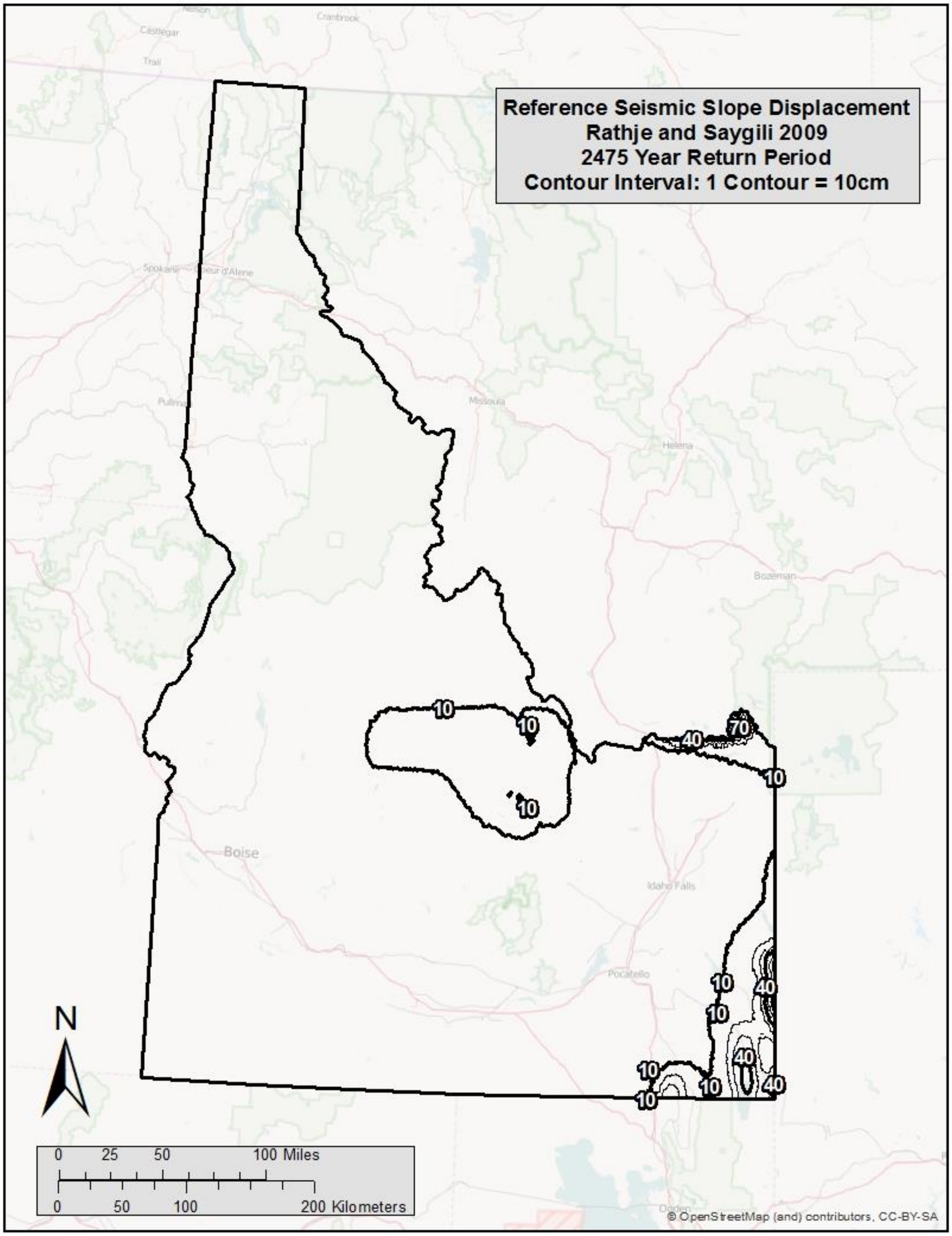

Figure B- 9 Rathje and Saygili (2009) Seismic Slope Displacement *(D^{ref})* Map for Idaho (Tr= 2,475)

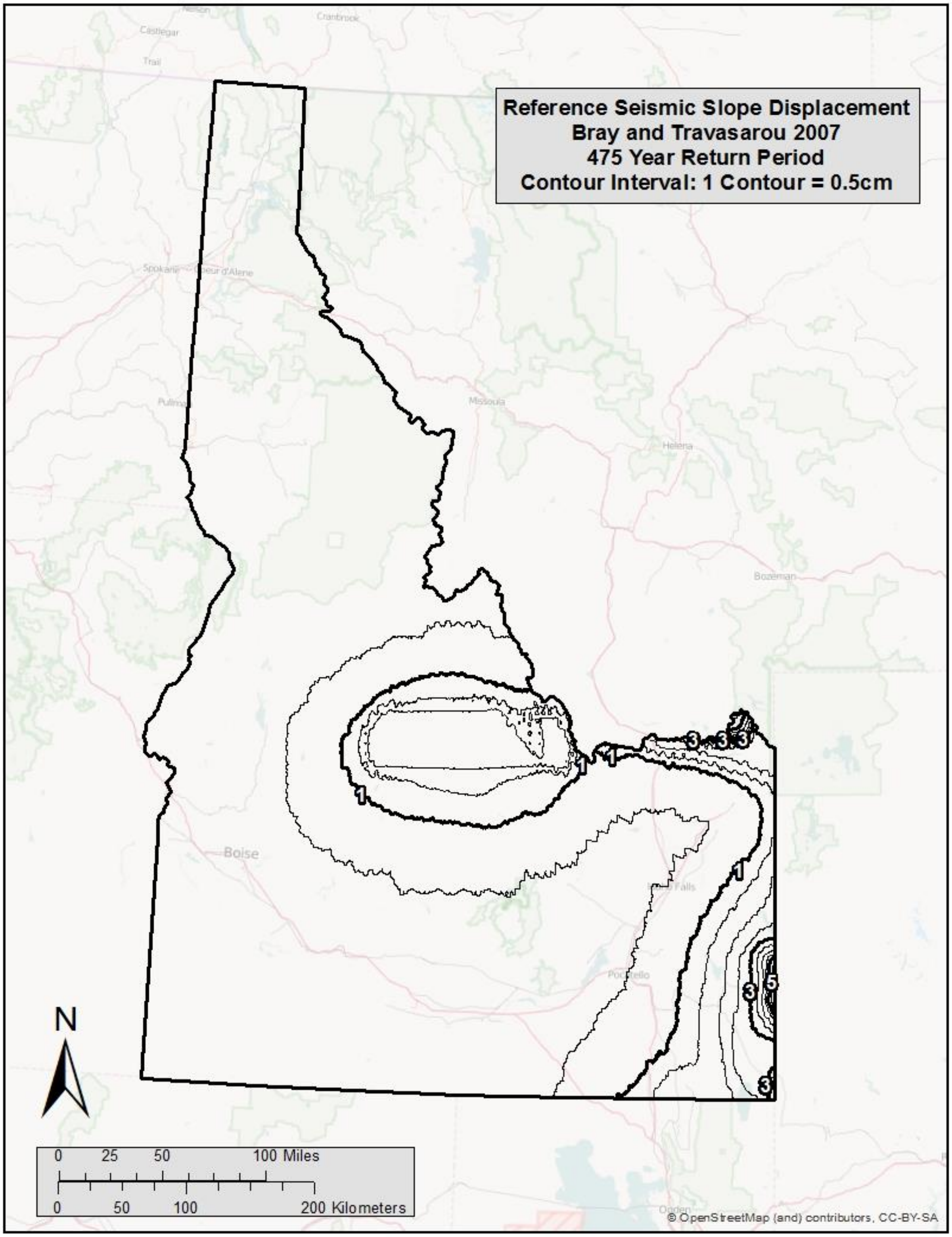

Figure B- 10 Bray and Travasarou (2007) Seismic Slope Displacement *(D^{ref})* Map for Idaho (Tr = 475)

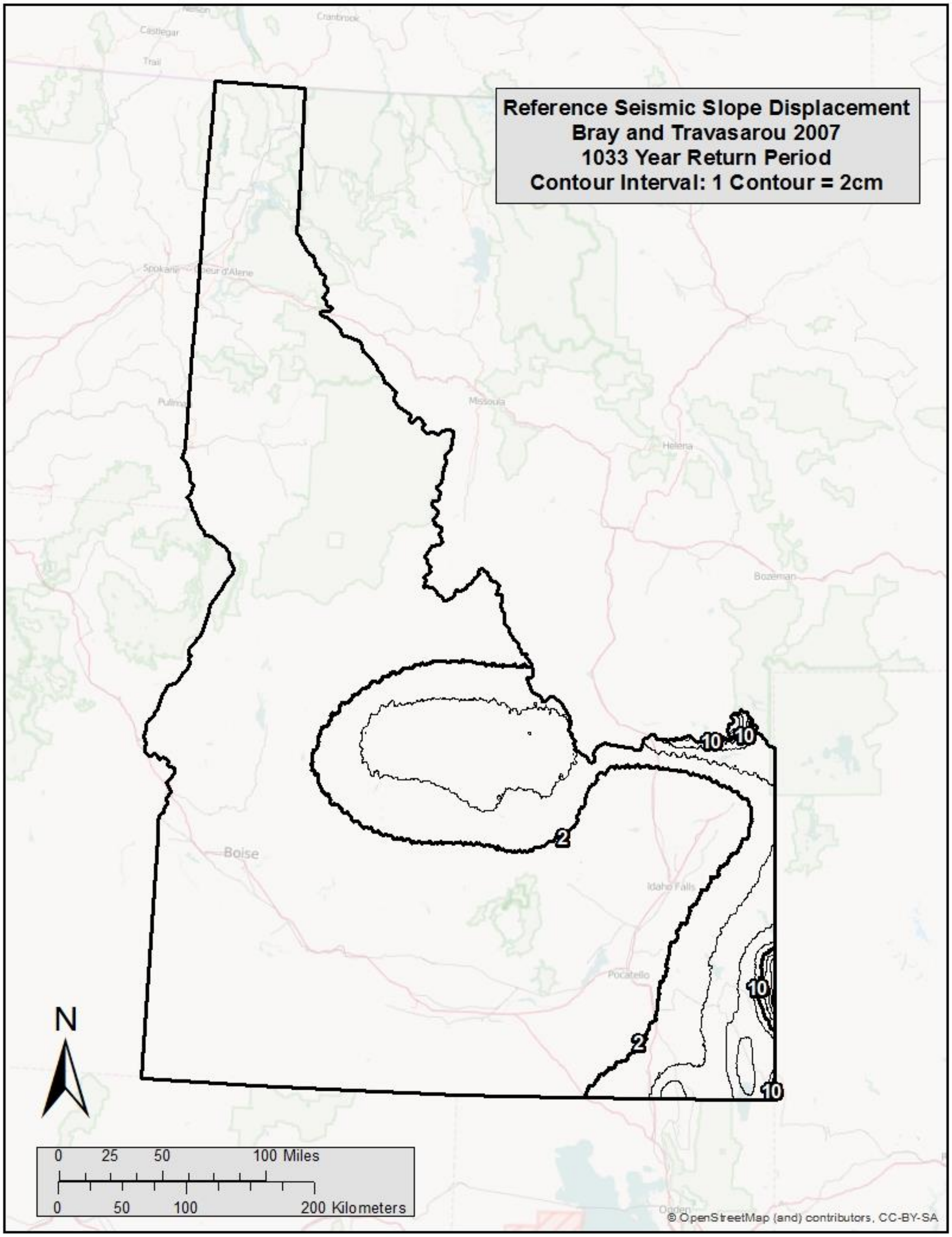

Figure B- 11 Bray and Travasarou (2007) Seismic Slope Displacement *(D^{ref})* Map for Idaho (Tr = 1,033)

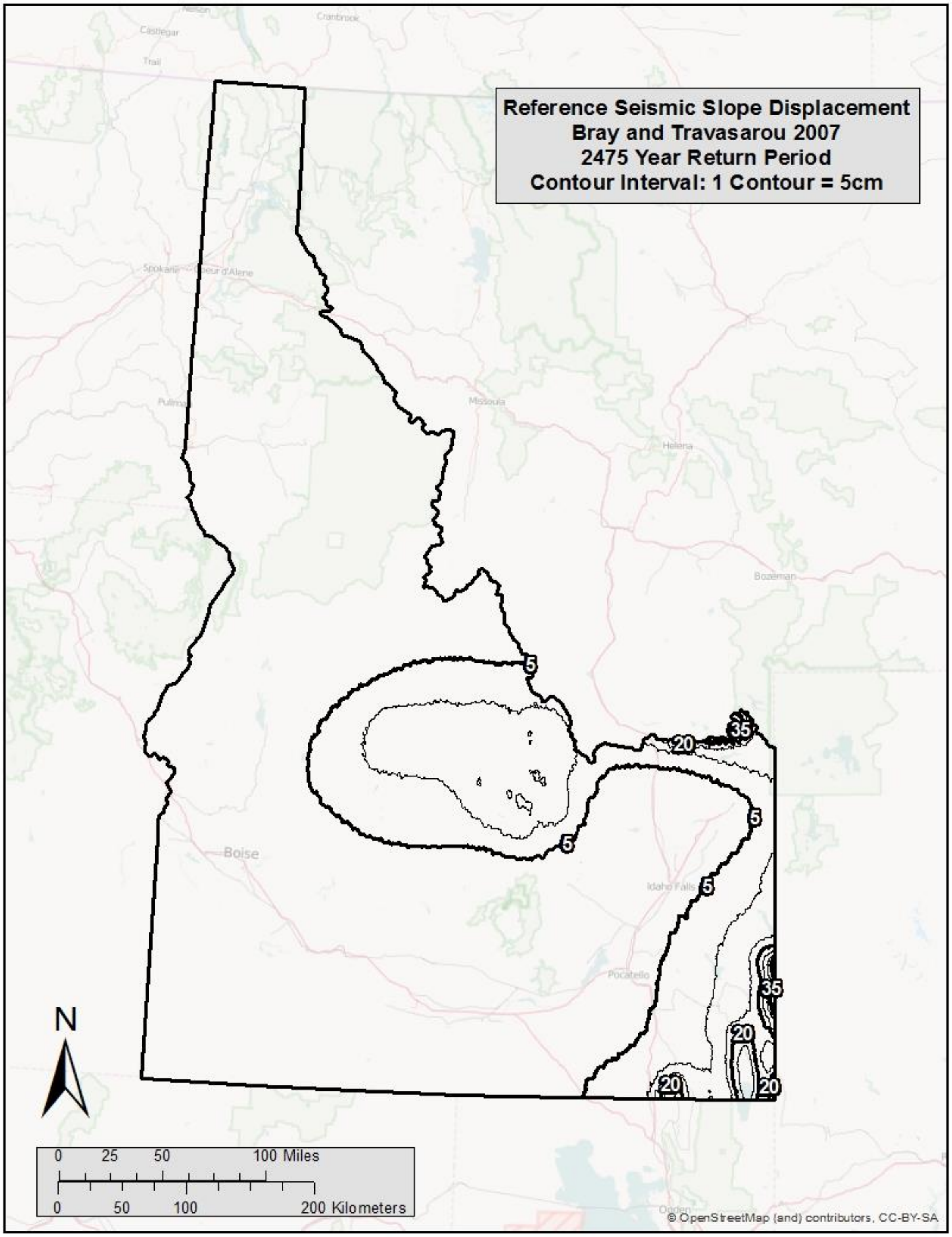

Figure B- 12 Bray and Travasarou (2007) Seismic Slope Displacement *(D^{ref})* Map for Idaho (Tr = 2,475)

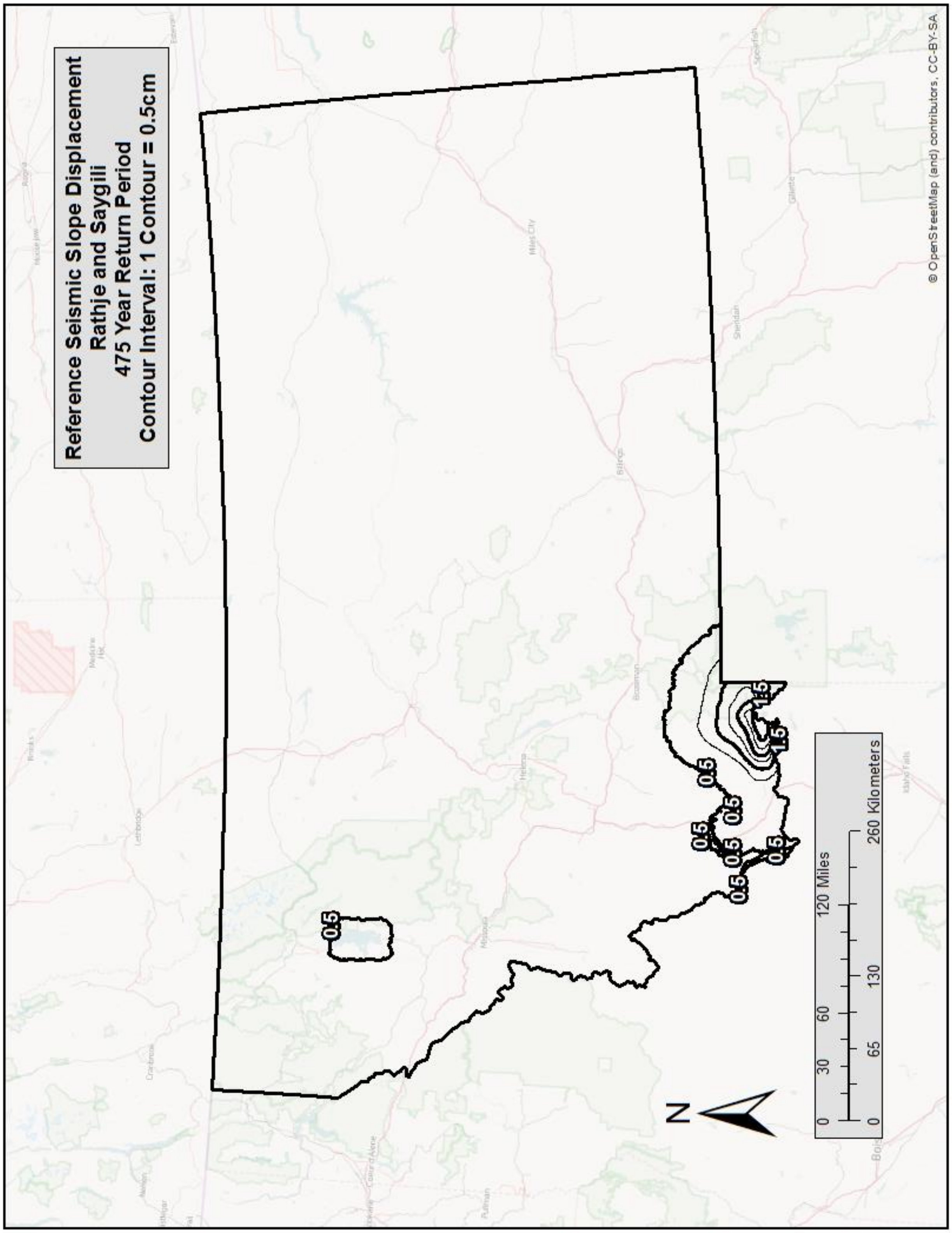

Figure B- 13 Rathje and Saygili (2009) Seismic Slope Displacement *(D^{ref})* Map for Montana (Tr = 475)

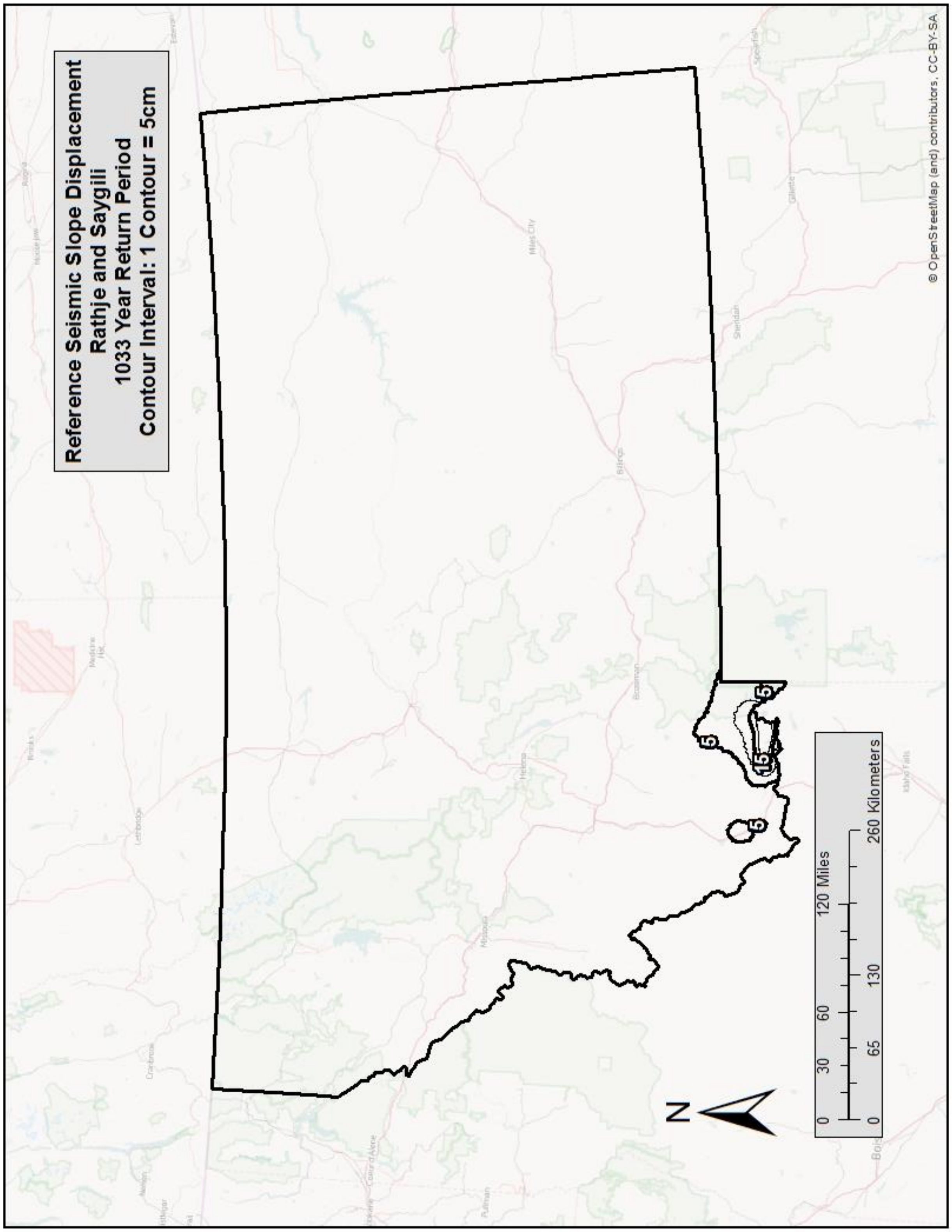

Figure B- 14 Rathje and Saygili (2009) Seismic Slope Displacement *(D^{ref})* Map for Montana (Tr = 1,033)

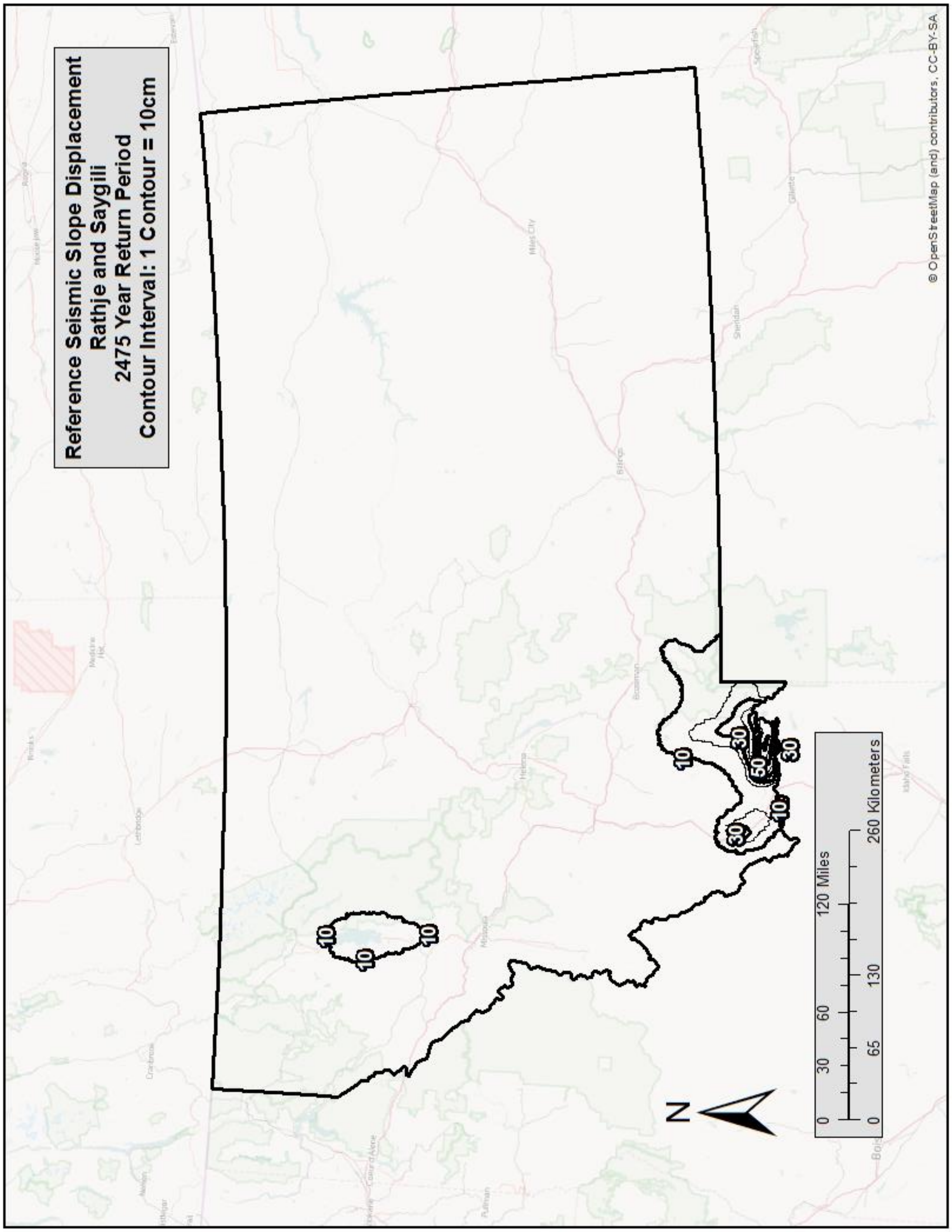

Figure B- 15 Rathje and Saygili (2009) Seismic Slope Displacement *(D^{ref})* Map for Montana (Tr = 2,475)

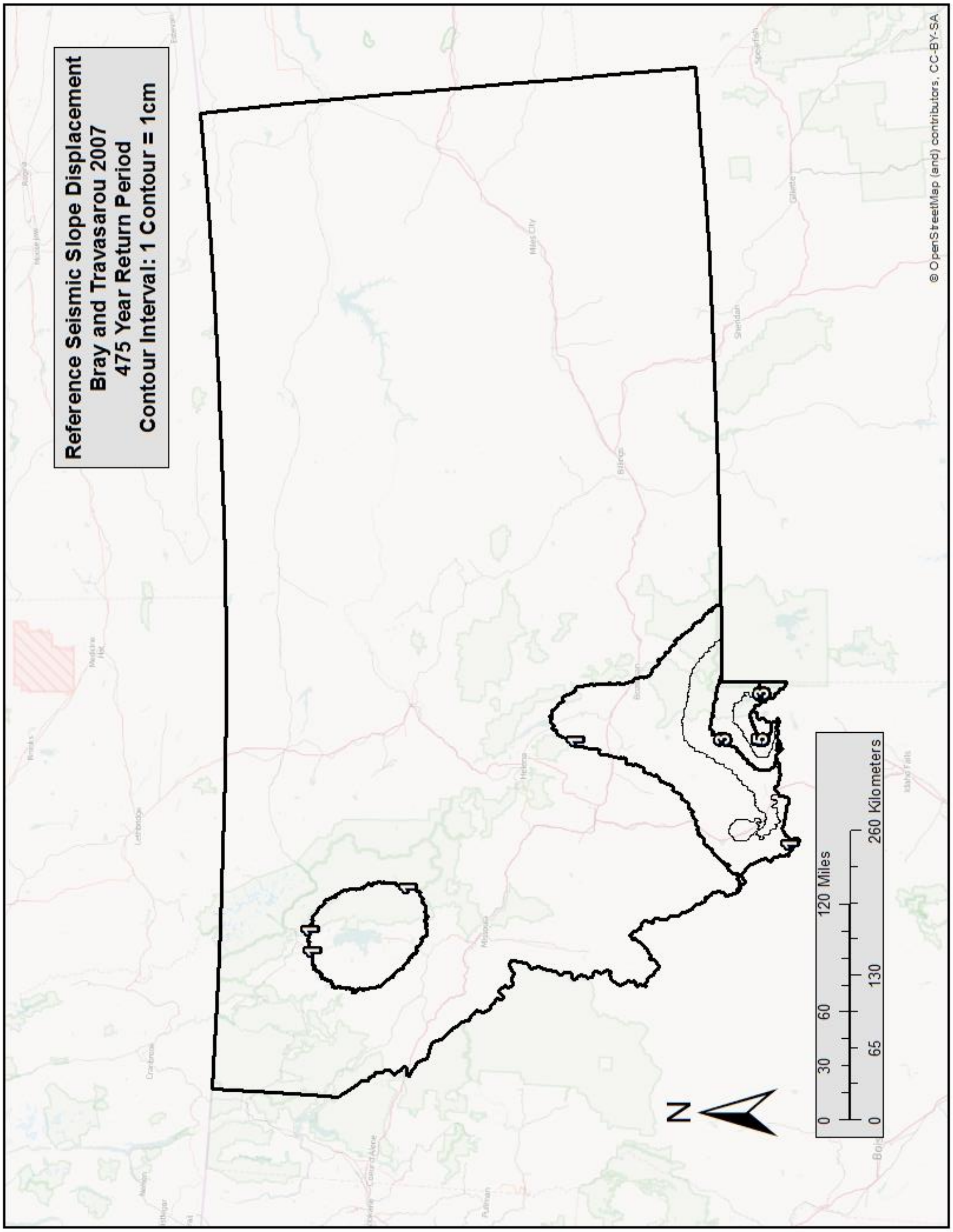

Figure B- 16 Bray and Travasarou (2007) Seismic Slope Displacement *(D^{ref})* Map for Montana (Tr = 475)

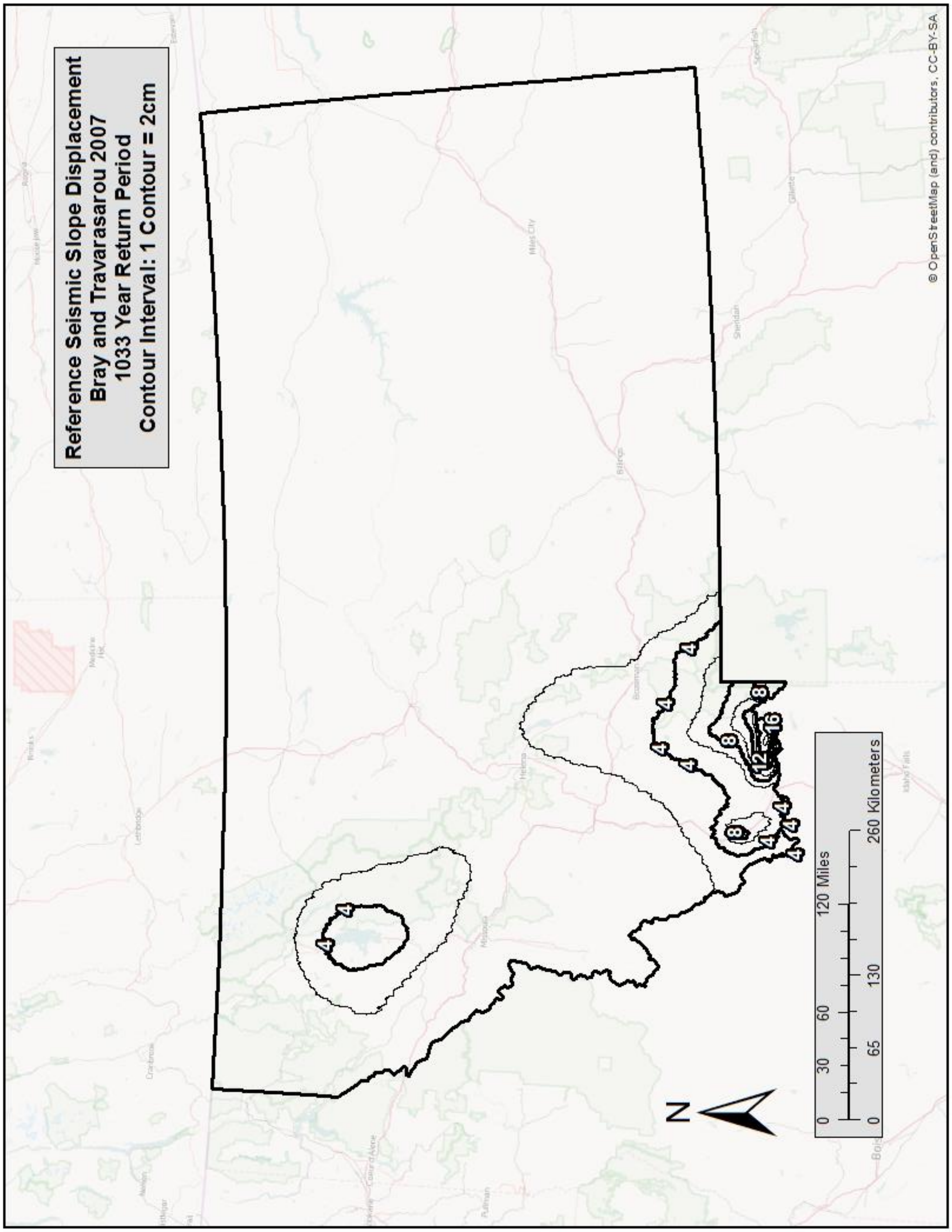

Figure B- 17 Bray and Travasarou (2007) Seismic Slope Displacement *(D^{ref})* Map for Montana (Tr = 1,033)

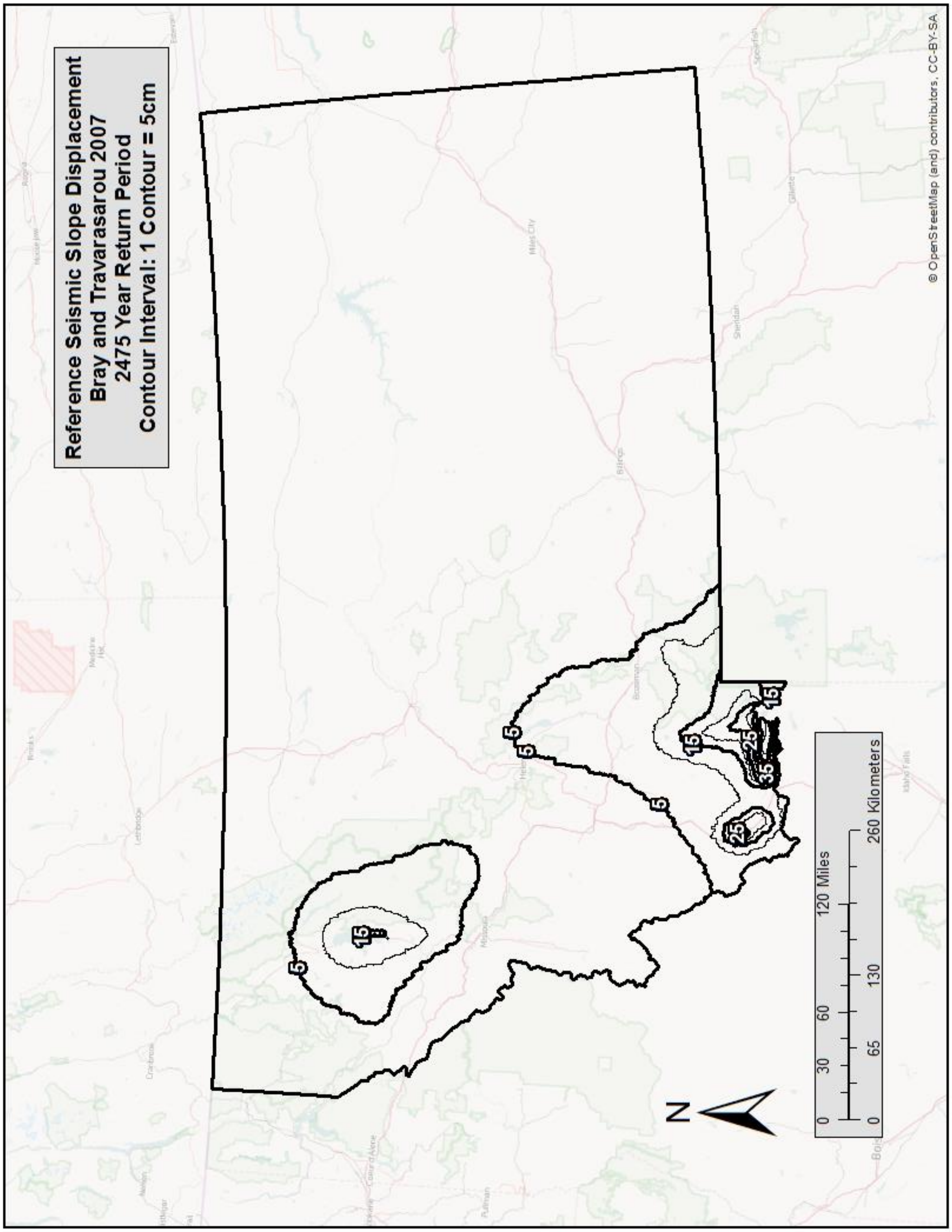

Figure B- 18 Bray and Travasarou (2007) Seismic Slope Displacement *(D^{ref})* Map for Montana (Tr = 2,475)

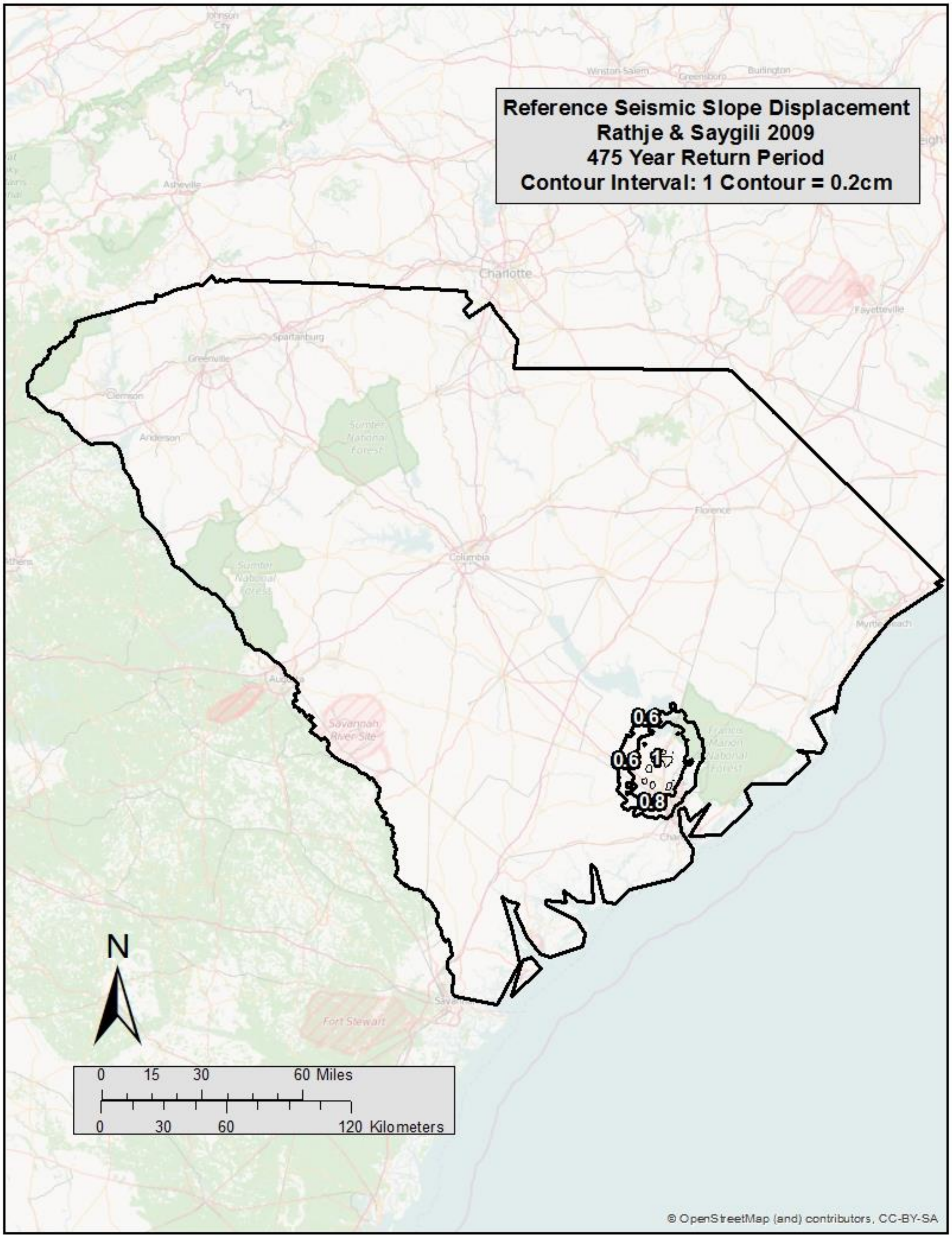

Figure B- 19 Rathje and Saygili (2009) Seismic Slope Displacement *(D^{ref})* Map for South Carolina (Tr = 475)

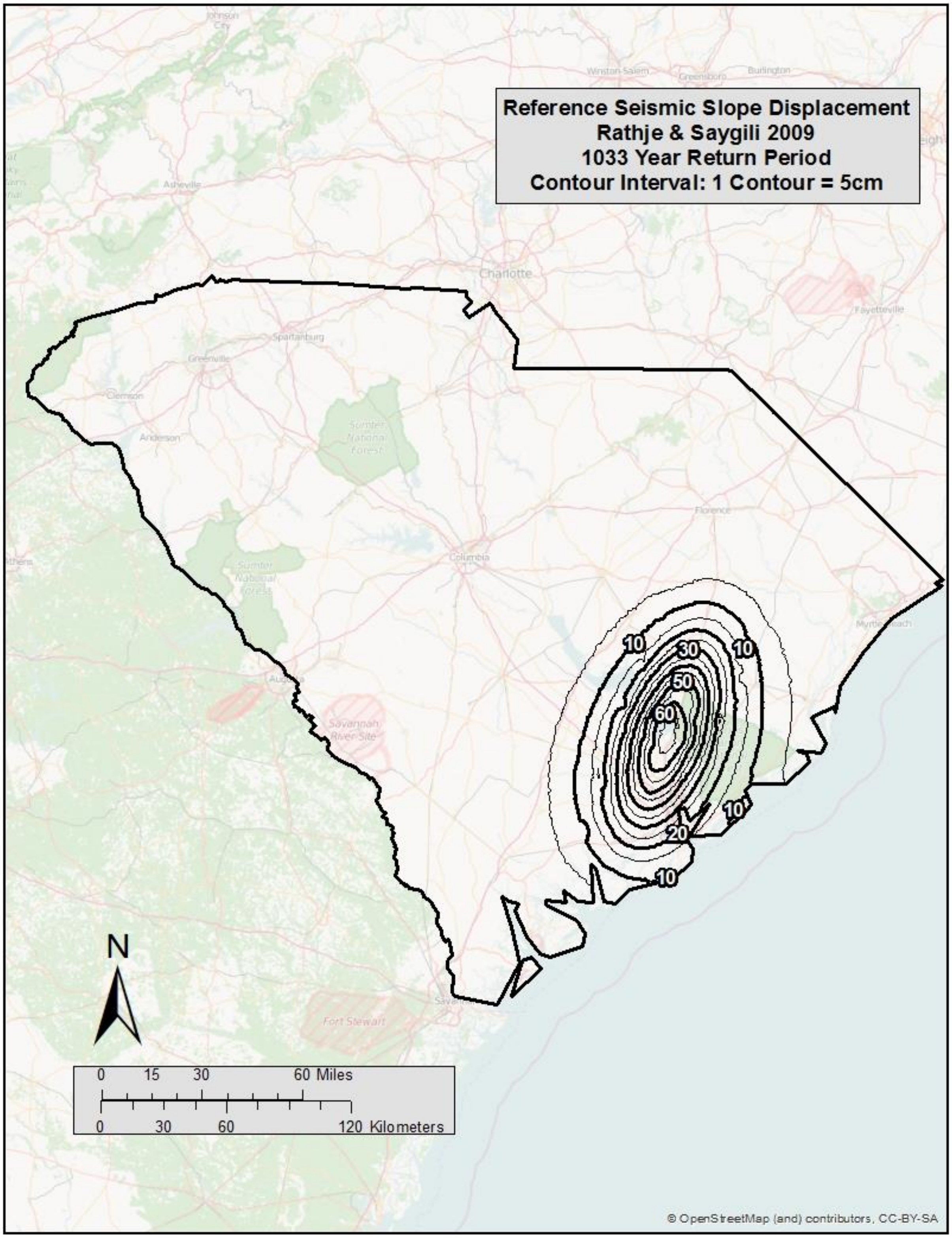

Figure B- 20 Rathje and Saygili (2009) Seismic Slope Displacement *(D^{ref})* Map for South Carolina (Tr = 1,033)

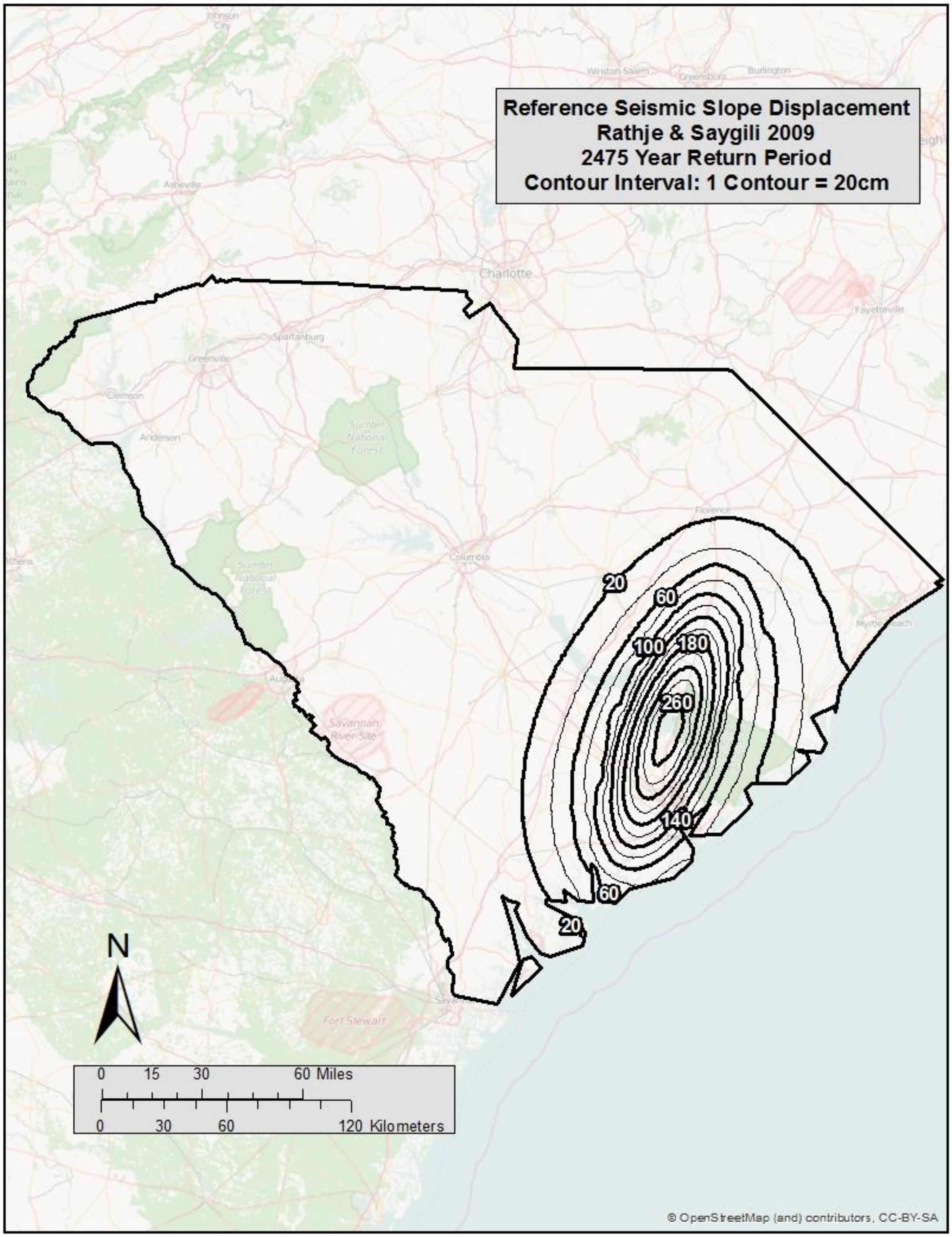

Figure B- 21 Rathje and Saygili (2009) Seismic Slope Displacement *(D^{ref})* Map for South Carolina (Tr = 2,475)

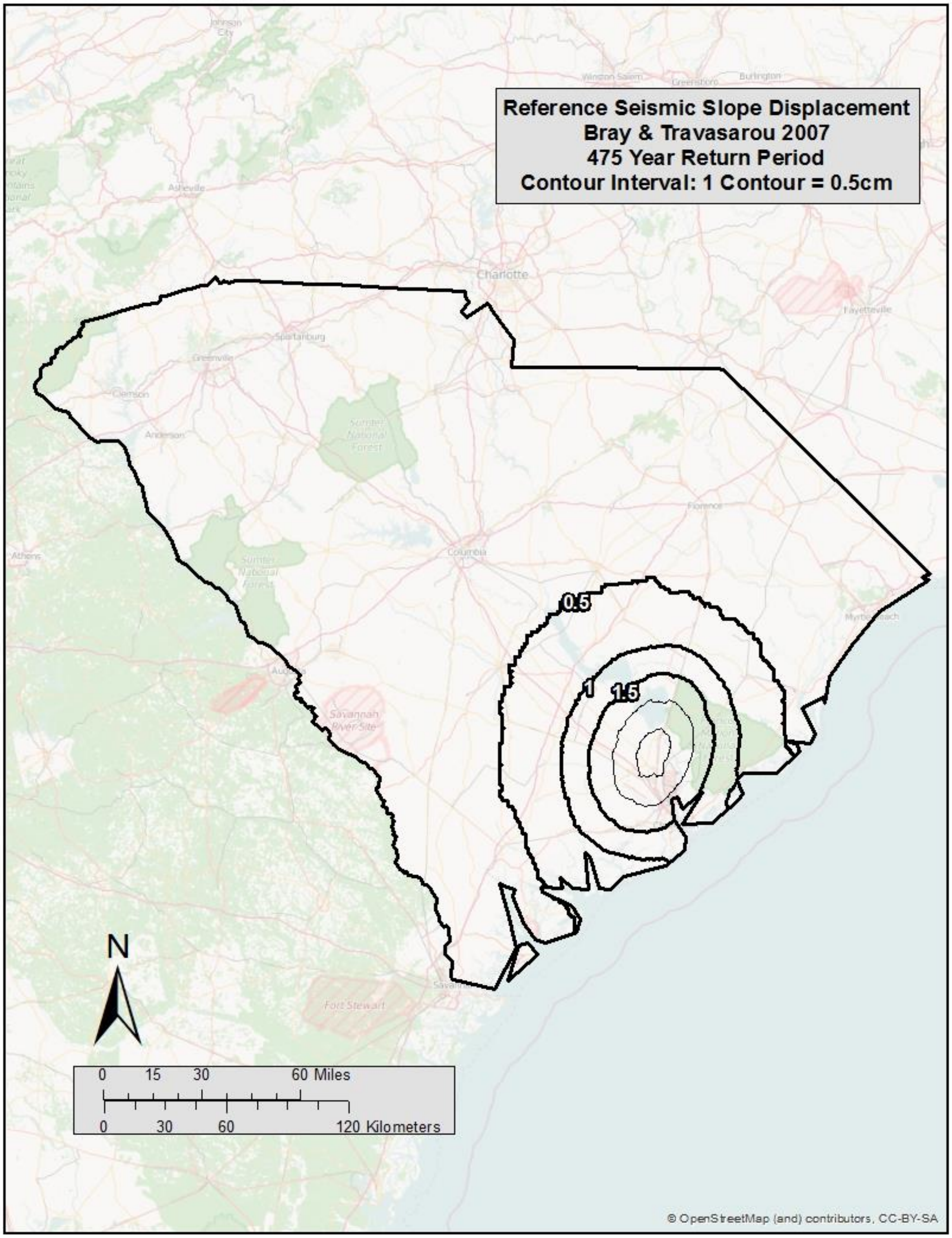

Figure B- 22 Bray and Travasarou (2007) Seismic Slope Displacement *(D^{ref})* Map for South Carolina (Tr = 475)

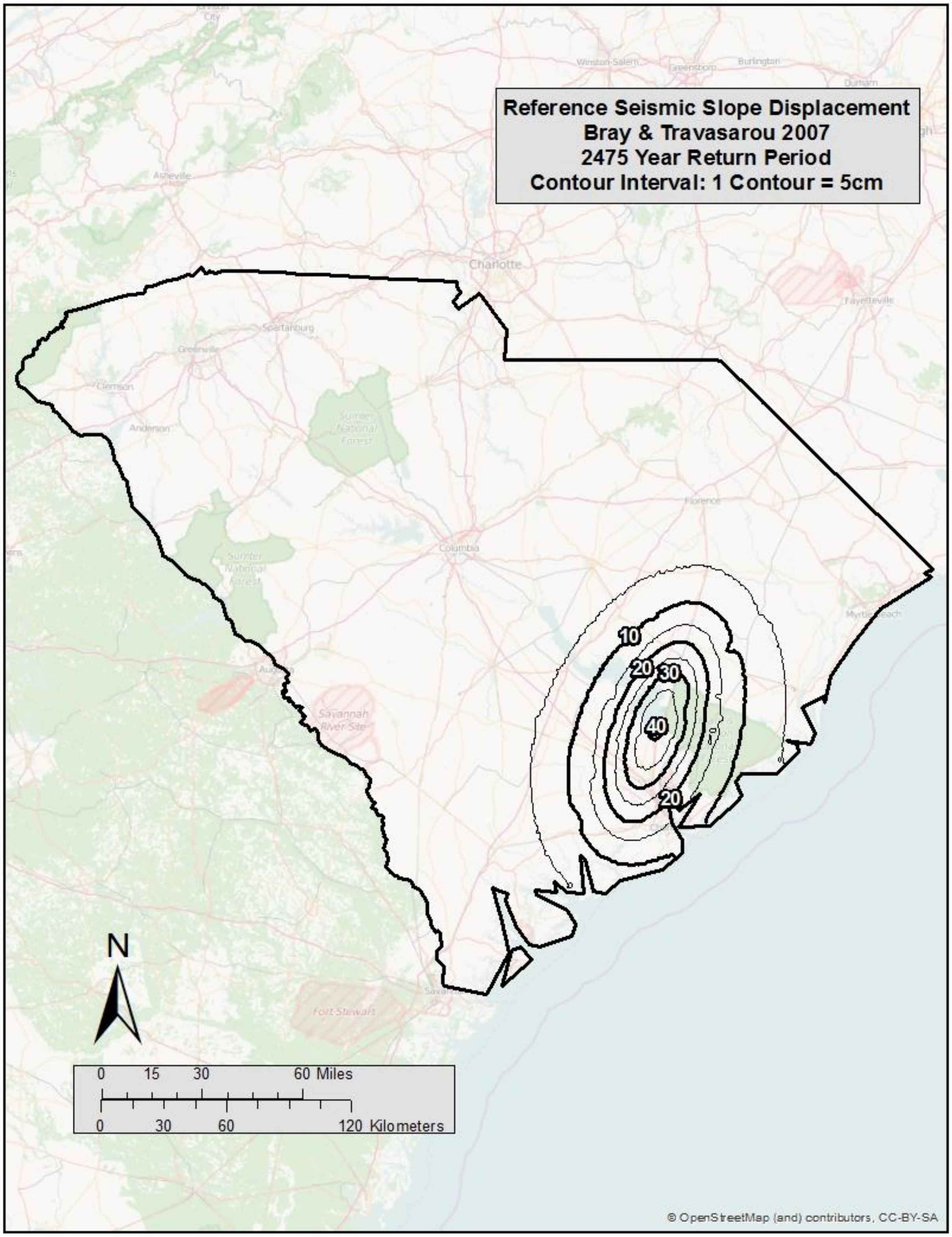

Figure B- 23 Bray and Travasarou (2007) Seismic Slope Displacement *(D^{ref})* Map for South Carolina (Tr = 1,033)

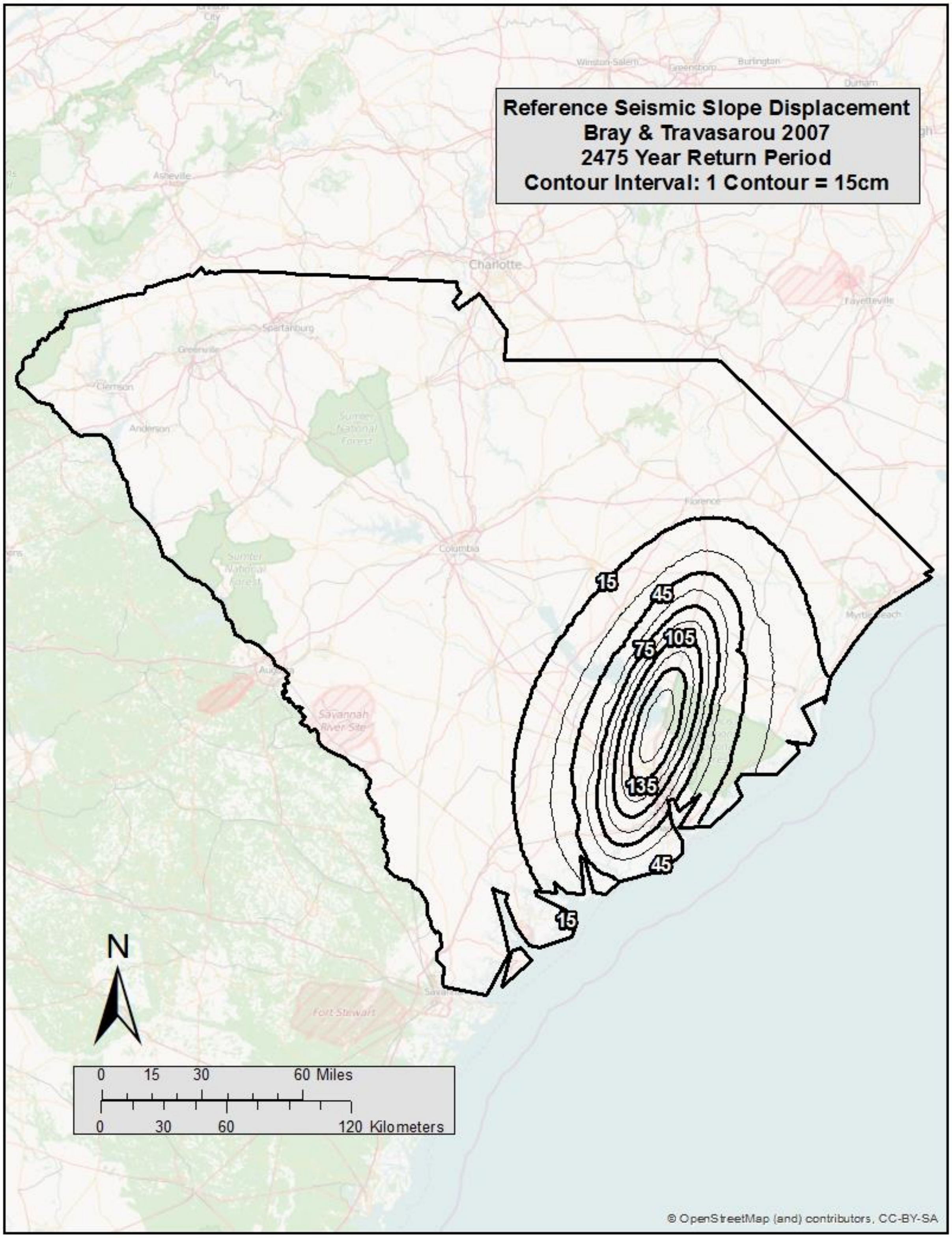

Figure B- 24 Bray and Travasarou (2007) Seismic Slope Displacement *(D^{ref})* Map for South Carolina (Tr = 2,475)

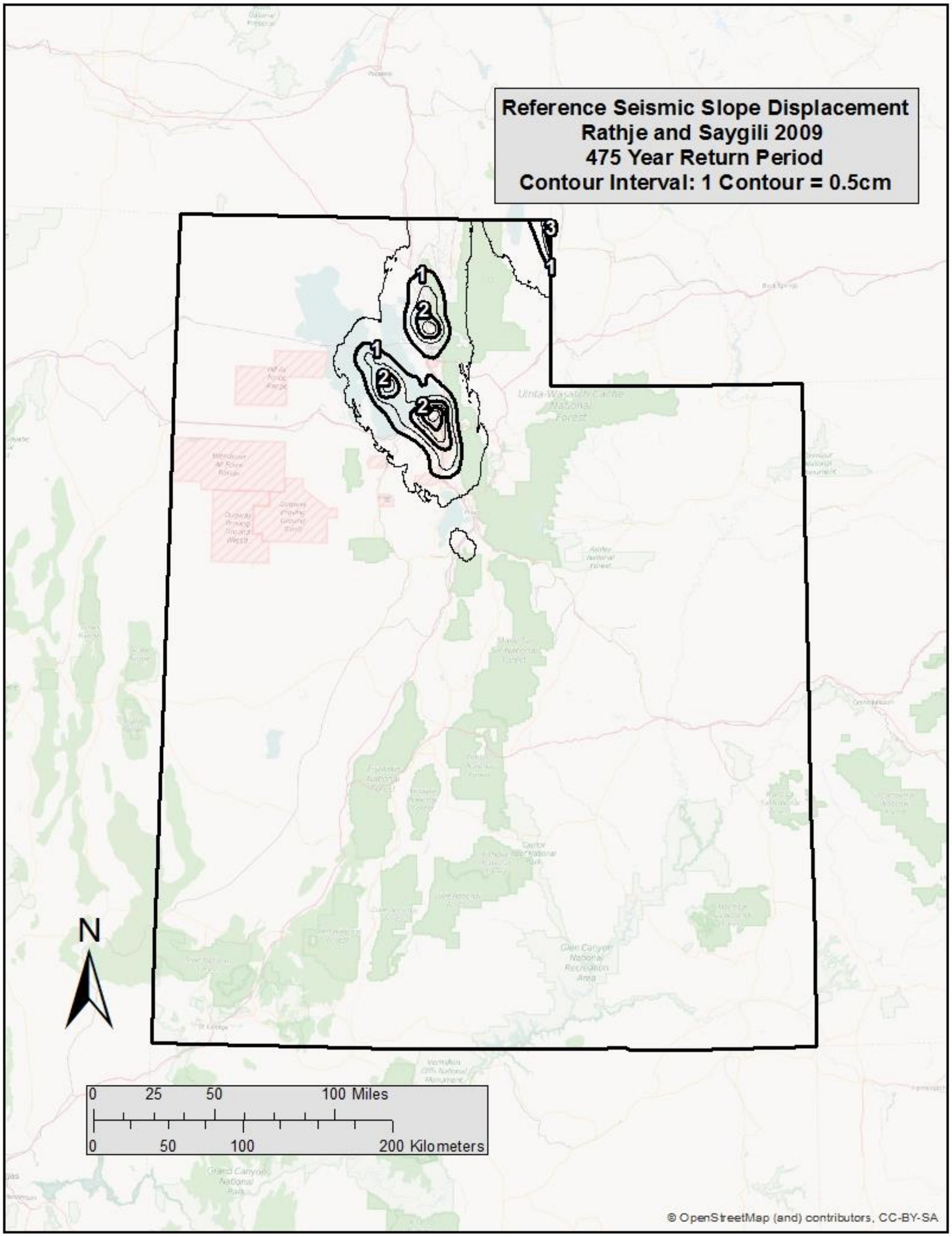

Figure B- 25 Rathje and Saygili (2009) Seismic Slope Displacement *(D^{ref})* Map for Utah (Tr= 475)

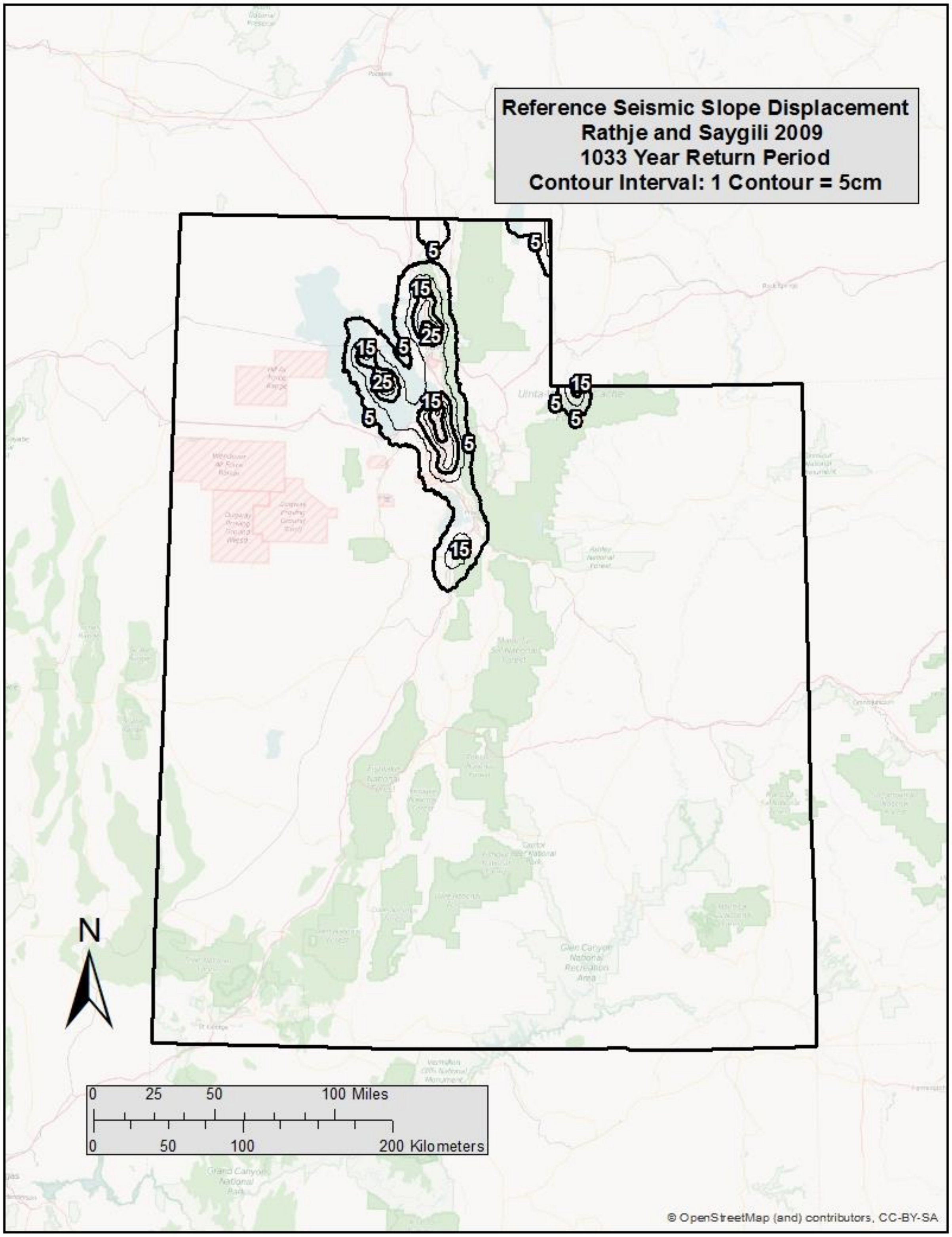

Figure B- 26 Rathje and Saygili (2009) Seismic Slope Displacement *(D^{ref})* Map for Utah (Tr= 1,033)

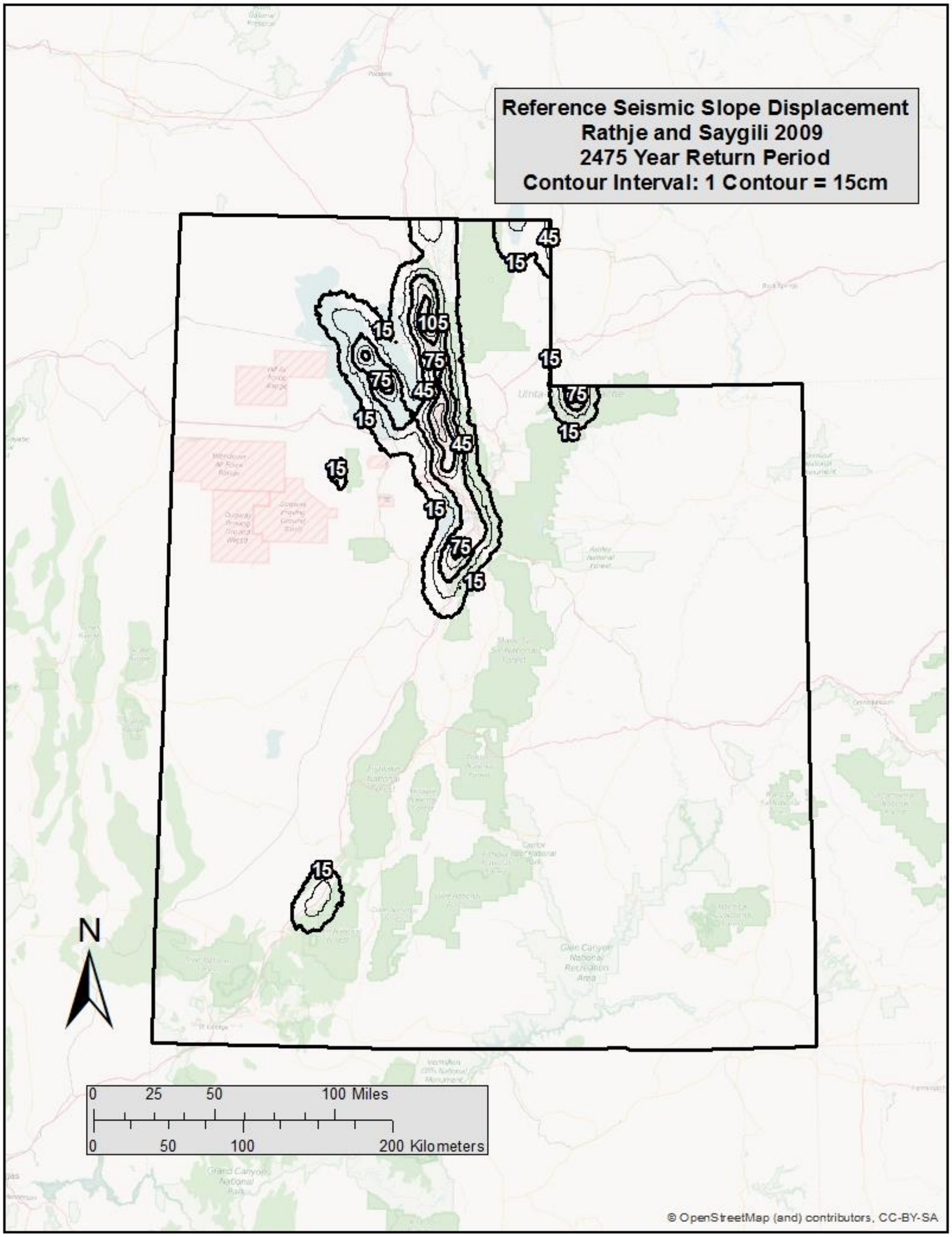

Figure B- 27 Rathje and Saygili (2009) Seismic Slope Displacement *(D^{ref})*Map for Utah (Tr= 2,475)

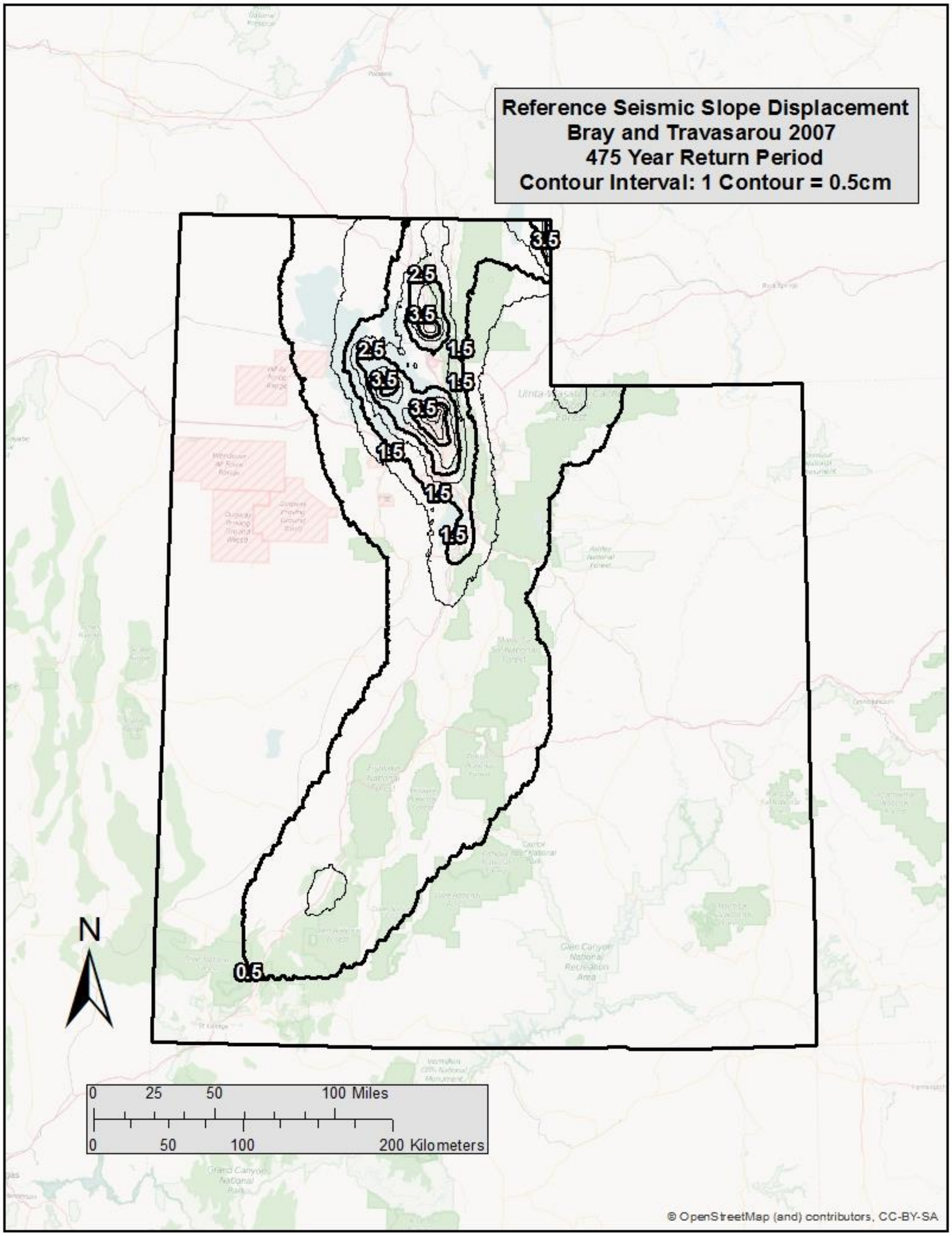

Figure B- 28 Bray and Travasarou (2007) Seismic Slope Displacement *(D^{ref})* Map for Utah (Tr = 475)

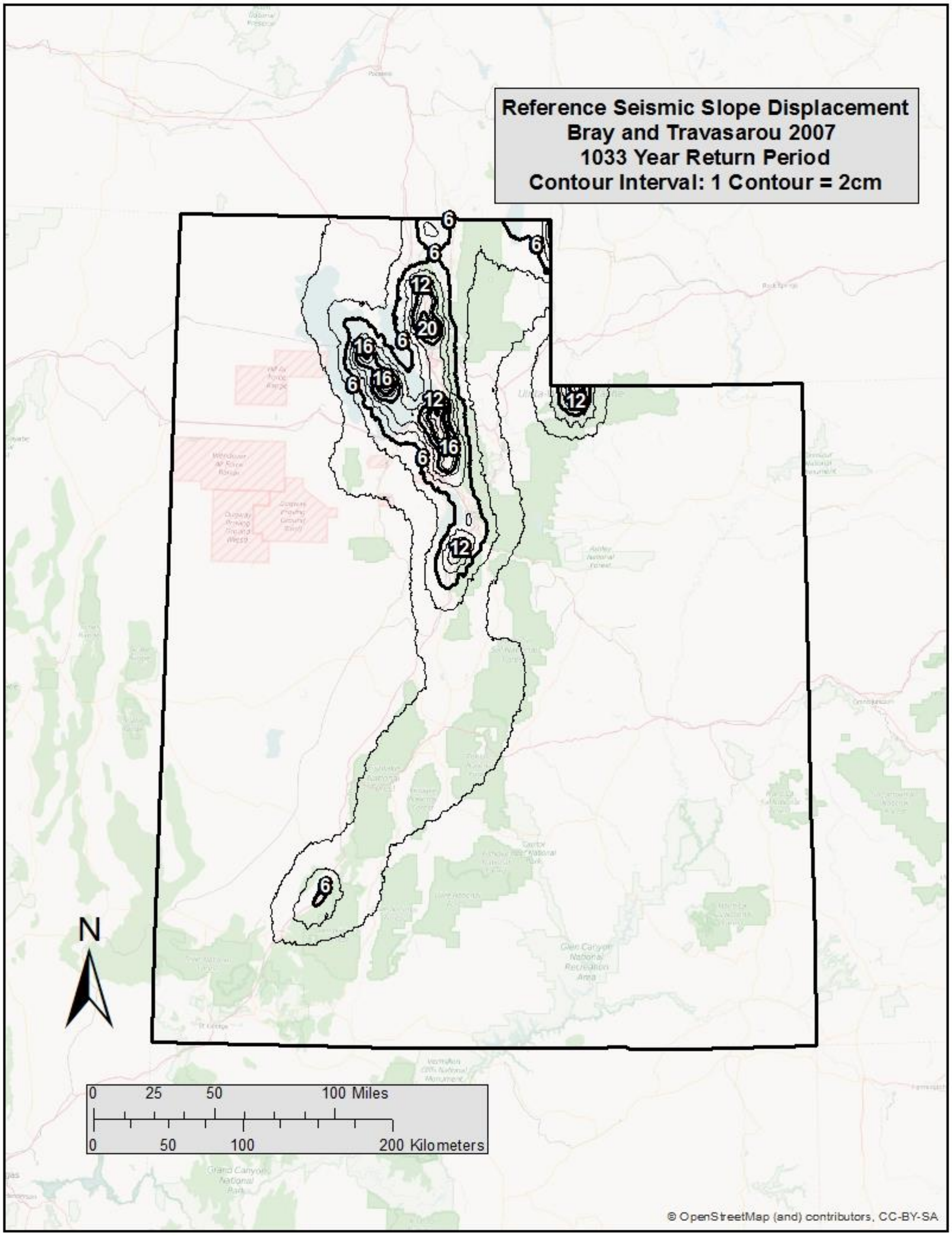

Figure B- 29 Bray and Travasarou (2007) Seismic Slope Displacement *(D^{ref})* Map for Utah (Tr = 1,033)

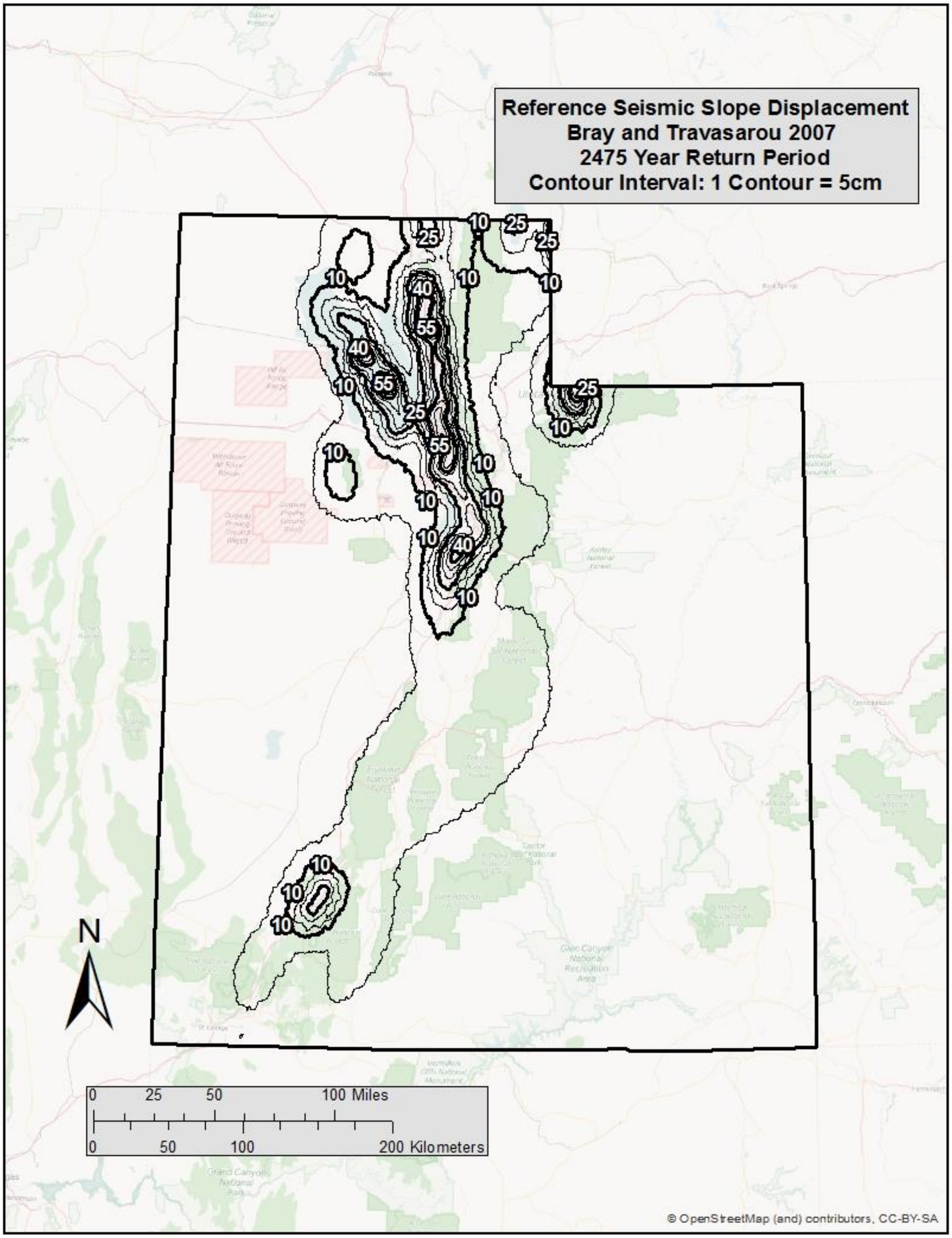

Figure B- 30 Bray and Travasarou (2007) Seismic Slope Displacement *(D^{ref})* Map for Utah (Tr = 2,475)